Electronic Supporting Information

N,O-Benzamide Difluoroboron Complexes as Near-infrared Probes for the Detection of *β*-amyloid and Tau Fibrils

Yimin Chen[a], Chang Yuan[a], Tianxin Xie[a], Yuying Li[a], Bin Dai[b], Kaixiang Zhou[a], Yi Liang[b], Jiapei Dai[c], Hongwei Tan*[, a], Mengchao Cui*[, a]

[a]*Key Laboratory of Radiopharmaceuticals, Ministry of Education, College of Chemistry, Beijing Normal University, Beijing 100875, People's Republic of China.*

[b]*State Key Laboratory of Virology, College of Life Sciences, Wuhan University, Wuhan 430072, People's Republic of China.*

[c]*Wuhan Institute for Neuroscience and Neuroengineering, South-Central University for Nationalities, Wuhan 430074, People's Republic of China.*

Corresponding Authors:

*Mengchao Cui, E-mail: cmc@bnu.edu.cn

*Hongwei Tan, Email: hongwei.tan@bnu.edu.cn

Table of contents

General Information.

All reagents used in synthesis were obtained commercially and used without further purification. The ^{1}H NMR and ^{13}C NMR spectra were obtained on JEOL (Japan Electron Optics Laboratory) JNM-ECZ400R or JNM-ECZ600R spectrometers in according solutions at room temperature with tetramethylsilane as an internal standard. MS was obtained by a LCQ FLEET (ESI) mass spectrometer (Thermo Scientific, USA) and HRMS were acquired by a Q Exactive (ESI) mass spectrometer (Thermo Scientific, USA). The fluorescence and ultraviolet spectra were measured on a Varian Cary Eclipse Fluorescence spectrophotometer (USA) and a Shimadzu UV-2450 UV−vis spectrophotometer (Japan). The absolute fluorescence quantum yields were measured by an Edinburgh FLS980 lifetime and steady state spectrometer (UK). Fluorescent and Gallyas-Braak staining images on tissue was recorded by a Life EVOS FL imaging microscope (USA). The quantitative binding affinity (K_d) was performed in black 96-well plate (Costar, USA) and measured by an Infinite M200 pro microplate reader (Tecan, Switzerland). *In vivo* and e*x vivo* NIR fluorescence imaging studies on living mice was performed on an IVIS Lumina III *in viv*o imaging system (PerkinElmer, USA) and data analysis was recorded by Living Image 4.2.1 software. *Ex vivo* fluorescence staining using frozen brain sections were prepared by a CM1900 freezing microtome (Leica, Germany). X-ray crystallography data was collected on a SuperNova X-ray diffractometer (Rigaku, Japan). Samples were analyzed using high performance liquid chromatography (HPLC, Primaide, Japan) equipped with a reverse column (Venusil MP C18, 5 μm, 4.6 mm×250 mm, Bonna-Agela Technologies, China) and eluted with a gradient of deionized water as phase A and acetonitrile as phase B at flow rate of 1.0 mL/min. Synthetic A$\beta_{1\text{-}42}$ peptides was purchased from Peptide Institute, Inc. (Osaka, Japan). The recombinant Tau-K18 fragment expressed by *escherichia coli* BL21 (DE3) was obtained from Wuhan University. The Tg-

A*β* mice (C57BL6, APPsw/PSEN1, 22 months old, male) and age-matched WT mice (C57BL6, 22 months old, male) were purchased from Zhishan (Beijing) Institute of Healthcare Research Co., Ltd. for *in vivo* near-infrared imaging. Tg-Tau mice tissue (rTg4510, P301L, 7 months old, female) were obtained from Xuanwu Hospital, Capital Medical University (Beijing, China). Human brain tissue from an AD patient (female, 95 years old; male) were provided by the Chinese Brain Bank Center. The normal ICR mice (male, 19 - 21 g) used for the quantitative brain uptake experiments were purchased from Vital River Laboratories (Beijing, China). All experiments were performed in compliance with the China Animal Management Regulations (2017 Edition), and were approved by the animal care committee of Beijing Normal University.

Chemistry

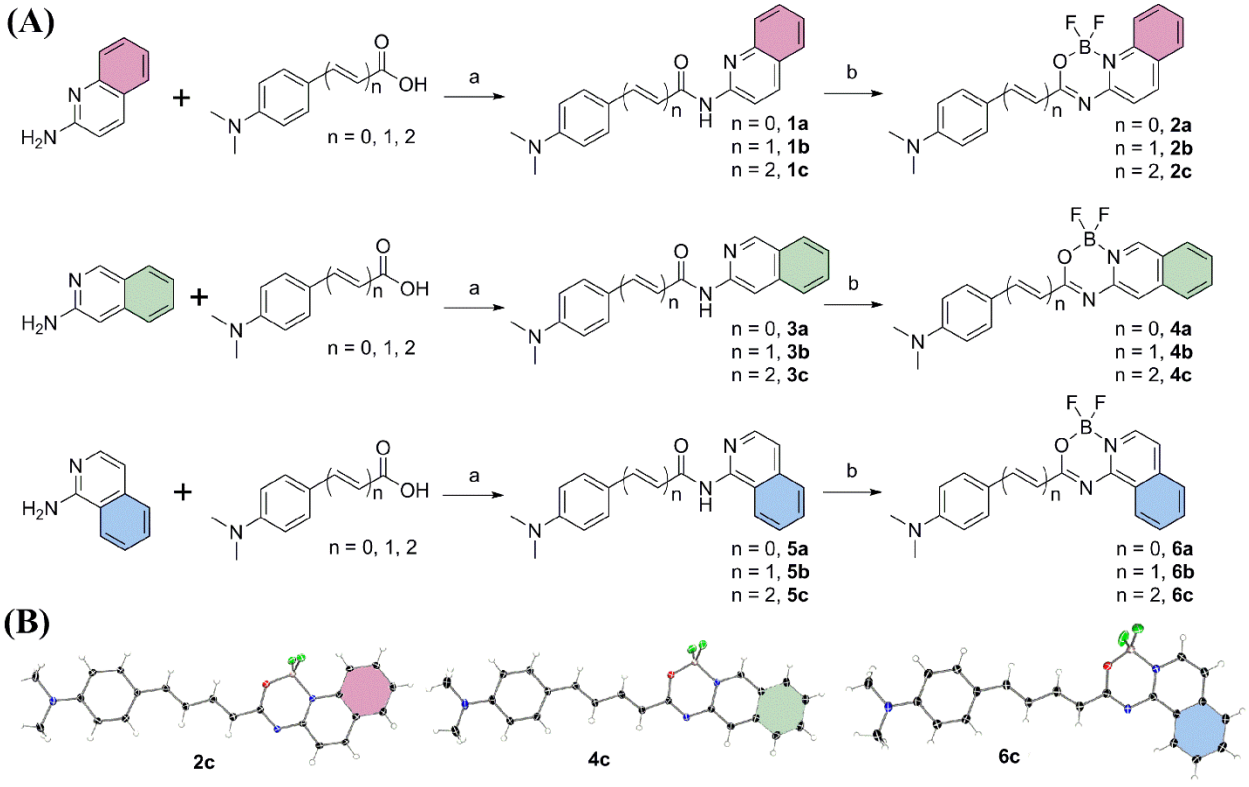

Scheme S1. (A) Reagents and conditions: (a) Acetonitrile, $POCl_3$, refluxed for 2 h; (b) CH_2Cl_2,

BF_3 ·Et_2O, Et_3N, r.t. 10 min. (B) The ORTEP diagrams of **2c**, **4c** and **6c**.

4-(Dimethylamino)-*N*-(quinolin-2-yl)benzamide (1a)

To a solution of 4-(dimethylamino)benzoic acid (826.0 mg, 5.0 mmol) and quinolin-2-amine (966.1 mg, 5.0 mmol) in acetonitrile and was added $POCl_3$ dropwise. The solution was refluxed for about 2 h. After cooling to room temperature, neutralized with aqueous NaOH (1 mol/L), and the reaction mixture extracted with CH_2Cl_2 (50 mL×5) then dried over anhydrous $MgSO_4$. The solvents were concentrated under reduced pressure and the crude product was purified by flash column chromatography (petroleum ether/ethyl acetate = 3 : 1, v/v). Compound **1a** was obtained as yellow solid (1201 mg, 82.4%). ^{1}H NMR (600 MHz, DMSO-d_6) δ 10.69 (s, 1H), 8.36 (s, 2H), 8.07 – 7.98 (m, 2H), 7.93 (dd, *J* = 8.1, 0.9 Hz, 1H), 7.86 (d, *J* = 8.3 Hz, 1H), 7.71 (ddd, *J* = 8.4, 6.9, 1.4 Hz, 1H), 7.50 (ddd, *J* = 8.0, 7.0, 1.0 Hz, 1H), 6.75 (d, *J* = 9.0 Hz, 2H), 3.02 (s, 6H). MS: m/z calculated for $C_{18}H_{18}N_3O$ 292.14; found 292.17, M + H^+.

(*E*)-3-(4-(Dimethylamino)phenyl)-*N*-(quinolin-2-yl)acrylamide (1b)

The same method described above for compound **1a** was used, and compound **1b** was obtained as yellow solid (652 mg, 68.5%). ^{1}H NMR (400 MHz, DMSO-d_6) δ 10.83 (s, 1H), 8.48 (d, *J* = 9.0 Hz, 1H), 8.35 (d, *J* = 9.1 Hz, 1H), 7.91 (dd, *J* = 8.1, 1.3 Hz, 1H), 7.86 – 7.76 (m, 1H), 7.71 (ddd, *J* = 8.4, 6.9, 1.5 Hz, 1H), 7.58 (d, *J* = 15.6 Hz, 1H), 7.51 – 7.42 (m, 3H), 6.84 (d, *J* = 15.5 Hz, 1H), 6.76 (d, *J* = 8.9 Hz, 2H), 2.99 (s, 6H). MS: m/z calculated for $C_{20}H_{20}N_3O$ 318.16; found 318.17, M + H^+.

(2*E*,4*E*)-5-(4-(Dimethylamino)phenyl)-*N*-(quinolin-2-yl)penta-2,4-dienamide (1c)

The same method described above for compound **1a** was used, and compound **1c** was obtained as yellow solid (92 mg, 13.4%). ^{1}H NMR (400 MHz, DMSO-d_6) δ 10.93 (s, 1H), 8.46 (d, *J* = 9.0 Hz, 1H), 8.35 (d, *J* = 9.0 Hz, 1H), 7.91 (d, *J* = 7.9 Hz, 1H), 7.81 (d, *J* = 8.4 Hz, 1H), 7.75 – 7.66 (m, 1H), 7.52

– 7.37 (m, 4H), 6.97 (d, *J* = 15.4 Hz, 1H), 6.85 (dd, *J* = 15.3, 11.0 Hz, 1H), 6.71 (d, *J* = 8.9 Hz, 2H), 6.44 (d, *J* = 14.8 Hz, 1H), 2.96 (s, 6H). MS: m/z calculated for $C_{22}H_{22}N_3O$ 344.14; found 344.00, M + H^+.

4-(Dimethylamino)-*N*-(isoquinolin-3-yl)benzamide (3a)

The same method described above for compound **1a** was used, and compound **3a** was obtained as light grey solid (200 mg, 68.7%). ^{1}H NMR (400 MHz, DMSO-d_6) δ 10.43 (s, 1H), 9.19 (s, 1H), 8.62 (s, 1H), 8.07 (d, J = 8.2 Hz, 1H), 8.03 – 7.97 (m, 2H), 7.92 (d, J = 8.1 Hz, 1H), 7.72 (ddd, J = 8.1, 6.9, 1.0 Hz, 1H), 7.59 – 7.48 (m, 1H), 6.76 (d, J = 9.0 Hz, 2H), 3.01 (s, 6H). MS: m/z calculated for $C_{18}H_{18}N_3O$ 292.14; found 292.33, M + H^+.

(*E*)-3-(4-(Dimethylamino)phenyl)-*N*-(isoquinolin-3-yl)acrylamide (3b)

The same method described above for compound **1a** was used, and compound **3b** was obtained as yellow solid (65 mg, 20.5%). ^{1}H NMR (600 MHz, $CDCl_3$)) δ 8.99 (s, 1H), 8.73 (s, 1H), 8.31 (s, 1H), 7.87 (dd, *J* = 25.0, 8.3 Hz, 2H), 7.75 (d, *J* = 15.4 Hz, 1H), 7.65 (t, *J* = 7.6 Hz, 1H), 7.48 (dt, *J* = 7.9, 3.0 Hz, 3H), 6.70 (d, *J* = 8.8 Hz, 2H), 6.40 (d, *J* = 15.3 Hz, 1H), 3.03 (s, 6H). MS: m/z calculated for $C_{20}H_{20}N_3O$ 318.16; found 318.08, M + H^+.

(2*E*,4*E*)-5-(4-(Dimethylamino)phenyl)-*N*-(isoquinolin-3-yl)penta-2,4-dienamide (3c)

The same method described above for compound **1a** was used, compound **3c** was obtained as yellow solid (208 mg, 60.6%). ^{1}H NMR (400 MHz, $CDCl_3$) δ 8.98 (s, 1H), 8.75 (s, 1H), 8.49 (s, 1H), 7.89 (dd, *J* = 20.1, 8.0 Hz, 2H), 7.68 (ddd, *J* = 8.2, 6.8, 1.2 Hz, 1H), 7.60 (dd, *J* = 14.6, 11.0 Hz, 1H), 7.53 – 7.49 (m, 1H), 7.39 (dd, *J* = 9.3, 2.4 Hz, 2H), 6.91 (d, *J* = 15.4 Hz, 1H), 6.82 – 6.68 (m, 3H), 6.09 (d, *J* = 14.7 Hz, 1H), 3.02 (s, 6H). MS: m/z calculated for $C_{22}H_{22}N_3O$ 344.14; found 344.33, M + H^+.

4-(Dimethylamino)-*N*-(isoquinolin-1-yl)benzamide (5a)

The same method described above for compound **1a** was used, and compound **5a** was obtained as yellow solid (135 mg, 46.3%). ^{1}H NMR (400 MHz, DMSO-d_6) δ 10.54 (s, 1H), 8.37 (d, J = 5.7 Hz, 1H), 8.02 – 7.90 (m, 4H), 7.77 (t, J = 6.5 Hz, 2H), 7.62 (t, J = 7.6 Hz, 1H), 6.79 (d, J = 9.0 Hz, 2H), 3.02 (s, 6H). MS: m/z calculated for $C_{18}H_{18}N_3O$ 292.14; found 292.25, M + H^+.

(*E*)-3-(4-(Dimethylamino)phenyl)-*N*-(isoquinolin-1-yl)acrylamide (5b)

The same method described above for compound **1a** was used, compound **5b** was obtained as yellow solid (100 mg, 31.5%). ^{1}H NMR (400 MHz, DMSO-d_6) δ 10.49 (s, 1H), 8.32 (d, J = 5.6 Hz, 1H), 7.99 (dd, J = 13.5, 8.3 Hz, 2H), 7.72 (tt, J = 15.2, 10.1 Hz, 4H), 7.51 (dd, J = 26.6, 12.1 Hz, 3H), 6.76 (d, J = 8.9 Hz, 2H), 2.98 (s, 6H). MS: m/z calculated for $C_{20}H_{20}N_3O$ 318.16; found 318.17, M + H^+.

(2*E*,4*E*)-5-(4-(Dimethylamino)phenyl)-*N*-(isoquinolin-1-yl)penta-2,4-dienamide (5c)

The same method described above for compound **1a** was used, and compound **5c** was obtained as yellow solid (75 mg, 21.8%). ^{1}H NMR (400 MHz, DMSO-d_6) δ 10.54 (s, 1H), 8.33 (d, J = 5.7 Hz, 1H), 8.03 – 7.95 (m, 2H), 7.80 – 7.59 (m, 3H), 7.44 (d, J = 8.8 Hz, 3H), 7.00 – 6.82 (m, 2H), 6.71 (d, J = 9.0 Hz, 2H), 6.43 (d, J = 14.9 Hz, 1H), 2.96 (s, 6H). MS: m/z calculated for $C_{22}H_{22}N_3O$ 344.14; found 344.17, M + H^+.

4-(1,1-Difluoro-1H-1l4,11l4-[1,3,5,2]oxadiazaborinino[3,4-a]quinolin-3-yl)-*N*,*N*-dimethylaniline (2a)

A solution of compound **1a** (100 mg, 0.34 mmol) and an appropriate amount of triethylamine in CH_2Cl_2 was stirred at room temperature, BF_3·Et_2O (1 mL, 4 mmol) was added dropwise for 0.5 h, the reaction mixture was washed with water and the organic phase was dried over anhydrous $MgSO_4$. After the solvents were concentrated under reduced pressure, the crude product was purified by flash column chromatography (petroleum ether/ethyl acetate = 3 : 1, v/v). Compound **2a** was obtained as yellow

solid (40 mg, 34.4%). ^{1}H NMR (400 MHz, $CDCl_3$) δ 8.57 (d, *J* = 9.0 Hz, 1H), 8.30 (d, *J* = 9.0 Hz, 2H), 8.24 (d, *J* = 8.9 Hz, 1H), 7.84 – 7.72 (m, 2H), 7.54 (t, *J* = 7.5 Hz, 1H), 7.38 (d, *J* = 8.9 Hz, 1H), 6.71 (d, *J* = 9.0 Hz, 2H), 3.11 (s, 6H). ^{13}C NMR (150 MHz, $CDCl_3$) δ 167.08, 156.71, 154.18, 142.83, 138.40, 132.23, 132.05, 128.30, 126.22, 125.79, 122.61, 122.43, 118.09, 110.94, 40.09. HRMS: m/z calculated for $C_{18}H_{17}BF_2N_3O$ 340.1433; found 340.1423, M + H^+.

(*E*)-4-(2-(1,1-Difluoro-1H-1l4,11l4-[1,3,5,2]oxadiazaborinino[3,4-a]quinolin-3-yl)vinyl)-*N*,*N*-dimethylaniline (2b)

The same method described above for compound **2a** was used, and compound **2b** was obtained as red solid (20 mg, 17.4%).^{1}H NMR (400 MHz, $CDCl_3$) δ 8.58 (d, *J* = 9.1 Hz, 1H), 8.33 (d, *J* = 8.8 Hz, 1H), 8.10 (d, *J* = 15.4 Hz, 1H), 7.92 – 7.73 (m, 2H), 7.60 (dd, *J* = 12.2, 8.2 Hz, 4H), 6.72 (d, *J* = 8.6 Hz, 3H), 3.09 (s, 6H). ^{13}C NMR (150 MHz, $CDCl_3$) δ 167.92, 156.27, 152.37, 147.62, 143.30, 138.40, 133.76, 132.34, 130.87, 128.50, 126.58, 125.95, 122.70, 122.52, 121.75, 111.93, 40.14. HRMS: m/z calculated for $C_{20}H_{19}BF_2N_3O$ 366.1589; found 366.1580, M + H^+.

4-((1*E*,3*E*)-4-(1,1-Difluoro-1H-1l4,11l4-[1,3,5,2]oxadiazaborinino[3,4-a]quinolin-3-yl)buta-1,3-dien-1-yl)-*N*,*N*-dimethylaniline (2c)

The same method described above for compound **2a** was used, and compound **2c** was obtained as black solid (52 mg, 57.0%).^{1}H NMR NMR (600 MHz, DMSO-d_6) δ 8.76 (d, *J* = 8.8 Hz, 1H), 8.38 (d, *J* = 8.5 Hz, 1H), 8.20 – 8.12 (m, 1H), 7.97 (ddd, *J* = 8.7, 7.0, 1.5 Hz, 1H), 7.81 (dd, *J* = 14.9, 11.3 Hz, 1H), 7.74 (t, *J* = 7.5 Hz, 1H), 7.55 – 7.46 (m, 3H), 7.22 (d, *J* = 15.3 Hz, 1H), 7.08 (dd, *J* = 15.2, 11.1 Hz, 1H), 6.77 (d, *J* = 9.0 Hz, 2H), 6.30 (d, *J* = 14.9 Hz, 1H), 3.03 (s, 6H). ^{13}C NMR (150 MHz, CF_3COOD) δ 159.82, 149.85, 141.27, 140.44, 137.33, 135.44, 130.57, 130.40, 128.21, 123.20, 122.34, 122.02, 120.63, 120.53, 114.79, 113.00, 106.92, 104.89, 39.60. HRMS: m/z calculated for

$C_{22}H_{21}BF_2N_3O$ 392.1746; found 392.1738, M + H^+.

4-(1,1-Difluoro-1H-1l4,11l4-[1,3,5,2]oxadiazaborinino[3,4-b]isoquinolin-3-yl)-*N*,*N*-dimethylaniline (4a)

The same method described above for compound **2a** was used, and compound **4a** was obtained as yellow solid (80 mg, 57.3%).^{1}H NMR (600 MHz, $CDCl_3$) δ 8.99 (s, 1H), 8.80 (s, 1H), 7.93 – 7.90 (m, 3H), 7.86 (d, *J* = 8.4 Hz, 1H), 7.72 – 7.62 (m, 1H), 7.49 (ddd, *J* = 8.0, 6.9, 0.9 Hz, 1H), 6.75 (d, *J* = 9.0 Hz, 2H), 3.07 (s, 6H). ^{13}C NMR (100 MHz, $CDCl_3$) δ 163.12, 153.41, 148.24, 143.20, 140.85, 134.28, 131.15, 129.18, 127.53, 126.60, 124.95, 119.31, 117.22, 110.95, 40.11. HRMS: m/z calculated for $C_{18}H_{17}BF_2N_3O$ 340.1433; found 340.1426, M + H^+.

(*E*)-4-(2-(1,1-Difluoro-1H-1l4,11l4-[1,3,5,2]oxadiazaborinino[3,4-b]isoquinolin-3-yl)vinyl)-*N*,*N*-dimethylaniline (4b)

The same method described above for compound **2a** was used, and compound **4b** was obtained as orange solid (8 mg, 13.9%).^{1}H NMR (400 MHz, $CDCl_3$) δ 9.17 (s, 1H), 8.08 (d, *J* = 8.4 Hz, 1H), 7.97 – 7.83 (m, 4H), 7.69 – 7.61 (m, 1H), 7.54 (d, *J* = 8.8 Hz, 2H), 6.71 (d, *J* = 8.8 Hz, 13), 3.06 (s, 6H). ^{13}C NMR (150 MHz, $CDCl_3$) δ 164.11, 151.99, 143.60, 143.49, 140.73, 134.66, 130.37, 129.82, 129.30, 128.05, 127.60, 126.85, 125.23, 122.91, 117.03, 111. 98, 40.19. HRMS: m/z calculated for $C_{20}H_{19}BF_2N_3O$ 366.1589; found 366.1581, M + H^+.

4-((1*E*,3*E*)-4-(1,1-Difluoro-1H-1l4,11l4-[1,3,5,2]oxadiazaborinino[3,4-b]isoquinolin-3-yl)buta-1,3-dien-1-yl)-*N*,*N*-dimethylaniline (4c)

The same method described above for compound **2a** was used, and compound **4c** was obtained as red solid (53 mg, 27.4%).^{1}H NMR (400 MHz, $CDCl_3$) δ 9.17 (s, 1H), 8.09 (d, *J* = 8.4 Hz, 1H), 8.04 – 7.85 (m, 3H), 7.84 – 7.73 (m, 1H), 7.67 (t, *J* = 7.6 Hz, 1H), 7.43 (d, *J* = 8.8 Hz, 2H), 7.00 – 6.82 (m, 2H),

6.74 (d, *J* = 7.3 Hz, 2H), 6.37 (d, *J* = 13.9 Hz, 1H), 3.04 (s, 6H). ^{13}C NMR (150 MHz, CF_3DCOOD) δ 166.71, 155.14, 146.58, 146.36, 142.56, 140.01, 138.20, 137.99, 135.42, 131.34, 130.40, 130.04, 127.97, 127.11, 127.02, 120.32, 112.78, 47.00. HRMS: m/z calculated for $C_{22}H_{21}BF_2N_3O$ 392.1746; found 392.1737, M + H^+

4-(4,4-Difluoro-4H-4l4,5l4-[1,3,5,2]oxadiazaborinino[4,3-a]isoquinolin-2-yl)-*N*,*N*-dimethylaniline (6a)

The same method described above for compound **2a** was used, and compound **6a** was obtained as yellow solid (30 mg, 25.8%).^{1}H NMR (400 MHz, $CDCl_3$) δ 9.08 (d, *J* = 8.4 Hz, 1H), 8.47 – 8.37 (m, 2H), 8.01 (d, *J* = 6.5 Hz, 1H), 7.89 (ddd, *J* = 8.1, 7.0, 1.2 Hz, 1H), 7.84 – 7.72 (m, 2H), 7.46 (d, *J* = 6.8 Hz, 1H), 6.80 (d, *J* = 9.1 Hz, 2H), 3.13 (s, 6H). ^{13}C NMR (150 MHz, $CDCl_3$) δ 167.35, 155.06, 153.95, 137.94, 133.86, 132.28, 129.81, 128.47, 128.08, 126.37, 124.92, 119.25, 117.11, 111.14, 40.25. HRMS: m/z calculated for $C_{18}H_{17}BF_2N_3O$ 340.1433; found 340.1426, M + H^+.

(*E*)-4-(2-(4,4-Difluoro-4H-4l4,5l4-[1,3,5,2]oxadiazaborinino[4,3-a]isoquinolin-2-yl)vinyl)-*N*,*N*-dimethylaniline (6b)

The same method described above for compound **2a** was used, and compound **6b** was obtained as red solid (61mg, 21.7%).^{1}H NMR (600 MHz, $CDCl_3$) δ 9.01 (d, *J* = 8.3 Hz, 1H), 8.07 (d, *J* = 15.6 Hz, 1H), 8.02 (d, *J* = 6.5 Hz, 1H), 7.90 (ddd, *J* = 8.2, 7.0, 1.2 Hz, 1H), 7.82 (d, *J* = 8.0 Hz, 1H), 7.76 (ddd, *J* = 8.2, 7.0, 1.1 Hz, 1H), 7.59 (d, *J* = 8.8 Hz, 1H), 7.51 (d, *J* = 6.8 Hz, 2H), 6.83 (s, 2H), 6.73 (d, *J* = 15.6 Hz, 1H), 3.08 (s, 6H). ^{13}C NMR (150 MHz, $CDCl_3$) δ 168.29, 154.94, 151.87, 146.84, 138.00, 134.01, 130.64, 130.51, 129.88, 128.68, 128.02, 126.40, 124.71, 117.70, 116.16, 112.23, 40.36. HRMS: m/z calculated for $C_{20}H_{19}BF_2N_3O$ 366.1589; found 366.1581, M + H^+.

4-((1*E*,3*E*)-4-(4,4-Difluoro-4H-4l4,5l4-[1,3,5,2]oxadiazaborinino[4,3-a]isoquinolin-2-yl)buta-

1,3-dien-1-yl)-*N*,*N*-dimethylaniline (6c)

The same method described above for compound **2a** was used, and compound **6c** was obtained as black solid (25 mg, 30.9%).^{1}H NMR (600 MHz, $CDCl_3$) δ 9.01 (t, *J* = 8.6 Hz, 1H), 8.06 (d, *J* = 6.7 Hz, 1H), 7.96 – 7.90 (m, 2H), 7.86 (d, *J* = 8.0 Hz, 1H), 7.79 (dd, *J* = 11.6, 4.5 Hz, 1H), 7.55 (d, *J* = 6.8 Hz, 1H), 7.49 (t, *J* = 9.5 Hz, 2H), 7.03 (d, *J* = 15.3 Hz, 1H), 7.01 – 6.74 (m, 3H), 6.40 (d, *J* = 14.9 Hz, 1H), 3.09 (s, 6H). ^{13}C NMR (150 MHz, $CDCl_3$) δ 167.95, 154.84, 151.28, 147.78, 143.13, 137.99, 134.05, 129.84, 129.19, 128.71, 128.01, 126.39, 124.72, 124.12, 122.26, 121.86, 117.86, 112.04, 40.19. HRMS: m/z calculated for $C_{22}H_{21}BF_2N_3O$ 392.1746; found 392.1737, M + H^+.

Purity Measurements

The purity of these probes (**2a** - **c**, **4a** - **c**, **6a** - **c**) was determined by High-Performance Liquid Chromatography (Hitachi Primaide, Japan) equipped with a reverse column (Venusil MP C18, 5 μm, 4.6 mm×250 mm, Bonna-Agela Technologies, China). Conditions: acetonitrile/water (85/15, v/v) at a flow rate of 1.0 mL/min.

Table S1. The purity of the probes (**2a** - **c**, **4a** - **c**, **6a** - **c**).

probe	t/min	purity/%	probe	t/min	purity/%	probe	t/min	purity/%
2a	7.387	97.065	**4a**	6.733	98.249	**6a**	8.240	99.748
2b	7.487	99.476	**4b**	6.740	99.358	**6b**	9.513	98.045
2c	9.313	96.719	**4c**	8.047	96.343	**6c**	12.340	98.672

The crystallographic data

Table S2. The crystallographic data of **2c**, **4c** and **6c**.

Probe		**2c**	**4c**	**6c**
Formula sum		C_{22} H_{20} B F_2 N_3 O	C_{22} H_{20} B F_2 N_3 O	C_{22} H_{20} B F_2 N_3 O
Formula weight		391.22	391.22	391.22
Temperature (K)		173.00(10)	172.99(10)	172.99(10)
Crystal system		triclinic	monoclinic	monoclinic
Space group		P-1	$P2_1/c$	$P2_1/n$
Cell length (Å)	a	7.9478(6)	7.3225(2)	7.1528(2)
	b	8.3539(5)	10.1109(4)	10.0789(2)
	c	14.6488(10)	25.0143(10)	26.7494(6)
Cell angle	α	74.878(6)	90	90
	β	76.982(6)	91.451(3)	96.597(2)
	γ	83.501(6)	90	90
Volume ($Å^3$)		913.27(11)	1851.39(12)	1915.66(8)
Z		2	4	4
Density		1.423 g/cm^3	1.404 g/cm^3	1.356 g/cm^3

Spectroscopic Determinations

The ultraviolet spectra, fluorescence spectra, and absolute quantum yields were measured by the previously reported methods.[1]

Table S3. Spectroscopic data for the probes. [a]Emission/Excitation maxima measured in PBS (10% DMSO). [b]Absolute quantum yield measured in CH_2Cl_2. [c]UV absorption maxima measured in CH_2Cl_2. [d]Calculated HOMO−LUMO energy gaps. n.d., not determined.

Probe	λ_{em1} (nm)[a]	λ_{ex1} (nm)[a]	*Φ*/%[b]	λ_{abs} (nm)[c]	ε ($L•mol^{-1}•cm^{-1}$)[c]	Gap (eV)[d]
2a	626	390	94.81	437	43890	5.67
2b	649	420	93.19	486	54400	5.30
2c	726	502	81.58	503	54800	5.02
4a	430	373	n.d.	374	33530	5.97
4b	536	478	0.96	436	50070	5.55
4c	630	425	0.86	454	41340	5.18
6a	561	388	75.27	434	44445	5.76
6b	610	482	72.81	480	43310	5.36
6c	710	516	73.81	498	54777	5.05

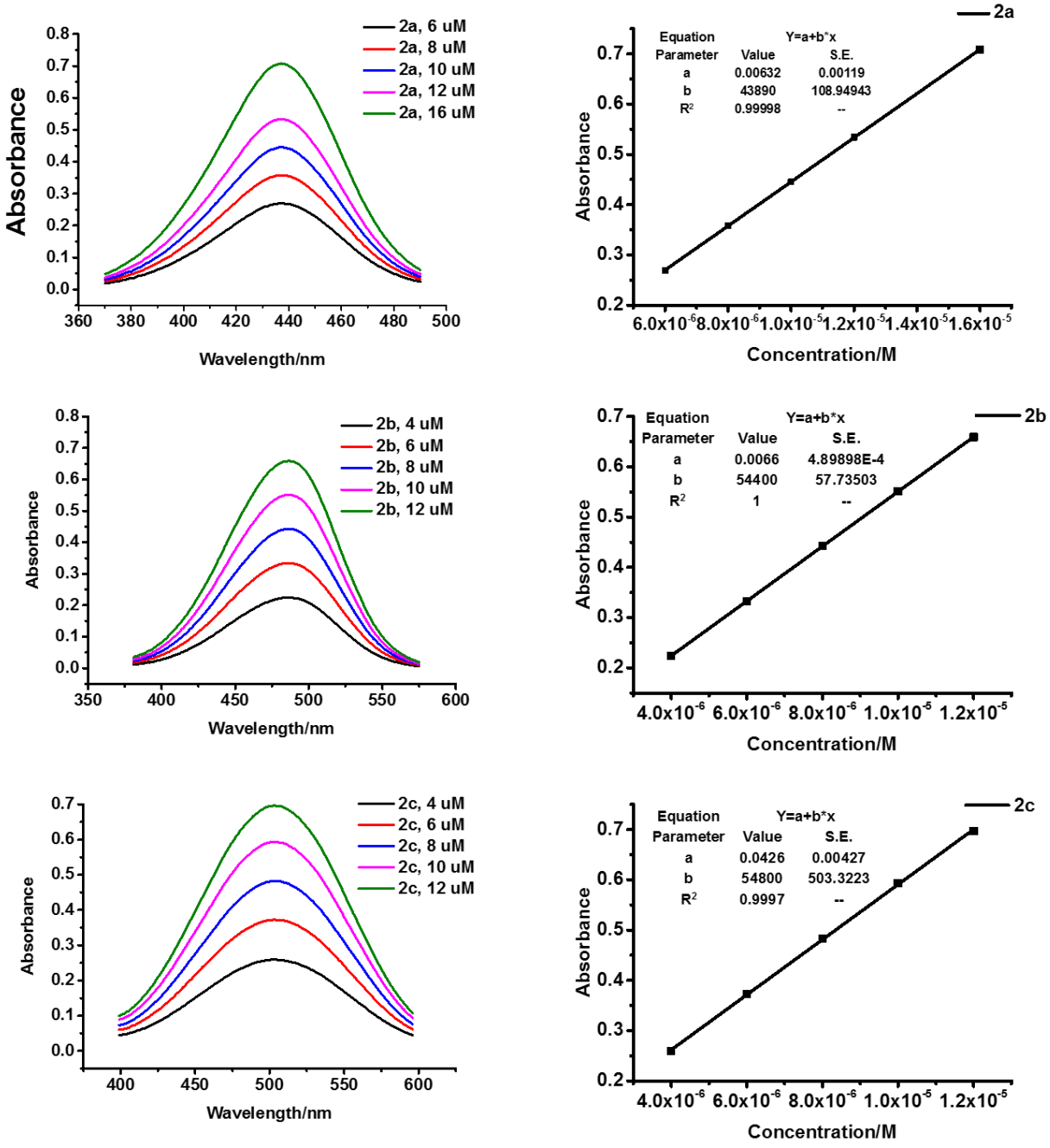

Figure S1. Absorption spectra (left) and linear fitting curve between absorbance and concentration (right) of **2a - c** in CH_2Cl_2, molar absorption coefficients (ε) equals to parameter b.

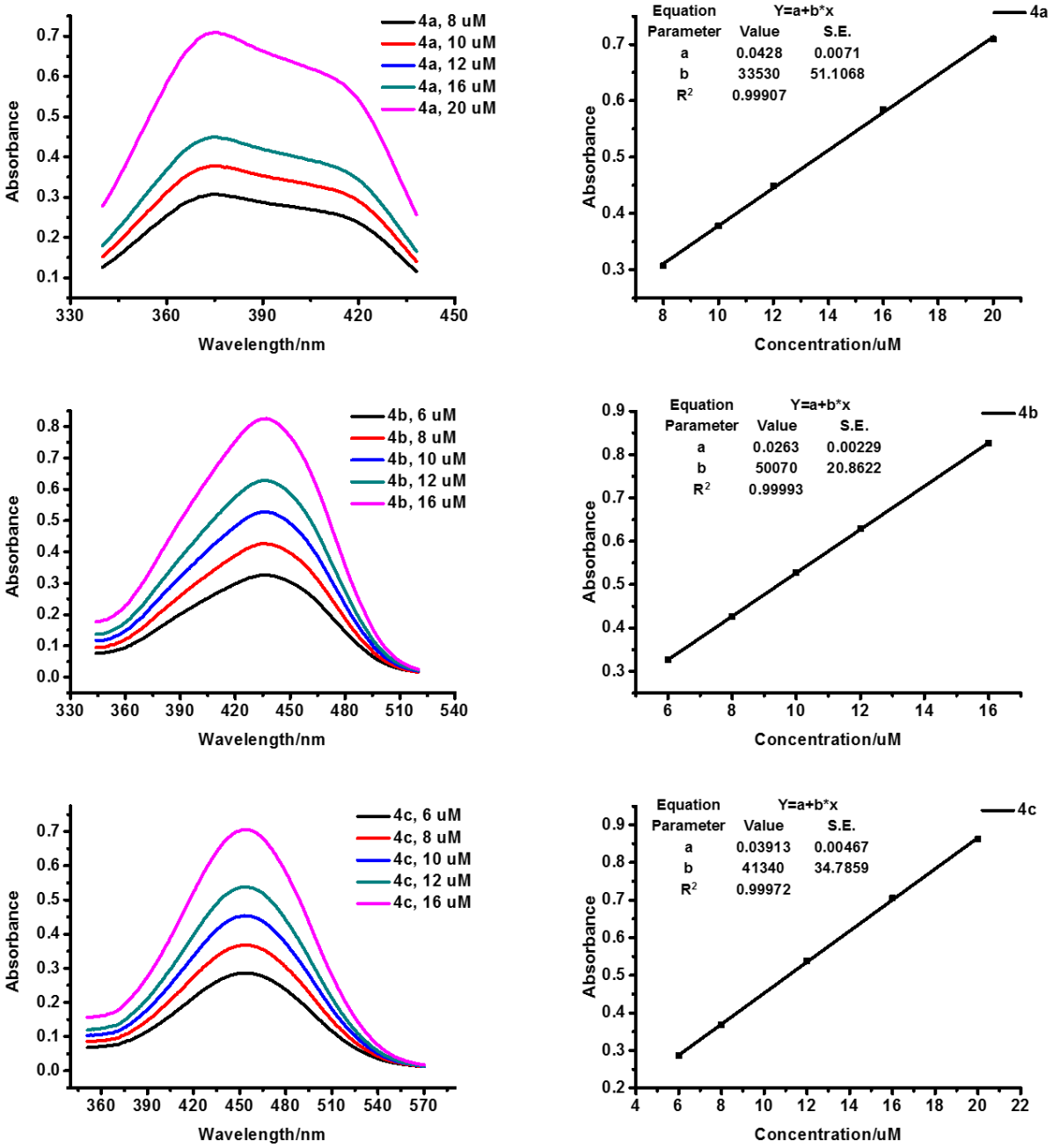

Figure S2. Absorption spectra (left) and linear fitting curve between absorbance and concentration (right) of **4a - c** in CH_2Cl_2, molar absorption coefficients (ε) equals to parameter b.

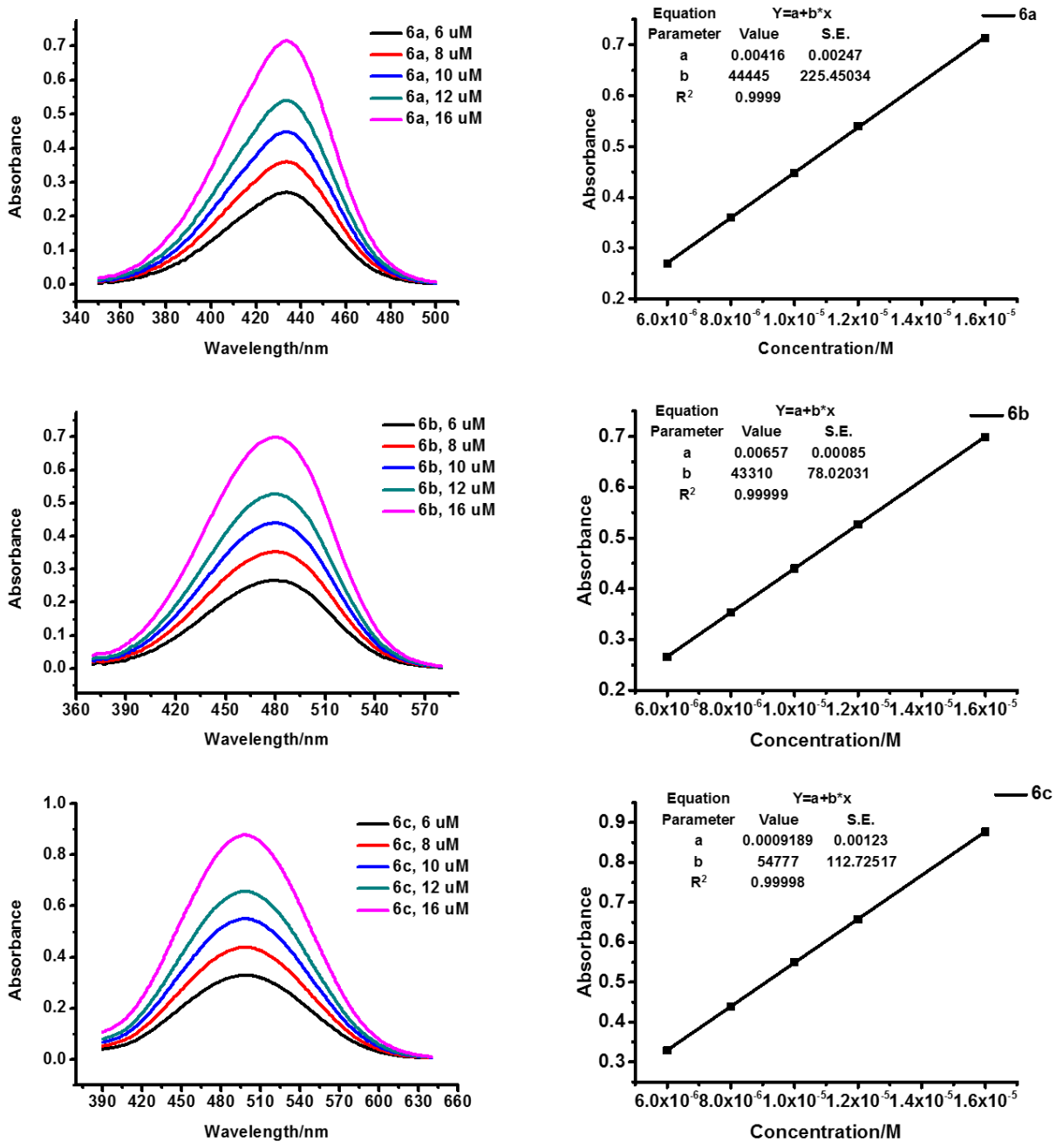

Figure S3. Absorption spectra (left) and linear fitting curve between absorbance and concentration (right) of **6a - c** in CH_2Cl_2, molar absorption coefficients (ε) equals to parameter b.

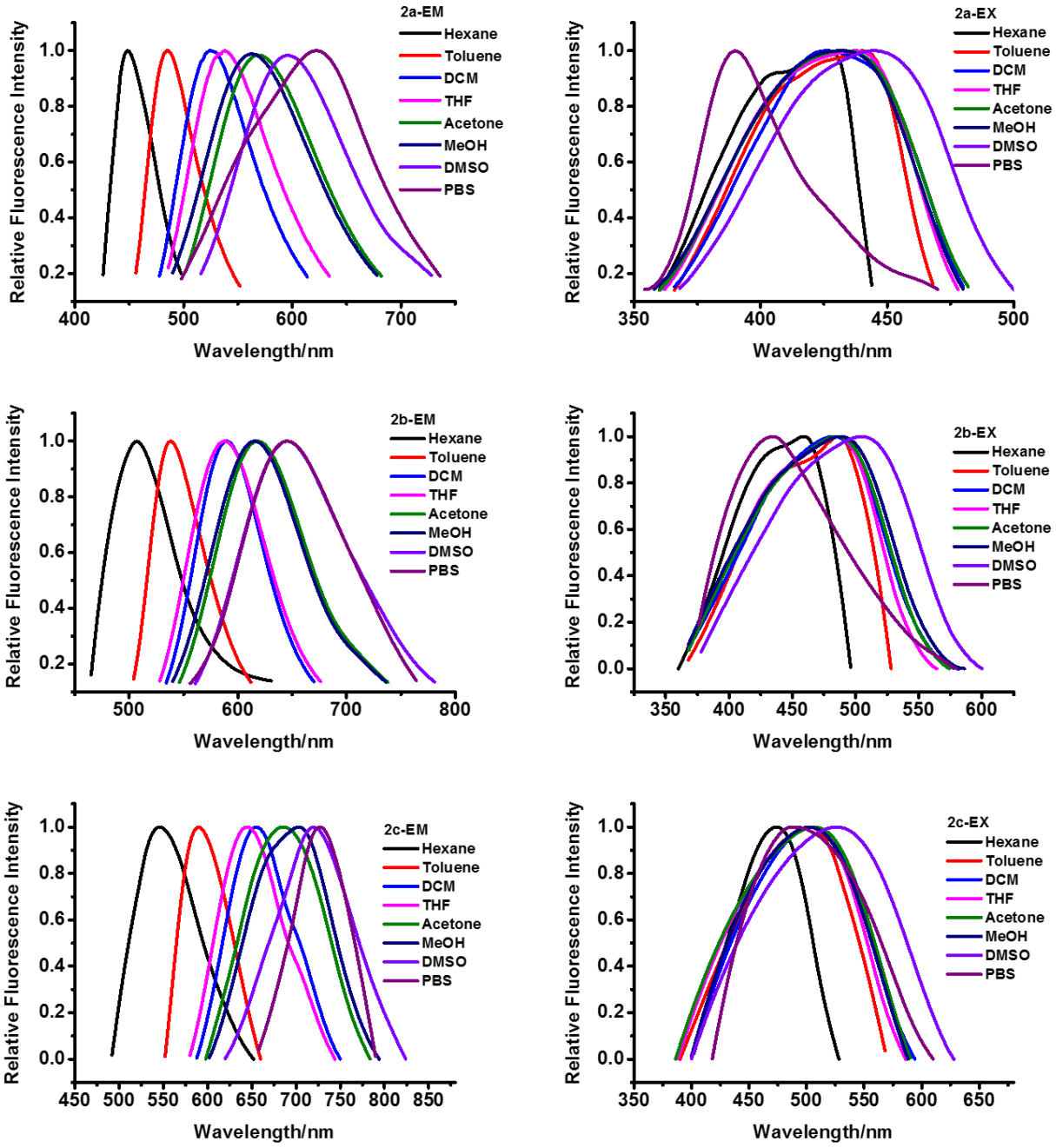

Figure S4. The emission (left) and excitation (right) fluorescence spectra of **2a - c** in solvents with different polarities: Hexane, Toluene, CH_2Cl_2, THF, Acetone, MeOH, DMSO and PBS (10% DMSO).

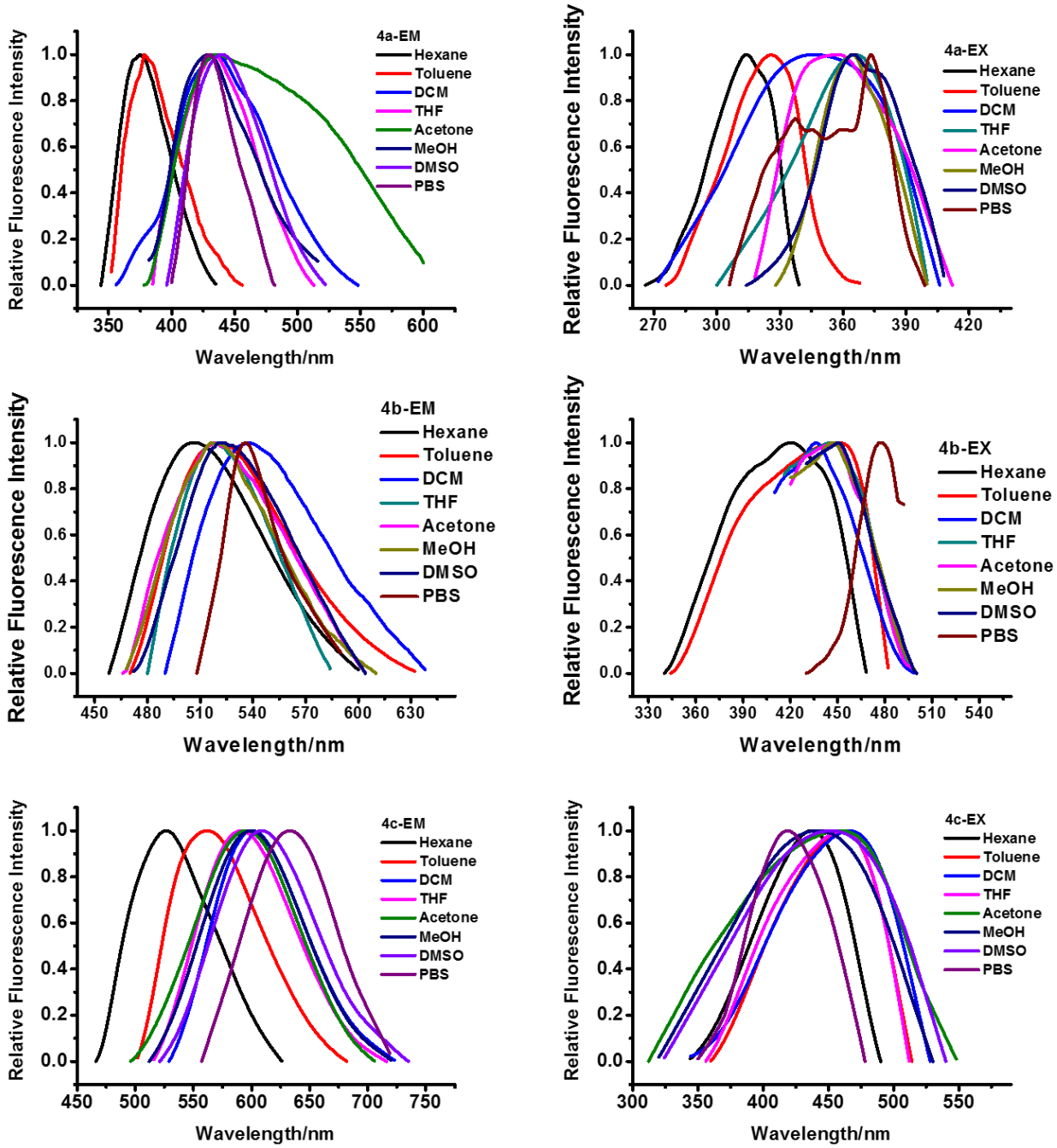

Figure S5. The emission (left) and excitation (right) fluorescence spectra of **4a - c** in solvents with different polarities: Hexane, Toluene, CH_2Cl_2 THF, Acetone, MeOH, DMSO and PBS (10% DMSO).

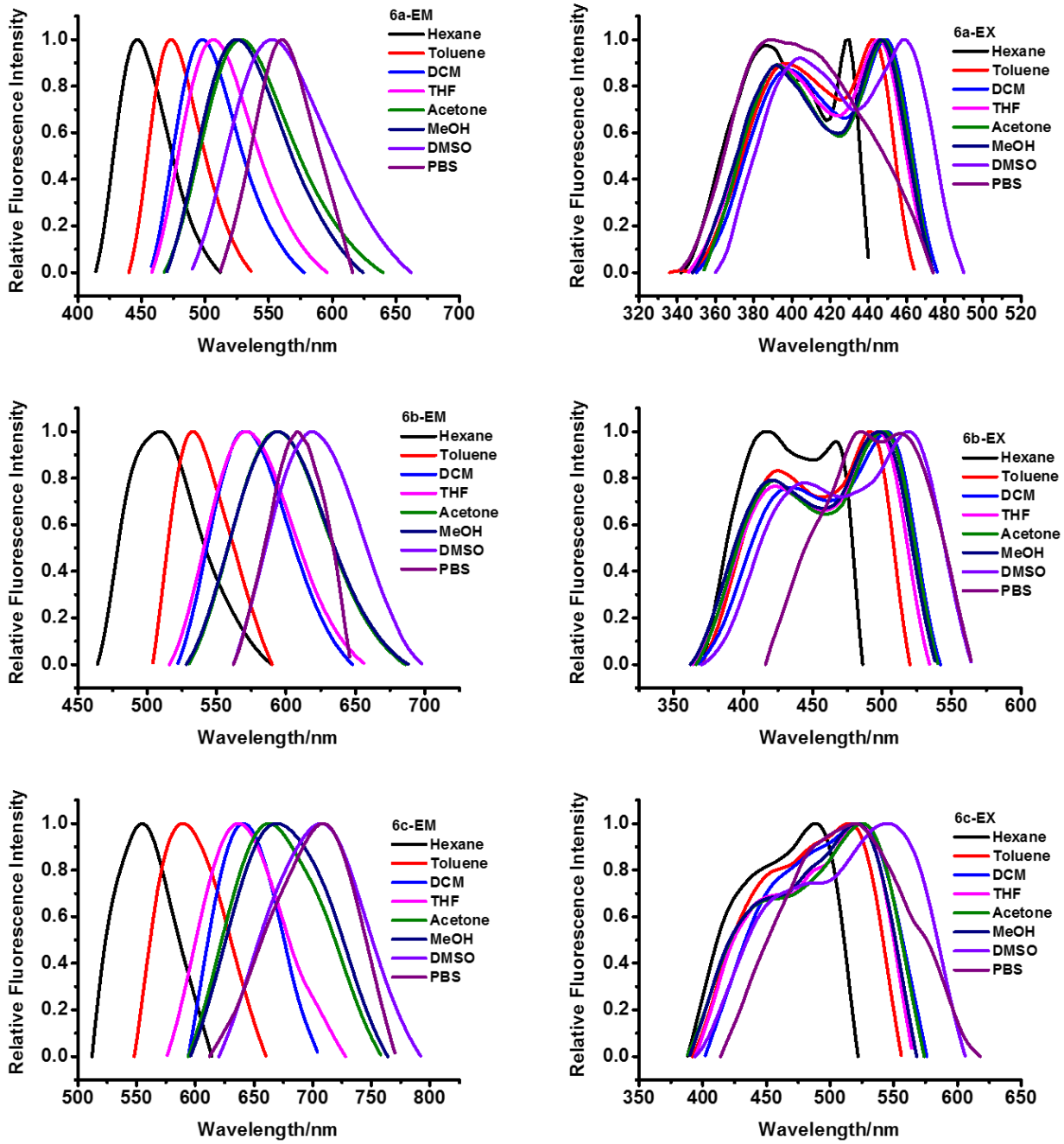

Figure S6. The emission (left) and excitation (right) fluorescence spectra of **6a - c** in solvents with different polarities: Hexane, Toluene, CH_2Cl_2 THF, Acetone, MeOH, DMSO and PBS (10% DMSO).

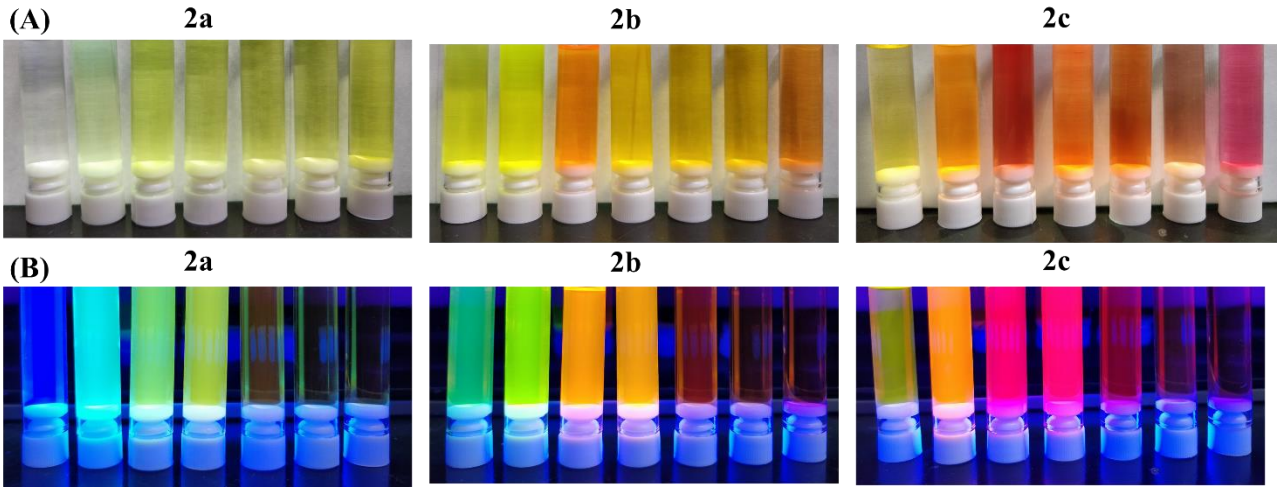

Figure S7. The color of the probes (**2a**, **2b**, **2c**) under natural light (A) and UV (365 nm) light (B) in solvents with different polarities: Hexane, Toluene, CH_2Cl_2, THF, Acetone, MeOH, DMSO.

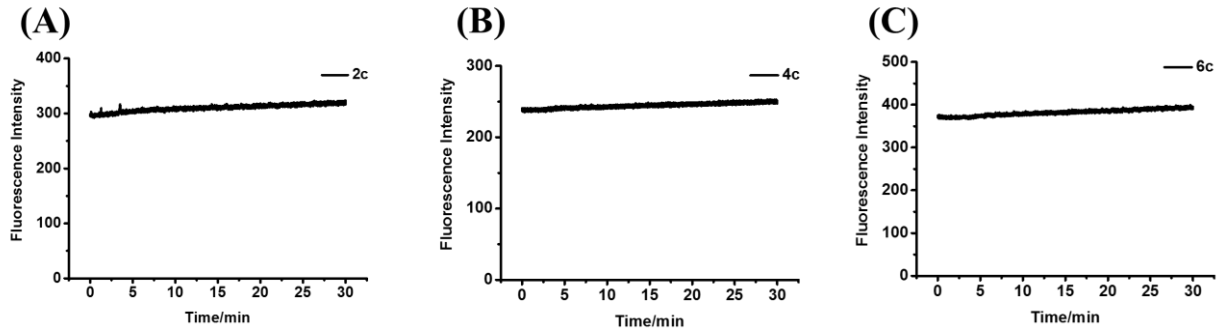

Figure S8. Photobleaching curves of **2c** (A), **4c** (B), and **6c** (C) in CH_2Cl_2 (20 μM).

DFT Calculations

Geometry structures of these probes were optimized by using the density functional method CAM-B3LYP with def2-SVP basis set. Also, def2-TZVP basis set was employed for further single point calculations to elucidate the frontier molecular orbitals (FMOs) and electronic density distributions of them.[2, 3]

DFT calculations were performed to gain deeper insights into the fluorescent properties of these probes. As shown in Figure S9, it's clear that the electron distribution is subjected to the general rule that the

highest occupied molecular orbitals (HOMO) are principally located on the dimethylaminophenyl group, while the lowest unoccupied molecular orbitals (LUMO) are mainly populated in the quinoline moiety. In general, the frontier molecular orbitals (FMO) of probes are combined by the fragments from the dimethylaminophenyl and quinoline (isoquinoline) parts. Therefore, the conjugation degree of FMO, which affects the emission wavelength, is dictated by if the fragment molecular orbitals from two groups are symmetry adapted. It is worthwhile mentioning that the conjugate π system of **4c** is dramatically different from that of **2c** and **6c**. From Figure 2, one can find that the fragment molecular orbital of the dimethylaminophenyl group cannot symmetrically match the isoquinoline ring in LUMO in **4c**, which results in that its LUMO is only populated on the isoquinoline. However, in **2c** and **6c**, the LUMOs are combined by the symmetry adapted fragments from the dimethylaminophenyl and quinoline/isoquinoline parts. Hence, the degree of conjugation of **2c** and **6c** is increased, which results in decreased HOMO-LUMO gap and longer emission maxima. The calculated energy gaps between the HOMO and the LUMO of these probes are shown in Table 1, which are highly consistent with the experimental absorption and emission maxima. By analyzing the frontier molecular orbitals of **2a - c**, the conjugate π system steadily grows and the energy gaps decrease (from 5.67 to 5.02 eV) in the order of **2a**, **2b** and **2c**, which are in accord with the observed continuous red shift in the emission wavelength (from 626 to 726 nm in PBS) in experiments. Probes **4a - c** and **6a - c** follow the same regular pattern, respectively. Meanwhile, comparing **4c** with **2c** (**6c**), evidently, **4c** (630 nm, in PBS) displayed shorter emission maxima than **2c** (726 nm, in PBS) and **6c** (710 nm, in PBS). As expected, the calculated energy gap (**2c**, 5.02 eV; **4c**, 5.18 eV; **6c**, 5.05 eV) supports it as well.

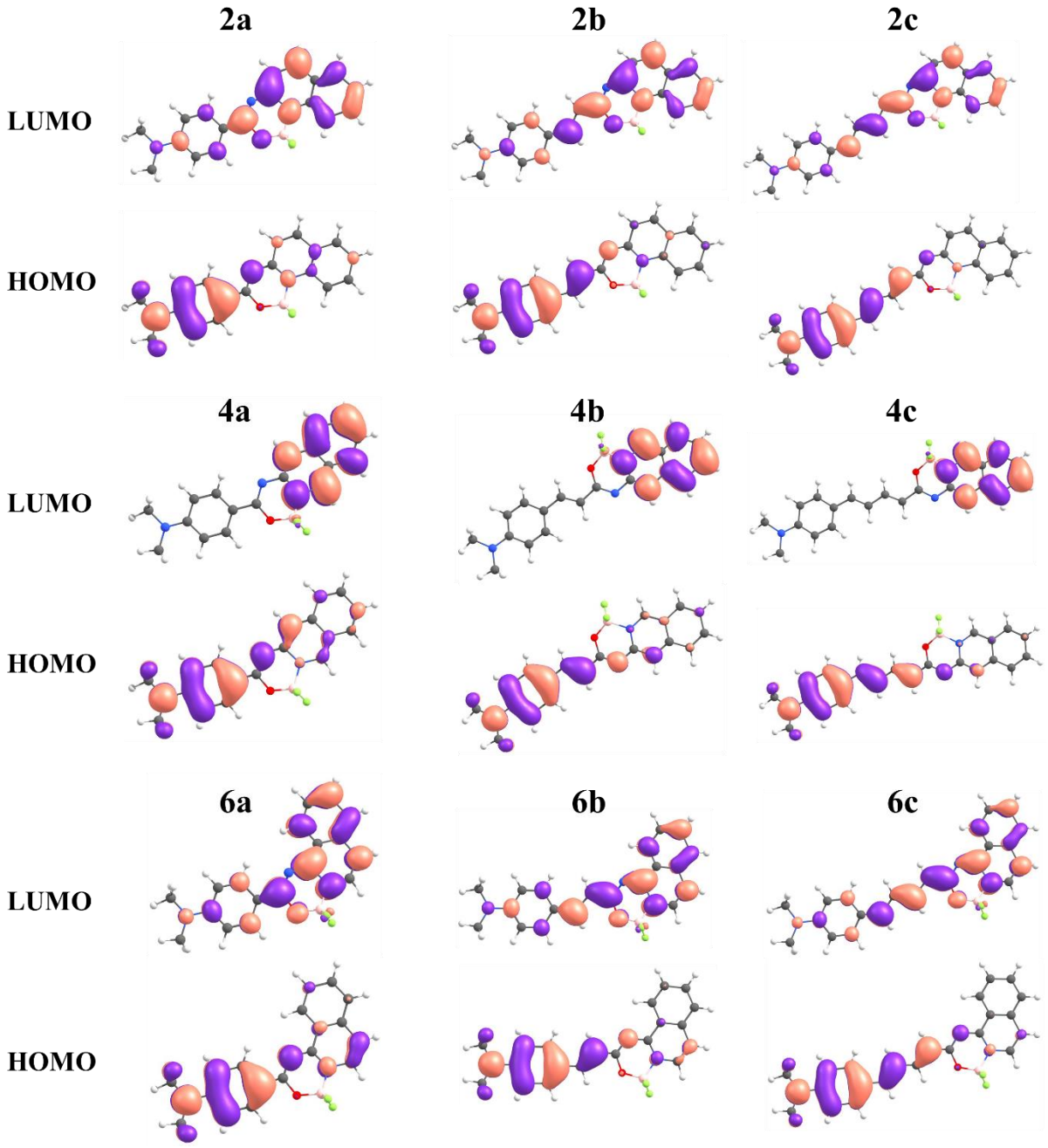

Figure S9. Frontier molecular orbitals of compounds **2a - c**, **4a - c**, **6a - c**.

Fluorescence Enhanced Experiment

The solutions of those probes (**2a - c**, **4a - c**, **6a - c**, 50 nM, final concentration) and A$\beta_{1\text{-}42}$ aggregates (8 μg/mL, final concentration), Tau-K18 aggregates (27 μg/mL, final concentration) or BSA (8 μg/mL, final concentration) in 3 mL PBS (pH = 7.4, 100 μL ethanol) was prepared in borosilicate glass tube

(12×75mm) and them were incubated at 37 ℃ with constant shaking (120 r/min) for 1h. Then, the solutions were measured by a fluorescence spectrophotometer to gain their emission and excitation spectra. The spectra of PBS background and probes (50 nM) in PBS were measured under the same condition.

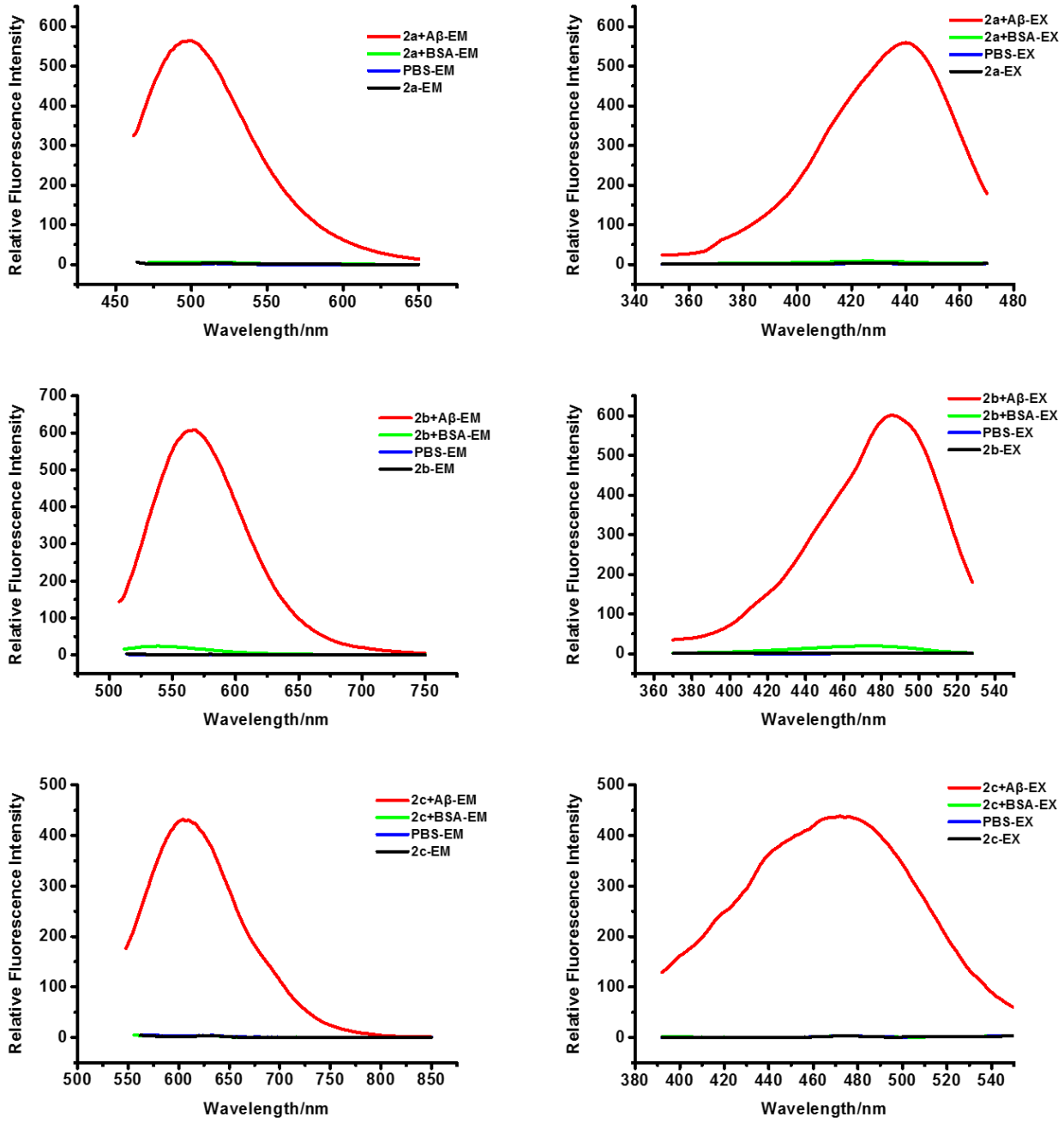

Figure S10. The fluorescence emission (left) and excitation (right) spectra of **2a - c** upon interaction with A$\beta_{1\text{-}42}$ aggregates and BSA.

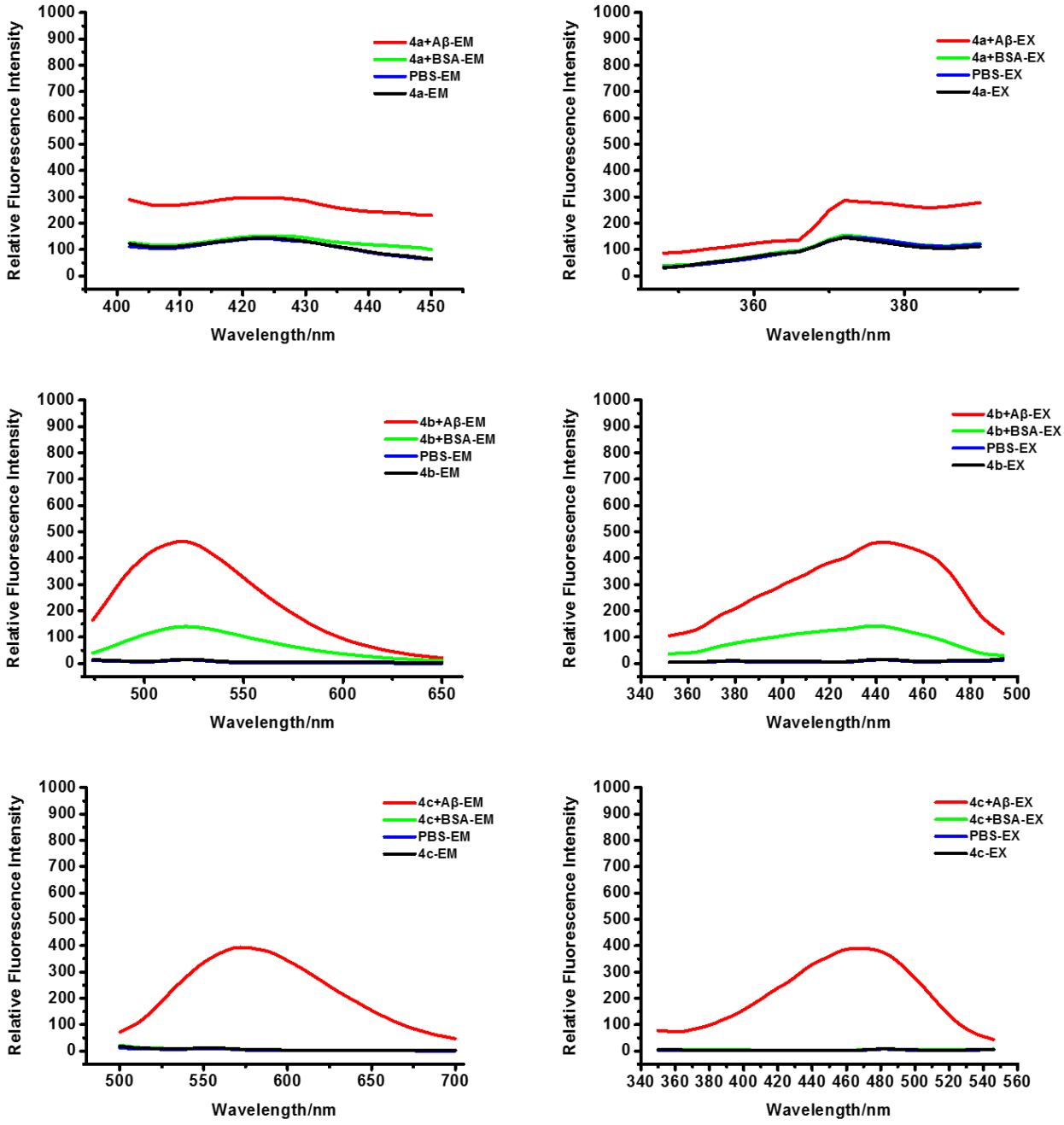

Figure S11. The fluorescence emission (left) and excitation (right) spectra of **4a - c** upon interaction with A$\beta_{1\text{-}42}$ aggregates and BSA.

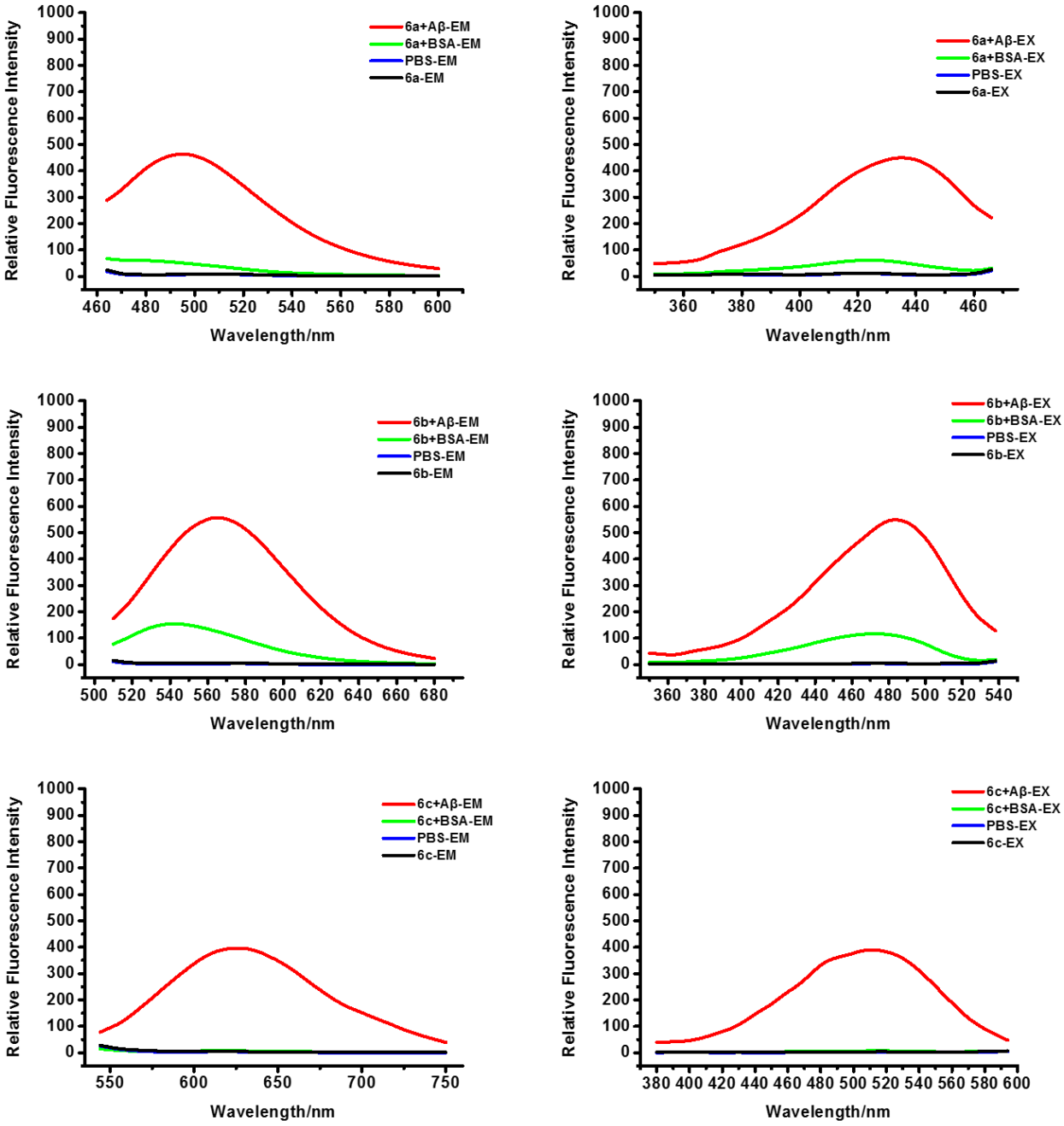

Figure S12. The fluorescence emission (left) and excitation (right) spectra of **6a - c** upon interaction with A$\beta_{1\text{-}42}$ aggregates and BSA.

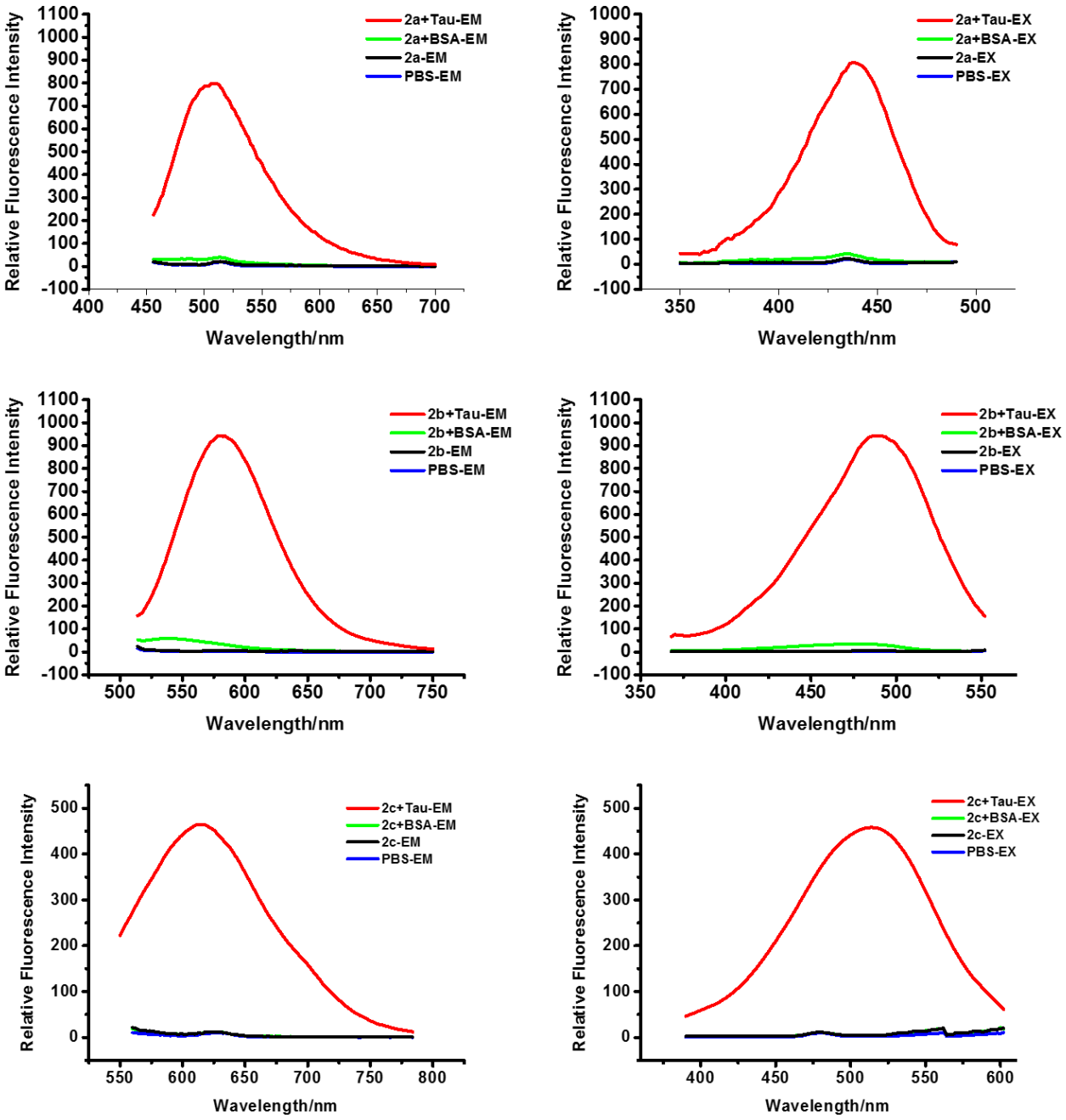

Figure S13. The fluorescence emission (left) and excitation (right) spectra of **2a - c** upon interaction with Tau (k18) aggregates and BSA.

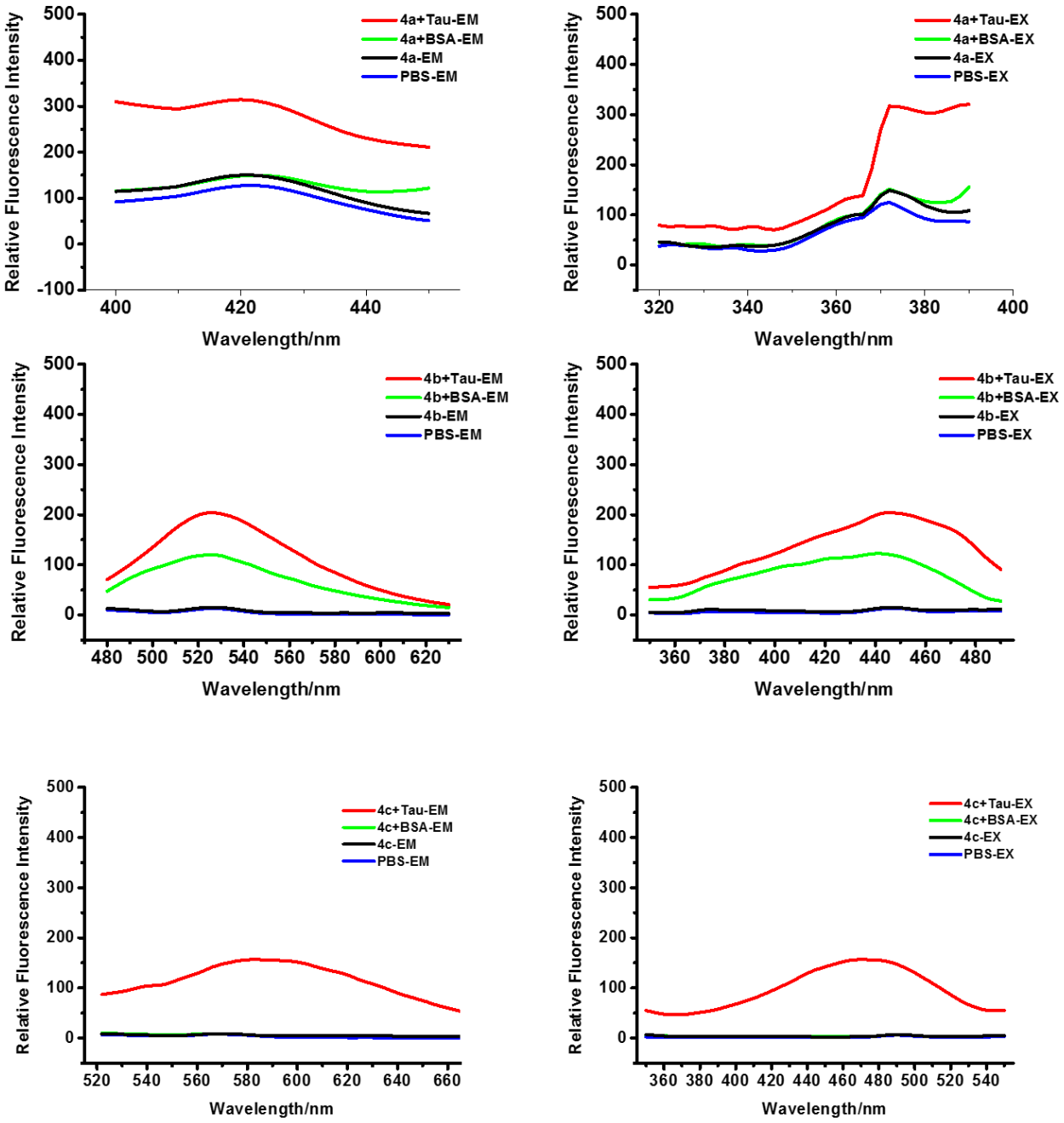

Figure S14. The fluorescence emission (left) and excitation (right) spectra of **4a - c** upon interaction with Tau (k18) aggregates and BSA.

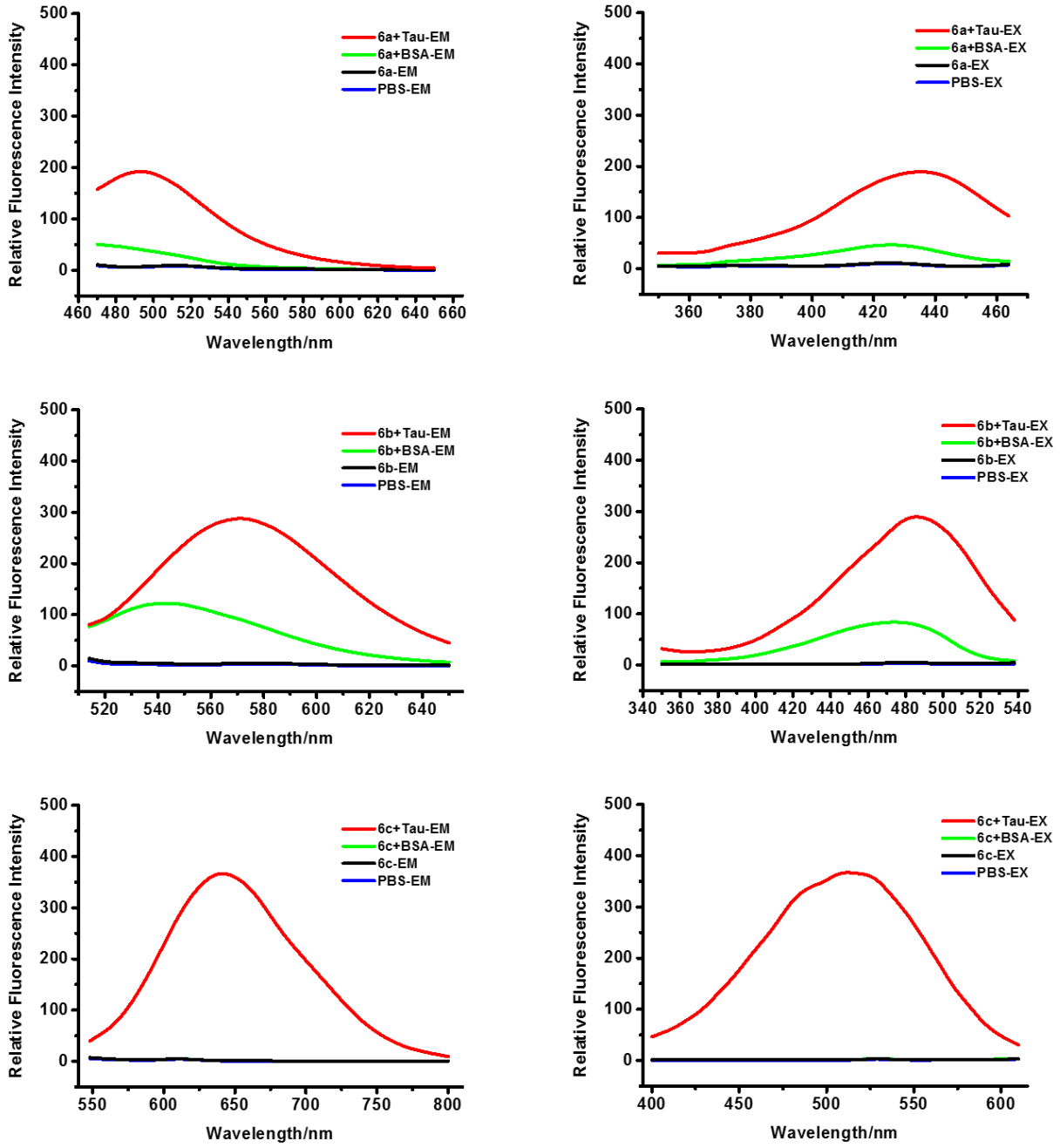

Figure S15. The fluorescence emission (left) and excitation (right) spectra of **6a - c** upon interaction with Tau (k18) aggregates and BSA.

***In Vitro* Saturation Binding Assay**

The solutions of those probes (**2a - c**, **4a - c**, **6a - c**, 1-5000 nM) and A$\beta_{1\text{-}42}$ or Tau (k18) (1 μg/mL, 2 μg/mL) in 1 mL PBS (pH = 7.4, 100 μL ethanol) were incubated at 37 ℃ with constant shaking (120 r/min) for 1 h in borosilicate glass tube (12×75mm). Then, those solutions were transferred to a black 96-well plate and measured by a microplate reader.

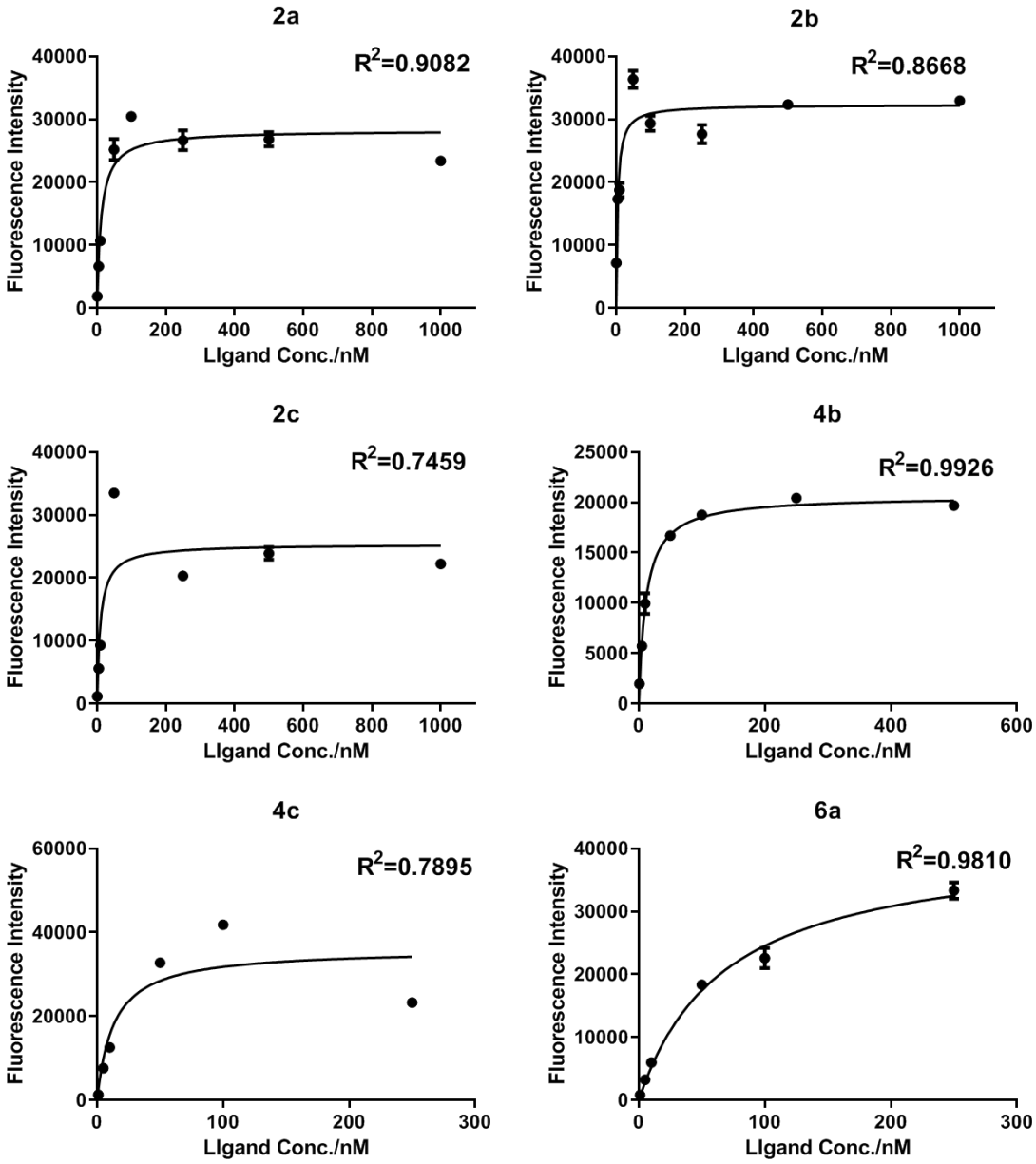

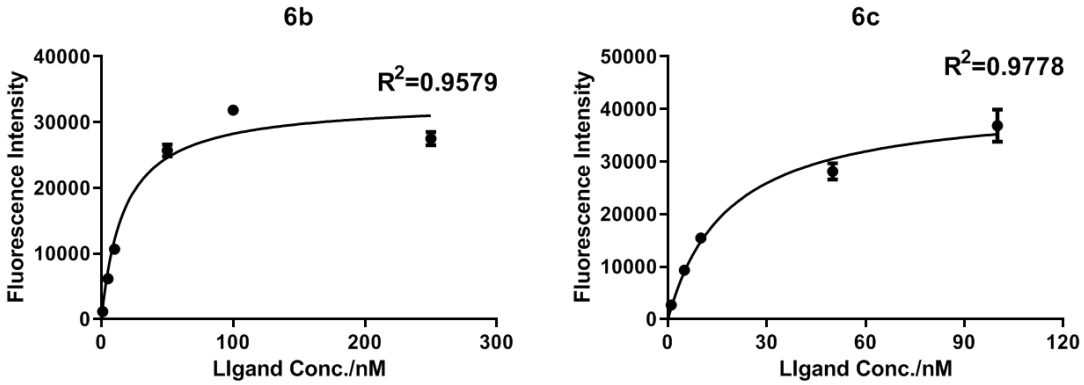

Figure S16. Saturation binding curves for ligands to A$\beta_{1\text{-}42}$ aggregates.

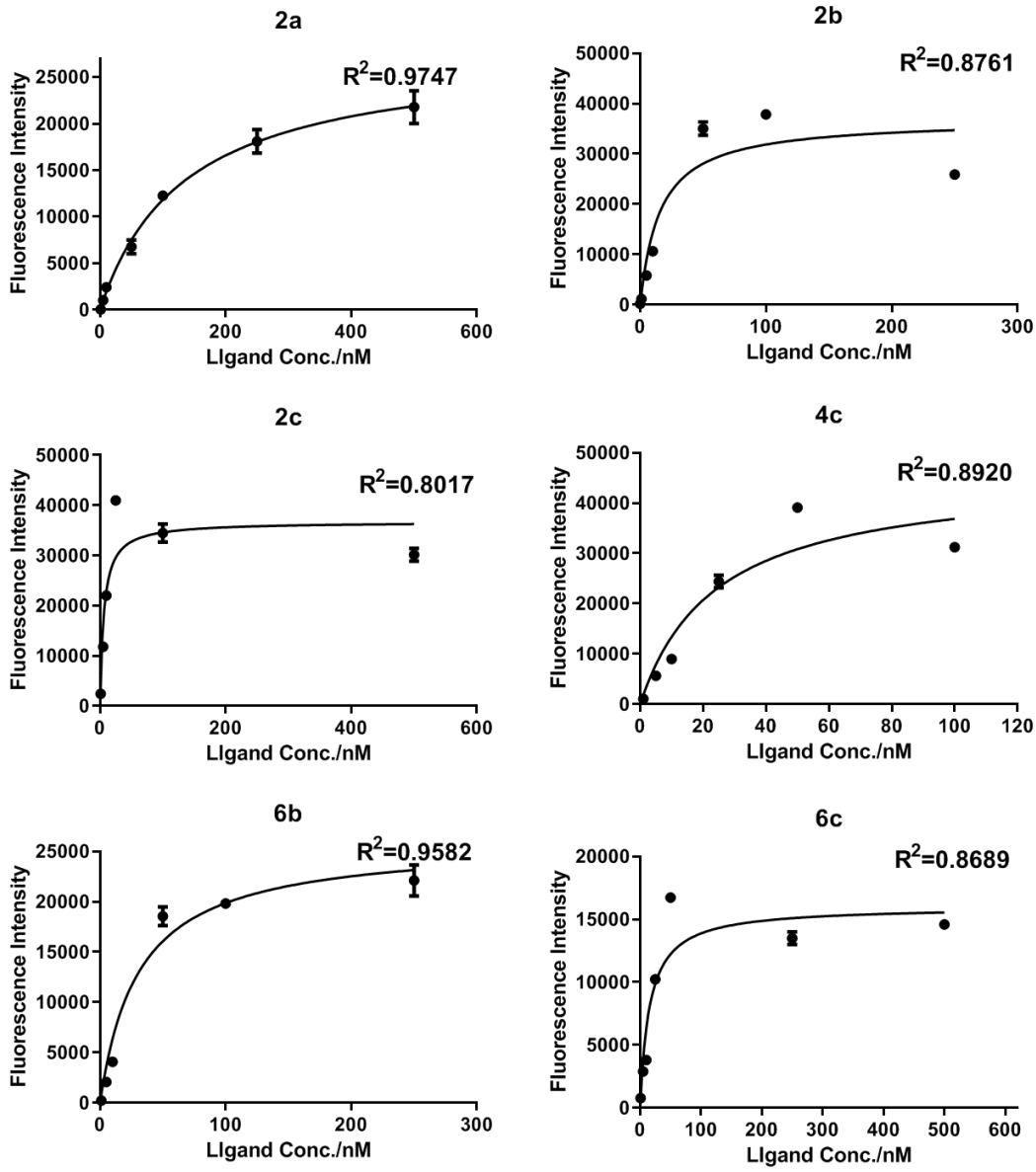

Figure S17. Saturation binding curves for ligands to Tau (k18) aggregates.

In Vitro Fluorescent Staining

Paraffin-embedded brain sections were prepared (xylene for 3 min, ethanol for 1 min and water for 1 min). Next, the solutions of **2c**, **4c**, **6c** (1 μM, 50% ethanol) were added to the sections and incubated for 2 minutes at room temperature, respectively. Then the sections were washed by 40% ethanol in water for 2 minutes. Fluorescent images were observed by the EVOS FL fluorescence microscope.

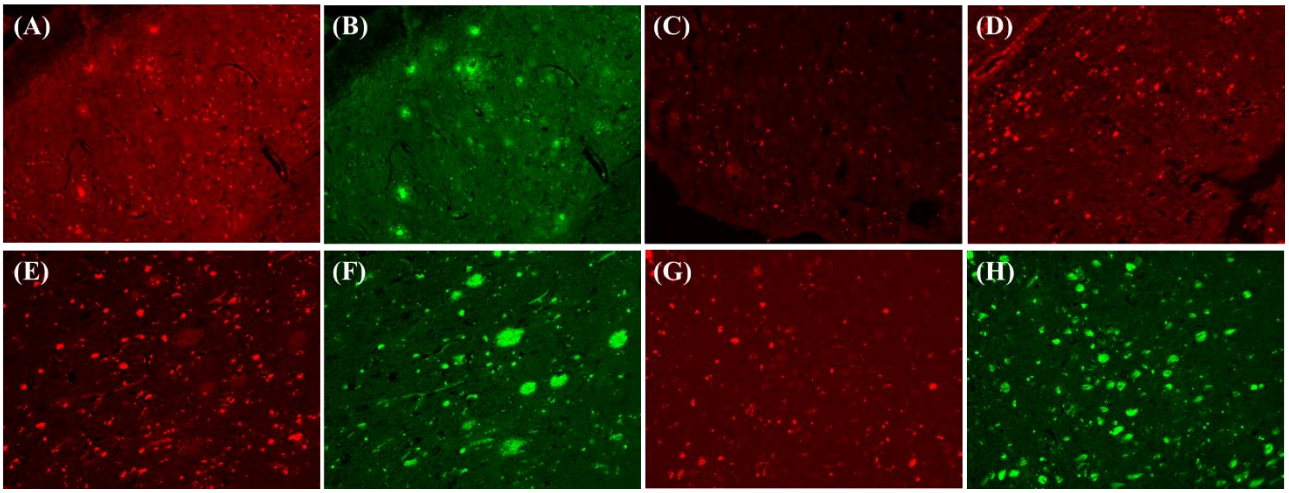

Figure S18. *In vitro* fluorescent staining images of **4c** (RFP filter). (A) Tg-Aβ mice (C57BL6, APPsw/PSEN1, 22 months old, male), 20×; (C) Tg-Tau mice (rTg4510, P301L, 7 months old, female); (D and E) AD patient (hippocampus, 95 years old, female), 20×; (G) AD patient (hippocampus, 88 years old, female), 20×; (B, F and H) Aβ plaques and neurofibrillary tangles were labeled by ThS (GFP filter).

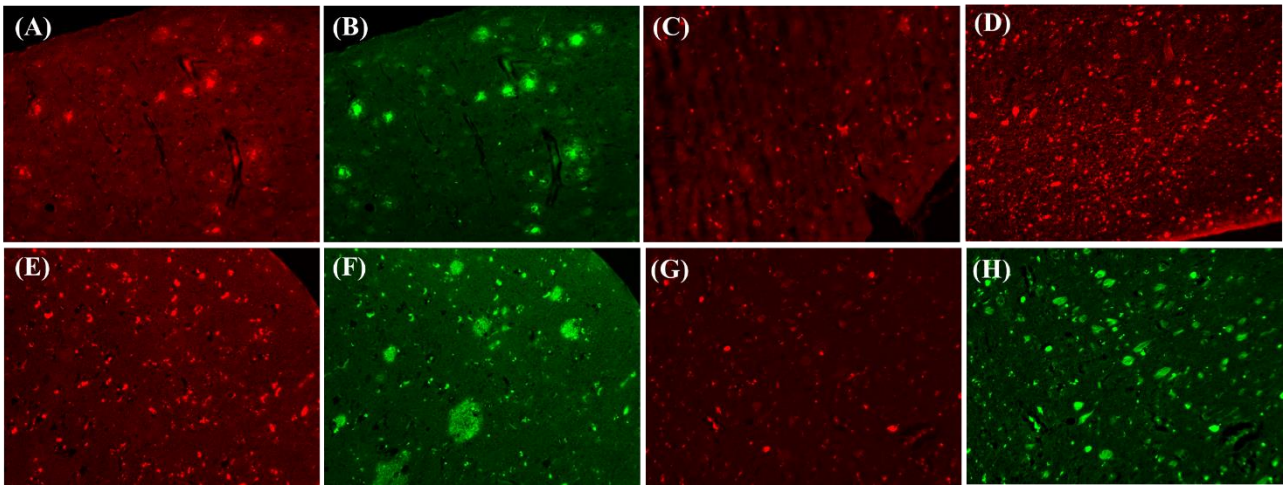

Figure S19. *In vitro* fluorescent staining images of **6c** (RFP filter). (A) Tg-Aβ mice (C57BL6, APPsw/PSEN1, 22 months old, male), 20×; (C) Tg-Tau mice (rTg4510, P301L, 7 months old, female); (D and E) AD patient (hippocampus, 95 years old, female), 20×; (G) AD patient (hippocampus, 88 years old, female), 20×; (B, F and H) Aβ plaques and neurofibrillary tangles were labeled by ThS (GFP filter).

Gallyas-Braak silver staining.

Gallyas-Braak silver staining was performed on paraffin-embedded tissue according to reported procedures with minor modification.[4] Brain tissue section were deparaffinized with xylene and ethanol in sequence and wash them with distilled water. Then, the brain slices were treated with 0.3% potassium permanganate solution for 10 minutes, 1% oxalic acid for 1 minute, and 0.5% lanthanum nitrate solution (including 2% sodium acetate) for 1 hour, and washed with distilled water for 5 min after each step. Next, they were treated with alkaline silver nitrate solution for 1 hour at 37 ℃ then washed with 1% acetic acid for 1 min. Next, the slices were developed for 5-20 minutes (monitor the color under a microscope) in developing solution prepared fresh by slow addition of equal volumes of solutions A, B and C with stirring and keeping in a shielded bottle (solution A: 50 g sodium carbonate in 1000 ml distilled water; solution B: 2 g silver nitrate, 2 g ammonium nitrate, 10 g tungstosilicic acid in 1000 ml distilled water; solution C: 2 g silver nitrate, 2 g ammonium nitrate, 10 g tungstosilicic acid and 6.1 ml 40% formaldehyde in 1000 ml distilled water). Last, the slices were washed with three times of 1% acetic acid for 1 min each and incubated with 0.5% gold chloride for a few seconds.

***Ex Vivo* Fluorescent Imaging of 2c**

A solution of **2c** (50% NMP and 50% propylene glycol, 100 μL, 0.5 mg/Kg) was injected via tail vein

of the Tg-Aβ mouse (C57BL6, APPsw/PSEN1, 22 months old, male) and WT mouse (C57BL6, 22 months old, male). The mice were sacrificed after 60 min and frozen sections (20 μm) were obtained.

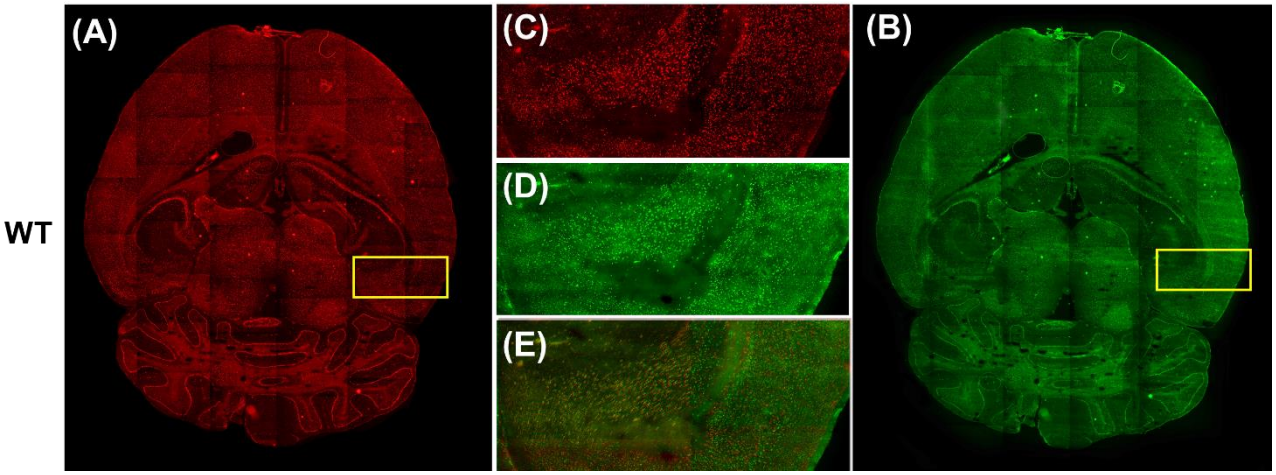

Figure S20. (A) *Ex vivo* histological staining of brain slices from WT mouse (C57BL6, 22 months old, male) after i.v. injection of **2c** at 1 h. (B) Counterstained by ThS. (C, D) Partially enlarged views. (E) Merged images showing the co-localization of **2c** and ThS.

In Vivo Fluorescent Imaging of 2c

Tg-Aβ mice (C57BL6, APPsw/PSEN1, 22 month-old, male) and age-matched WT mice (C57BL6, 22-month-old, male) were shaved before background imaging and were intravenous injected with **2c** (0.1 mg/Kg). The fluorescence signals of the brain are collected and recorded on an IVIS Lumina III system, and the semi-quantitative NIR fluorescence imaging data (draw the same size ROI around the brain area) was analyzed by Living Image Software (Living software® 4.2.1). A filter set (excitation at 520 nm, and emission at 670 nm) was used for the measurement. The mice were kept under anesthesia with 2.5% isoflurane gas in an oxygen flow (0.8 L/min) during the imaging process.

Molecular docking studies.

Molecular docking studies were performed for **A**$\beta_{1\text{-}42}$ (PDB ID: 5OQV) and Tau (PDB ID: 5O3T) fibrils. The structures of **2c**, **4c**, and **6c** were optimized according to the method mentioned in the DFT calculations above and used for docking in Autodock software. All rotatable bonds in this molecules remained in free-rotation state.

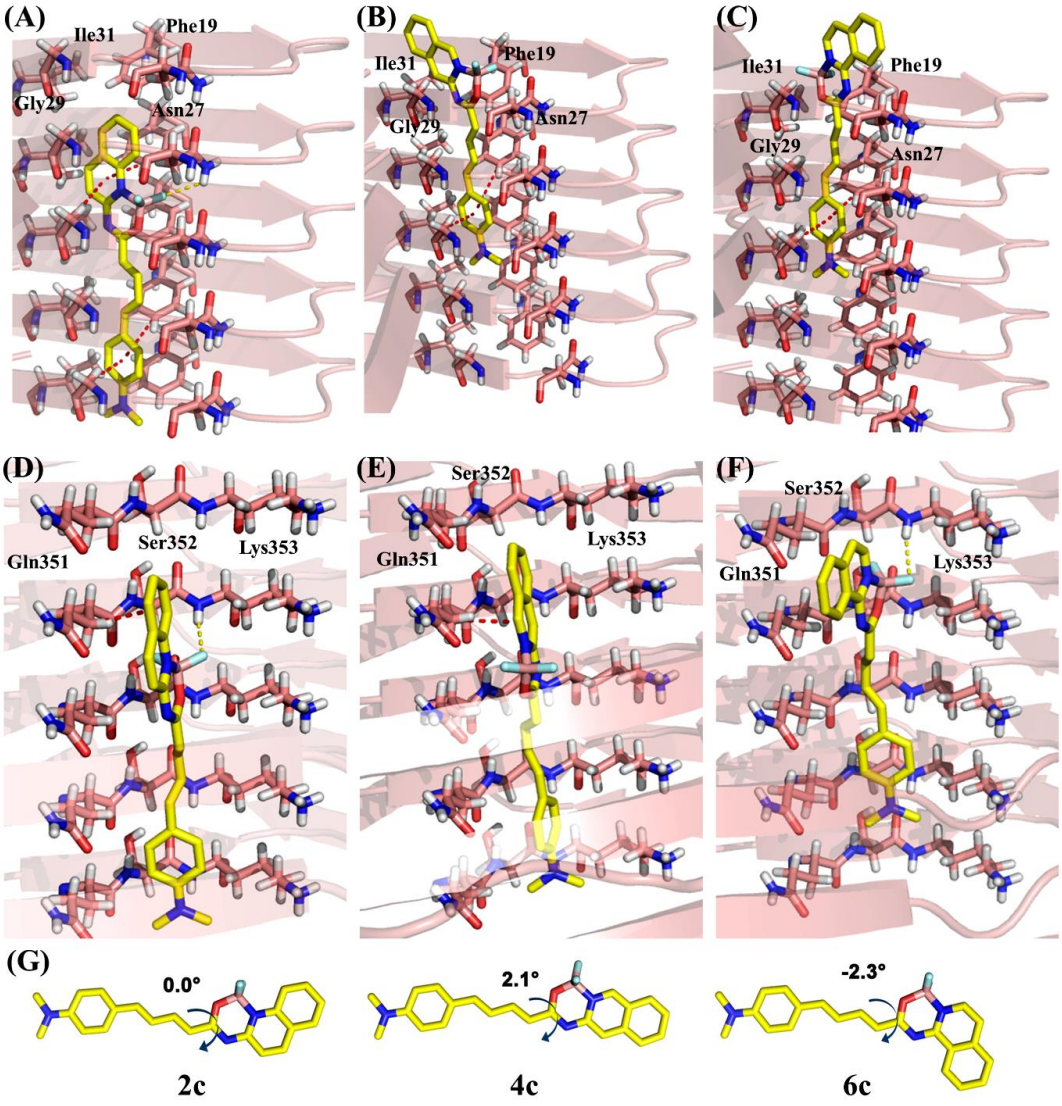

Figure S21. The optimal binding conformation of (A) **2c** - **A**$\beta_{1\text{-}42}$, (B) **4c** - **A**$\beta_{1\text{-}42}$, (C) **6c** - **A**$\beta_{1\text{-}42}$, (D) **2c** - **Tau**, (E) **4c** - **Tau,** and (F) **6c** - **A**$\beta_{1\text{-}42}$ complex in docking studies. (G)The theoretical molecular model of probes (**2c**, **4c** and **6c**). The probes are represented as stick, with carbon, oxygen, nitrogen,

boron and fluorin atoms colored yellow, red, blue, pink and cyan, respectively. The crystal structure of **A**$\beta_{1\text{-}42}$ and Tau are represented as cartoon, in which the key residues are represented as sticks, with carbon, oxygen, nitrogen and hydrogen atoms colored pink, red, blue and white, respectively. Hydrophobic and hydrophilic interactions are indicated as red and yellow dotted line, respectively.

Blood-Brain Barrier Penetrability of 2c

The Blood-Brain Barrier (BBB) penetration was tested by a conventional HPLC based method in normal ICR mice.[5] A solution of **2c** (30% DMSO and 70% propylene glycol, 100 μL, 0.1 mg/Kg) was injected via tail vein of ICR mice (19-21 g, male). % ID/g was given as the mean ± SD (n = 3). HPLC conditions: acetonitrile/water (85/15, v/v) at a flow rate of 1.0 mL/min, the UV detector is 491 nm.

Cytotoxicity Study of 2c

The cytotoxicity study of **2c** was performed by MTT (3-(4,5-dimethylthiazol-2-yl)-2,5-diphenyltetrazolium bromide) assay using human neuroblastoma cells (SH-SY5Y, 1×10^5/mL) to quantify cell viability at different concentrations (0.10, 0.25, 0.50, 1.00, 2.50, 5.00 μM). SH-SY5Y cells were seeded into a transparent 96-well plate for 18 h (37 ℃, 5% CO_2) and then treated with various concentrations of **2c** at various concentration for 24 h. Next, an MTT solution (final concentration 0.5 mg/mL) was added and incubated for 4 hours after removing **2c** using PBS. Finally, the formazan crystals produced by the live cells were dissolved by 300 μL of DMSO and determined the absorption values with a microplate reader at 570 nm (n=5).

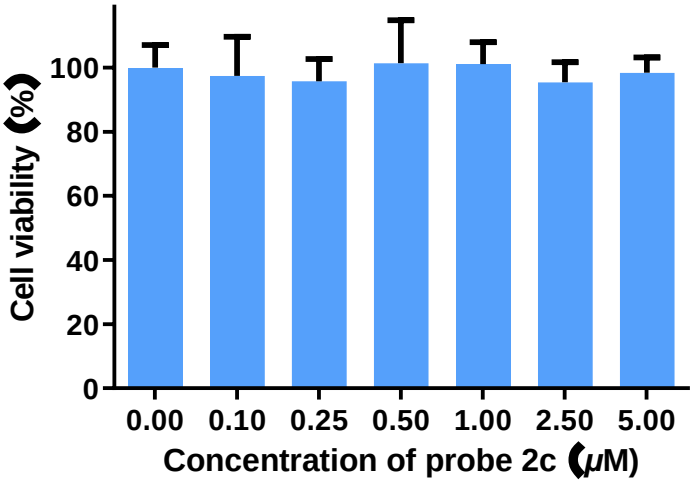

Figure S22. Cell viability after incubation of **2c** at different concentrations. Error bars designate standard deviation (n=5).

NMR and MS Spectra of Compounds

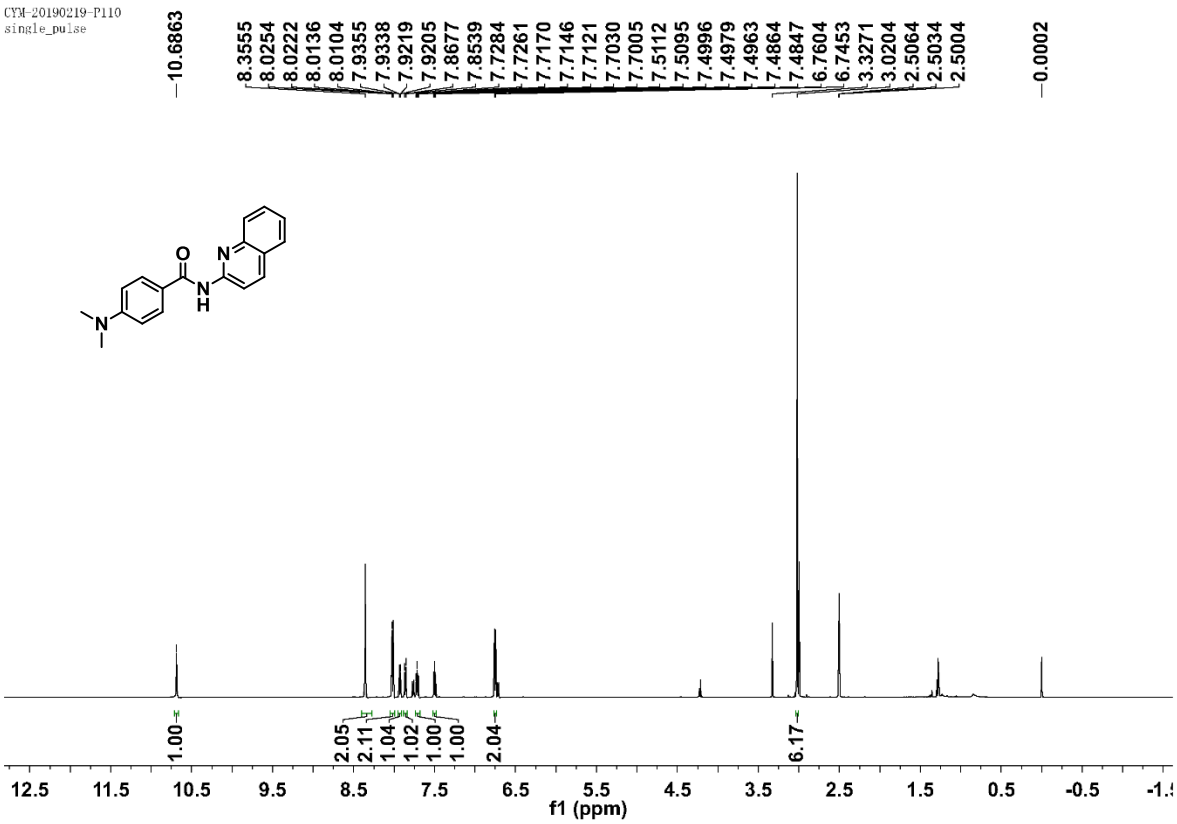

^{1}H NMR (DMSO-d_6) spectrum of compound **1a**

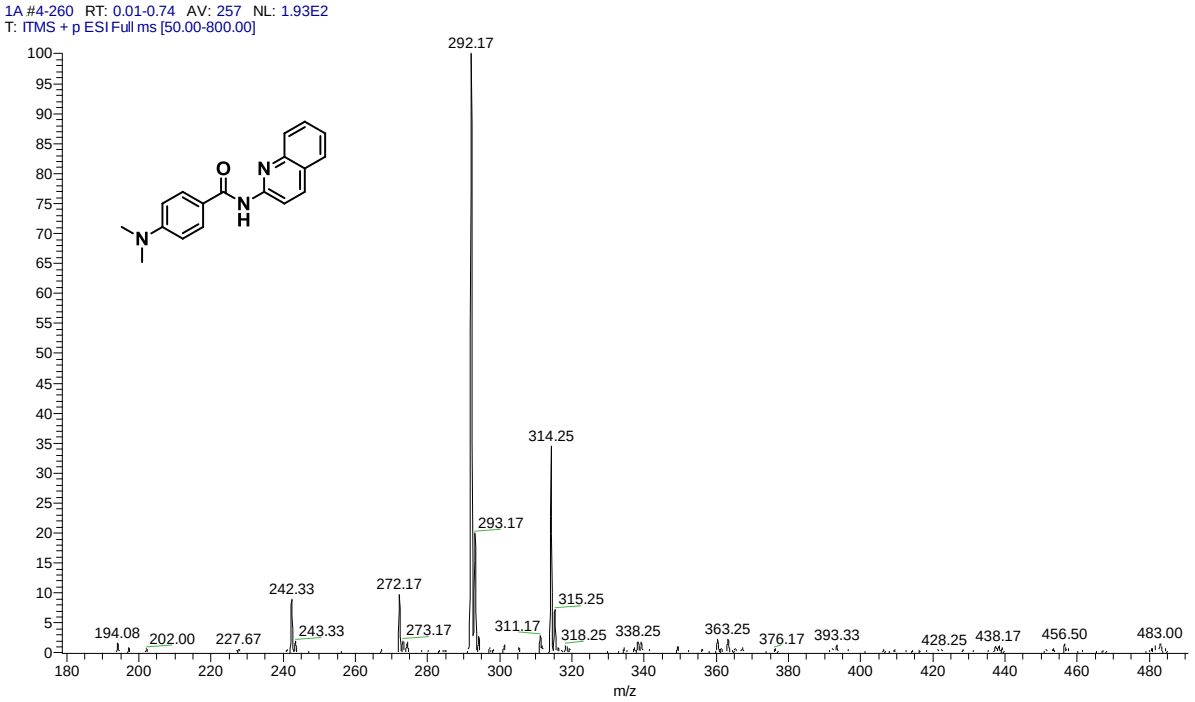

MS spectrum of compound **1a**

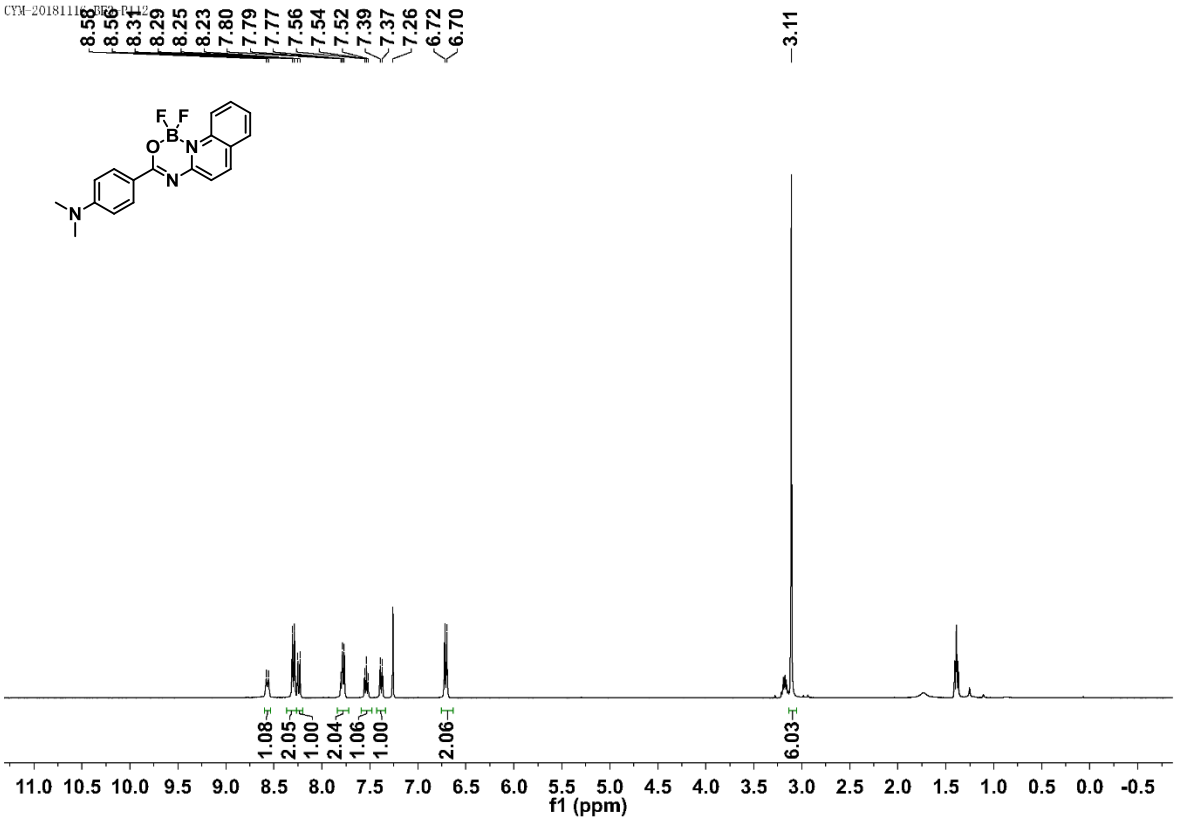

^{1}H NMR ($CDCl_3$) spectrum of compound **2a**

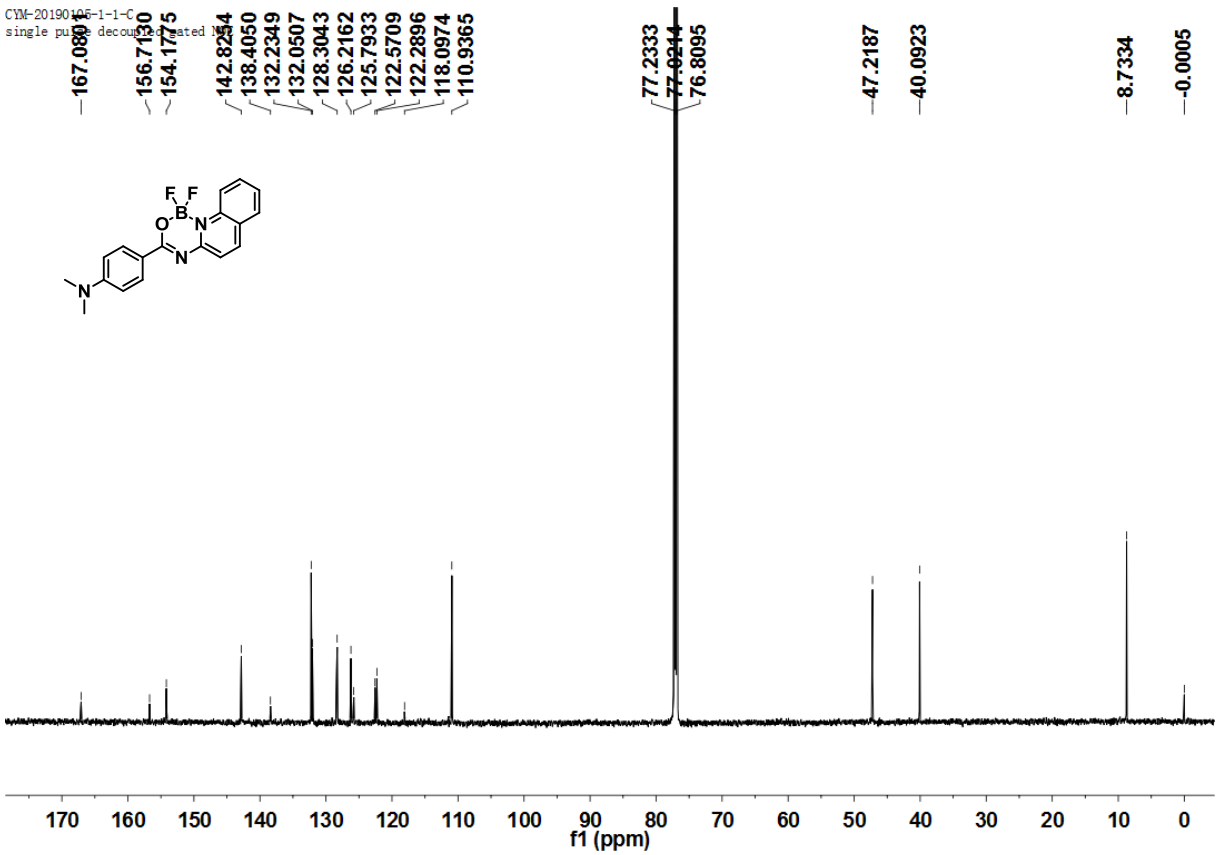

^{13}C NMR ($CDCl_3$) spectrum of compound **2a**

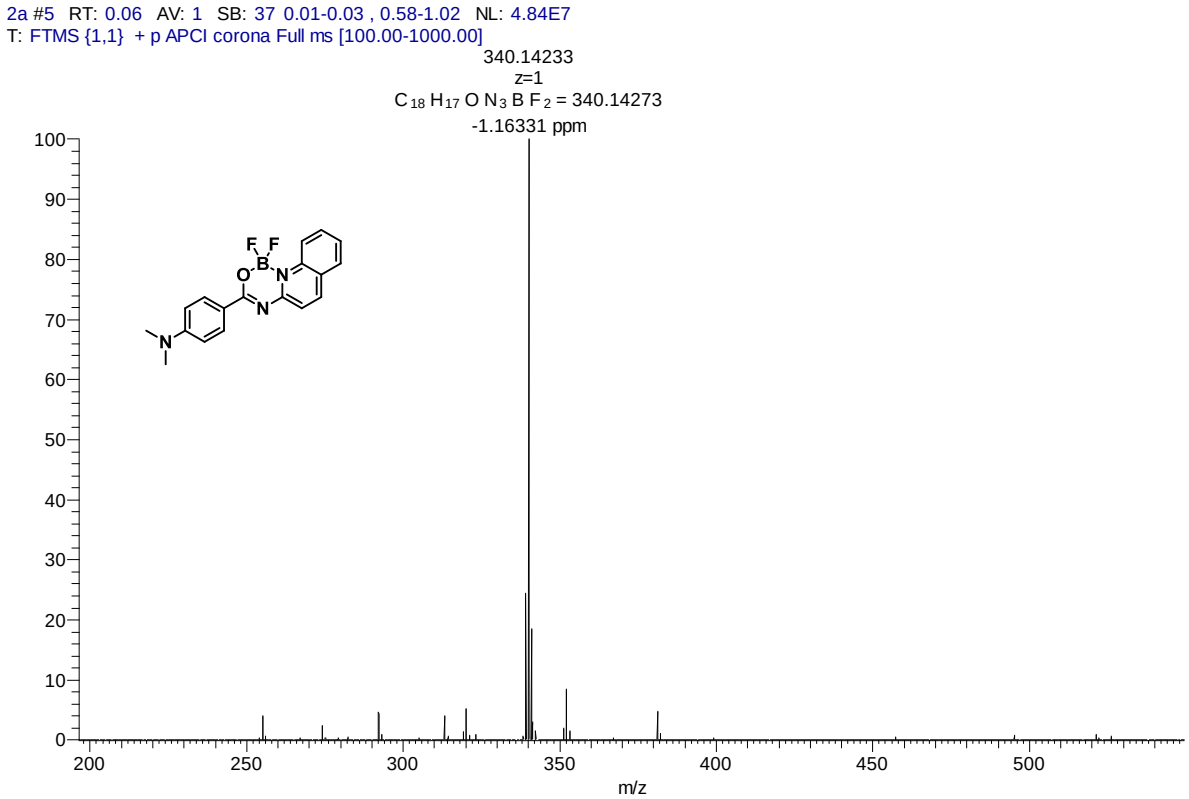

HRMS spectrum of compound **2a**

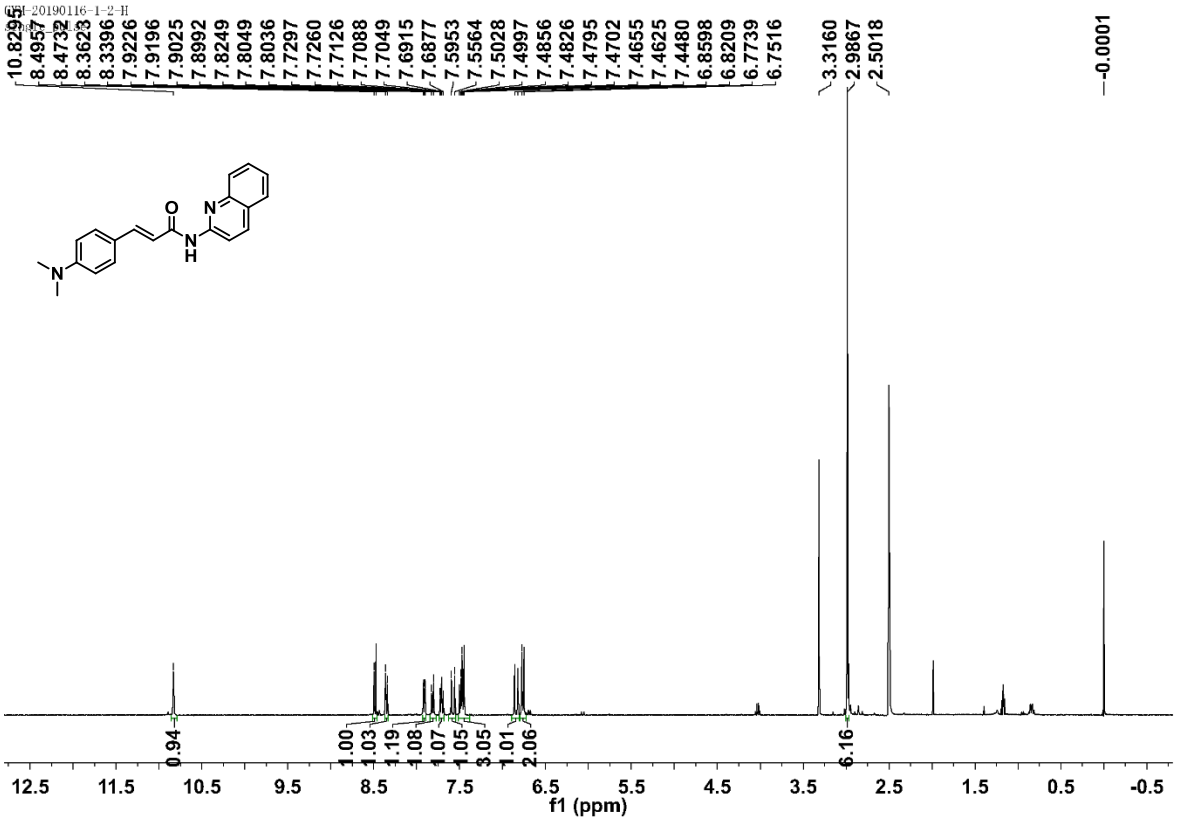

^{1}H NMR (DMSO-d_6) spectrum of compound **1b**

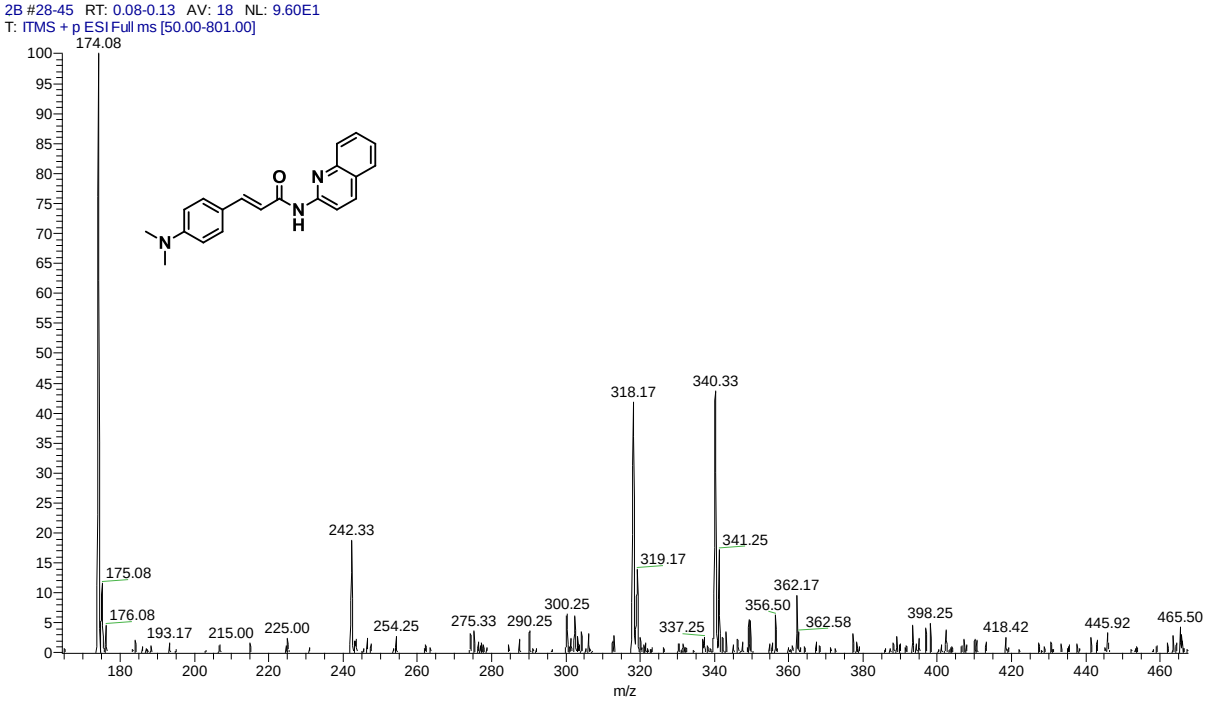

MS spectrum of compound **1b**

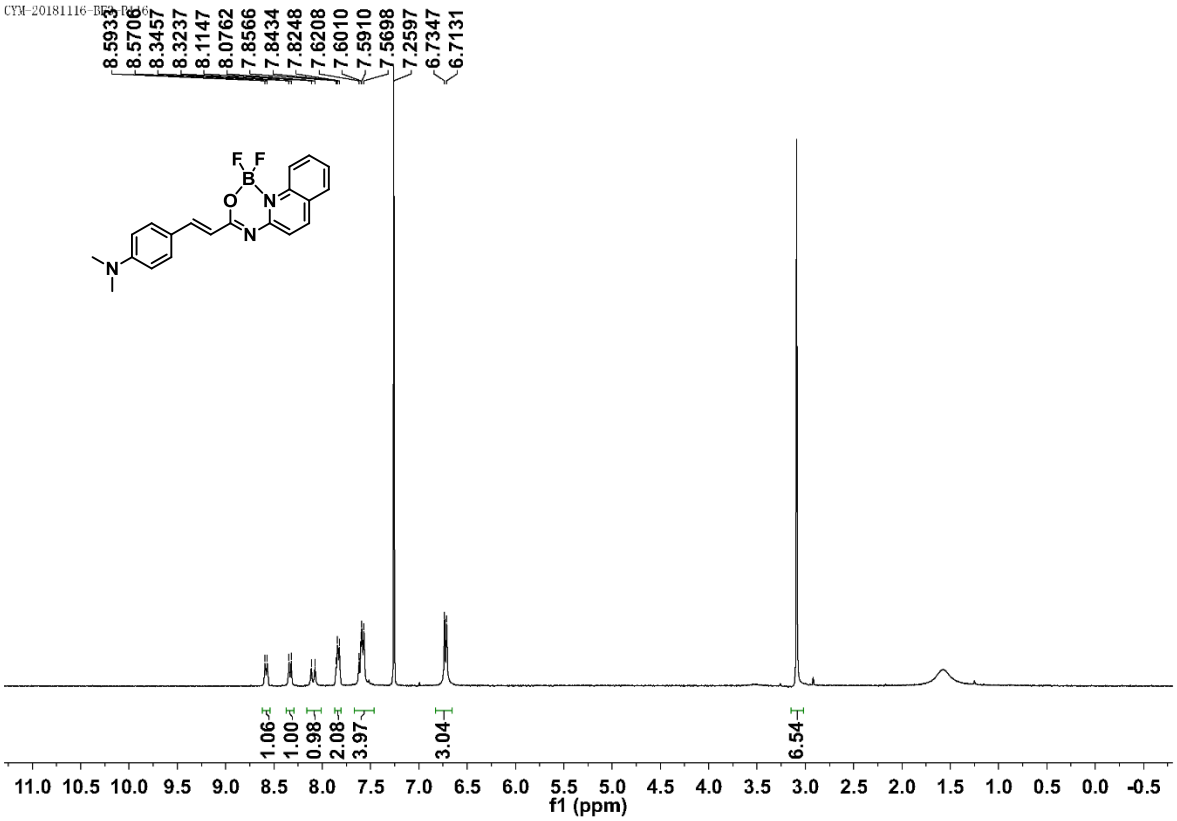

^{1}H NMR ($CDCl_3$) spectrum of compound **2b**

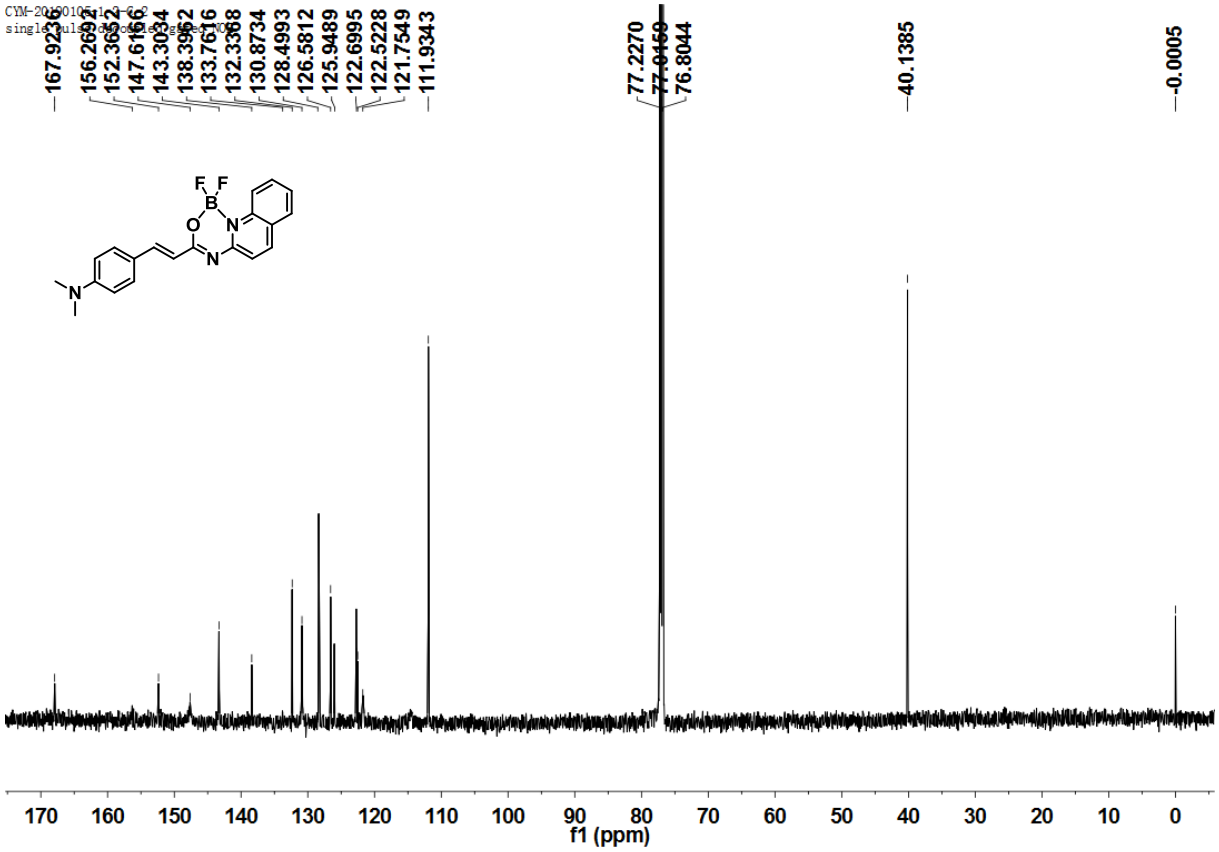

^{13}C NMR ($CDCl_3$) spectrum of compound **2b**

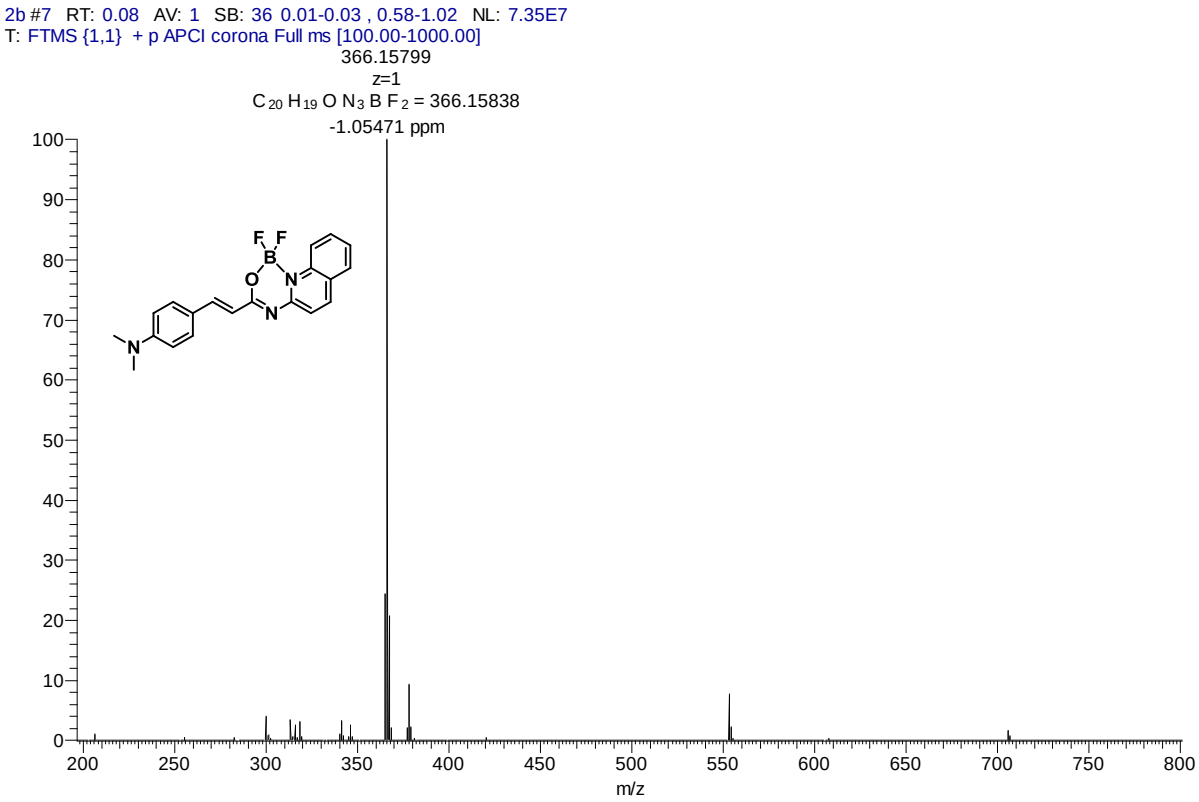

HRMS spectrum of compound **2b**

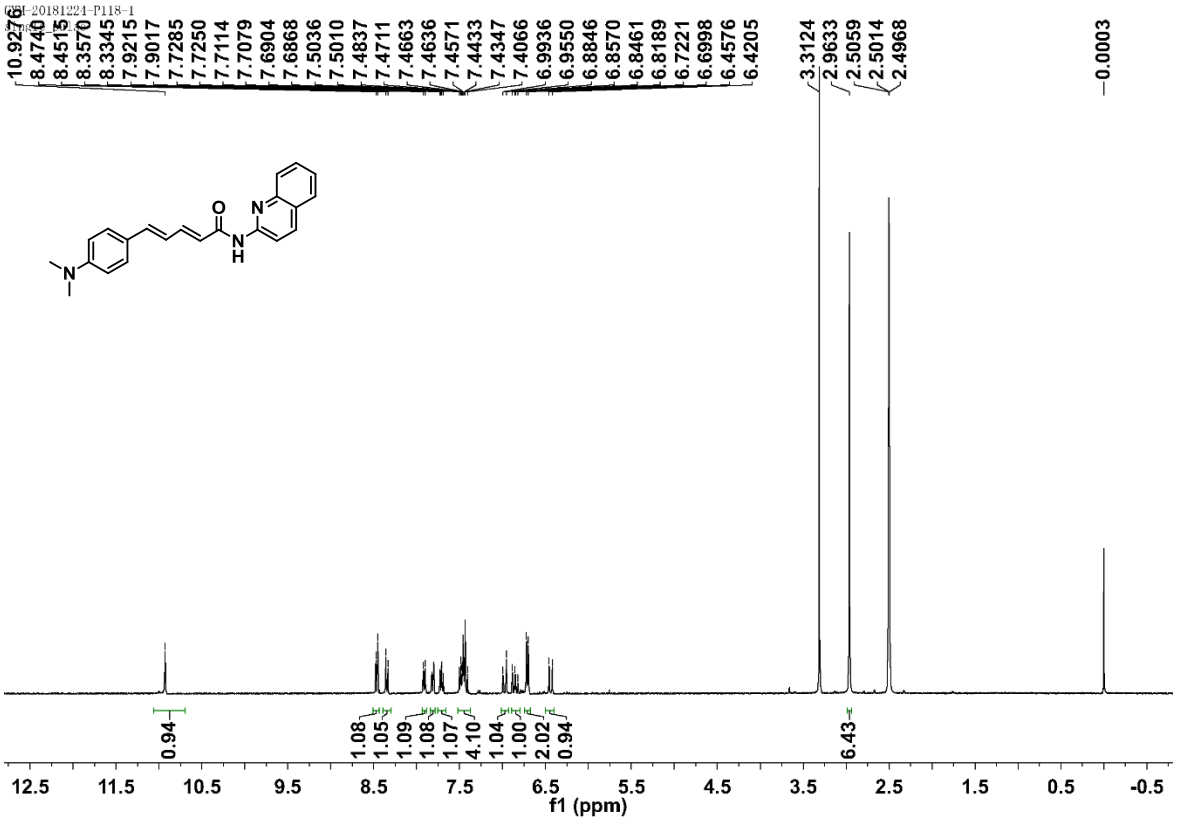

^{1}H NMR (DMSO-d_6) spectrum of compound **1c**

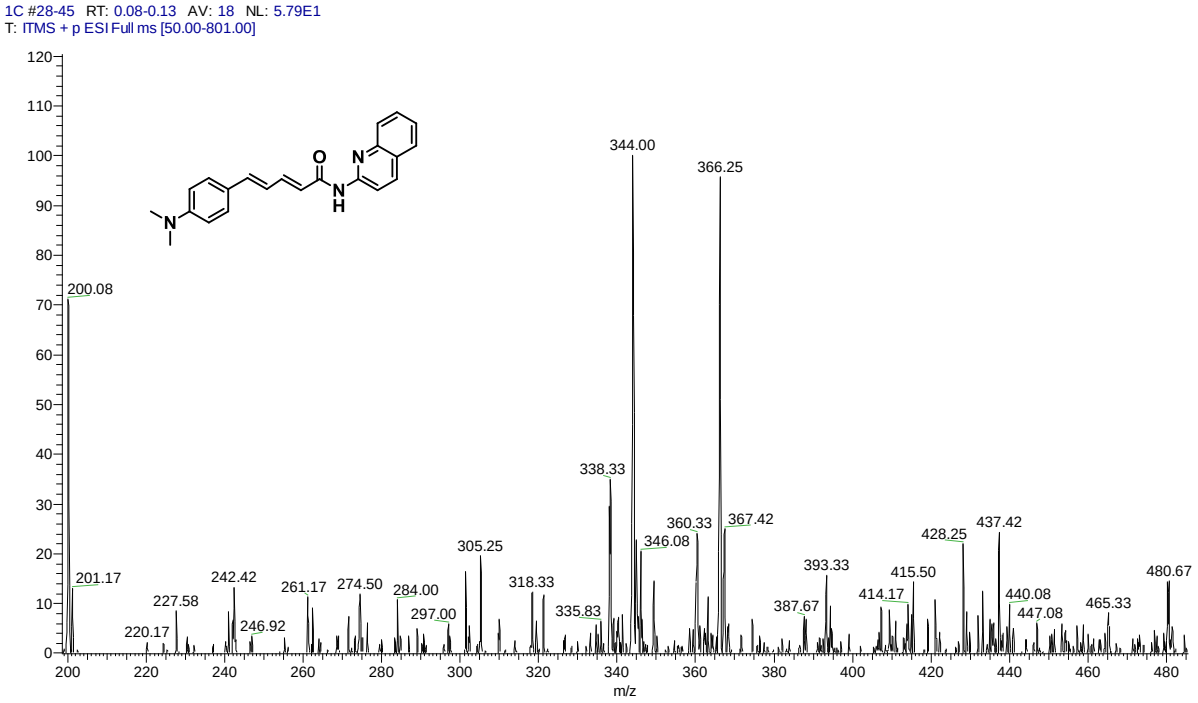

MS spectrum of compound **1c**

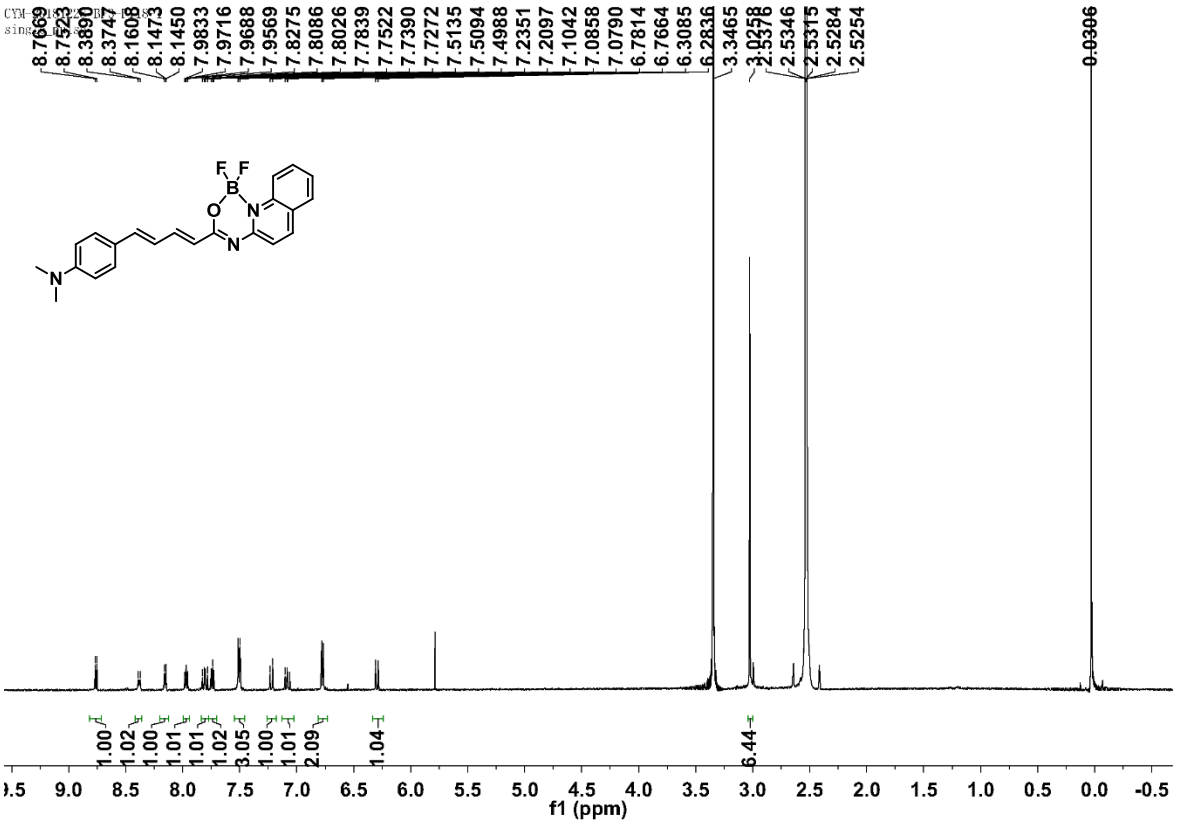

^{1}H NMR (DMSO-d_6) spectrum of compound **2c**

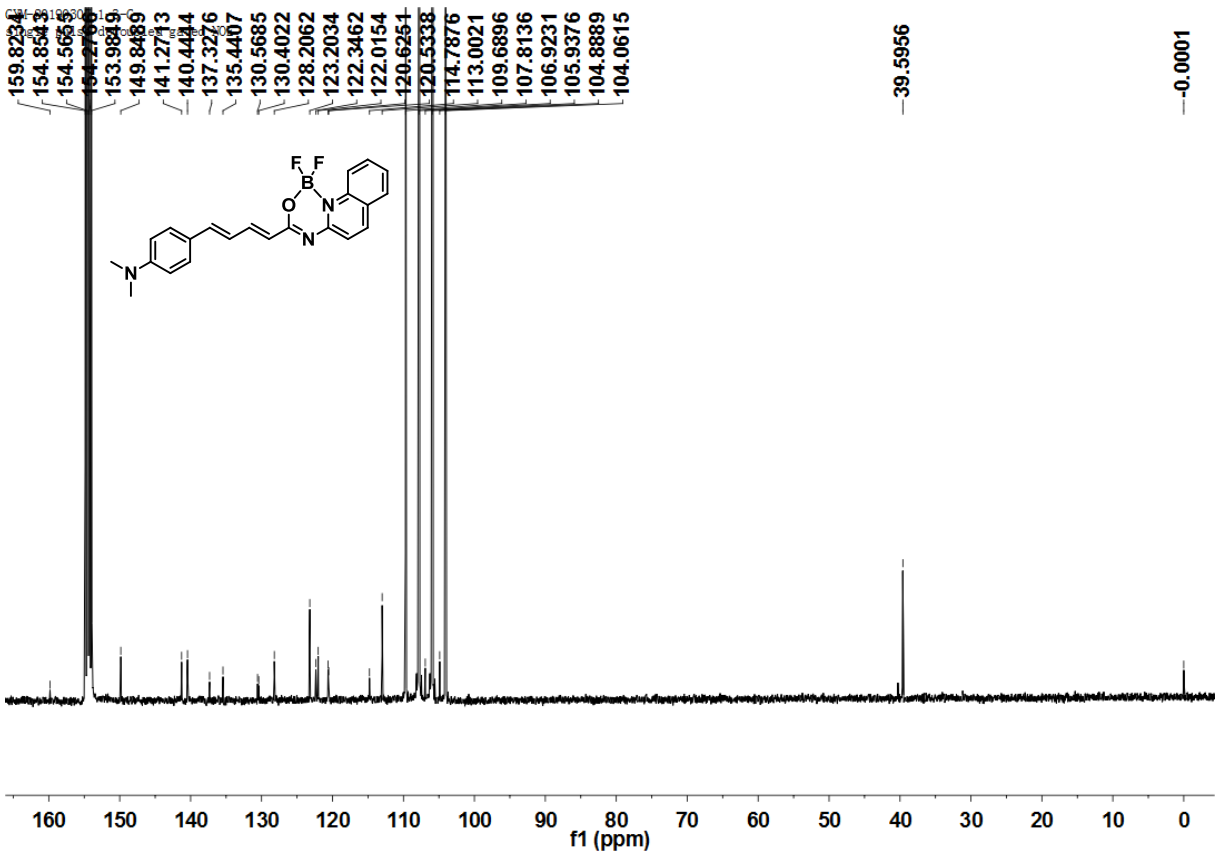

^{13}C NMR ($C_2DF_3O_2$) spectrum of compound **2c**

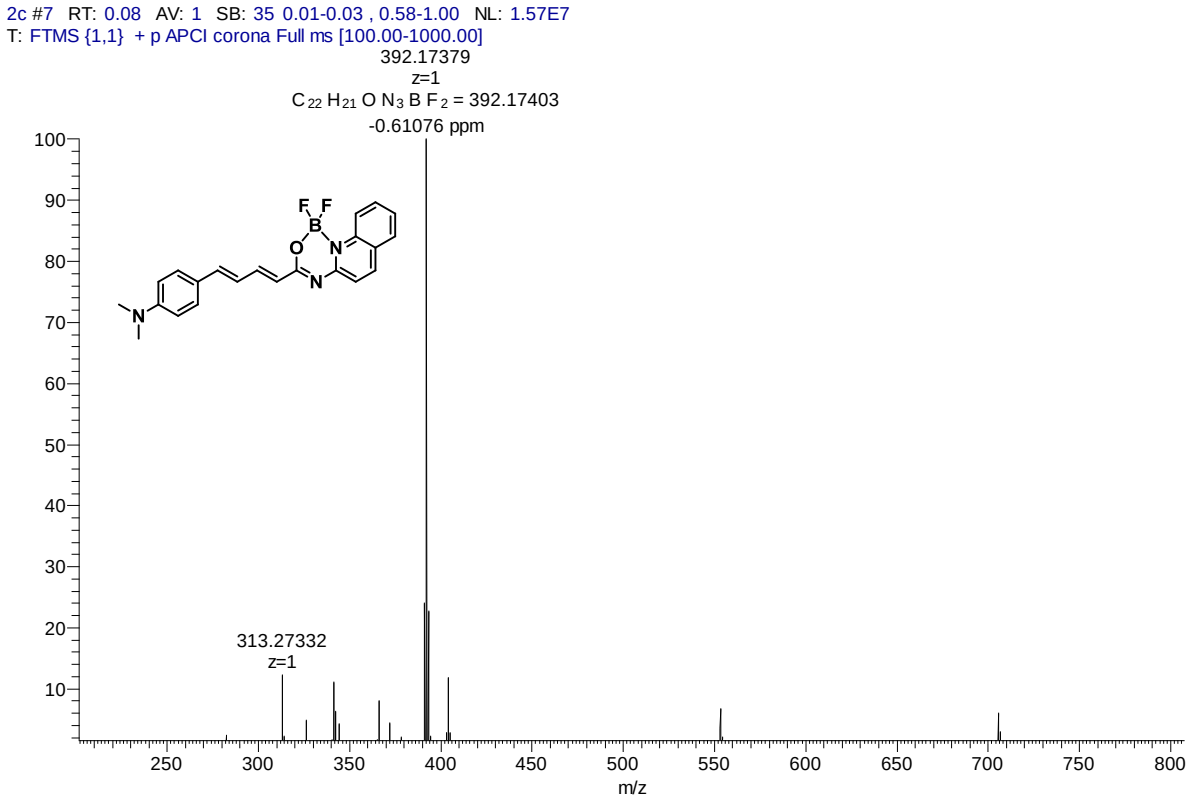

HRMS spectrum of compound **2c**

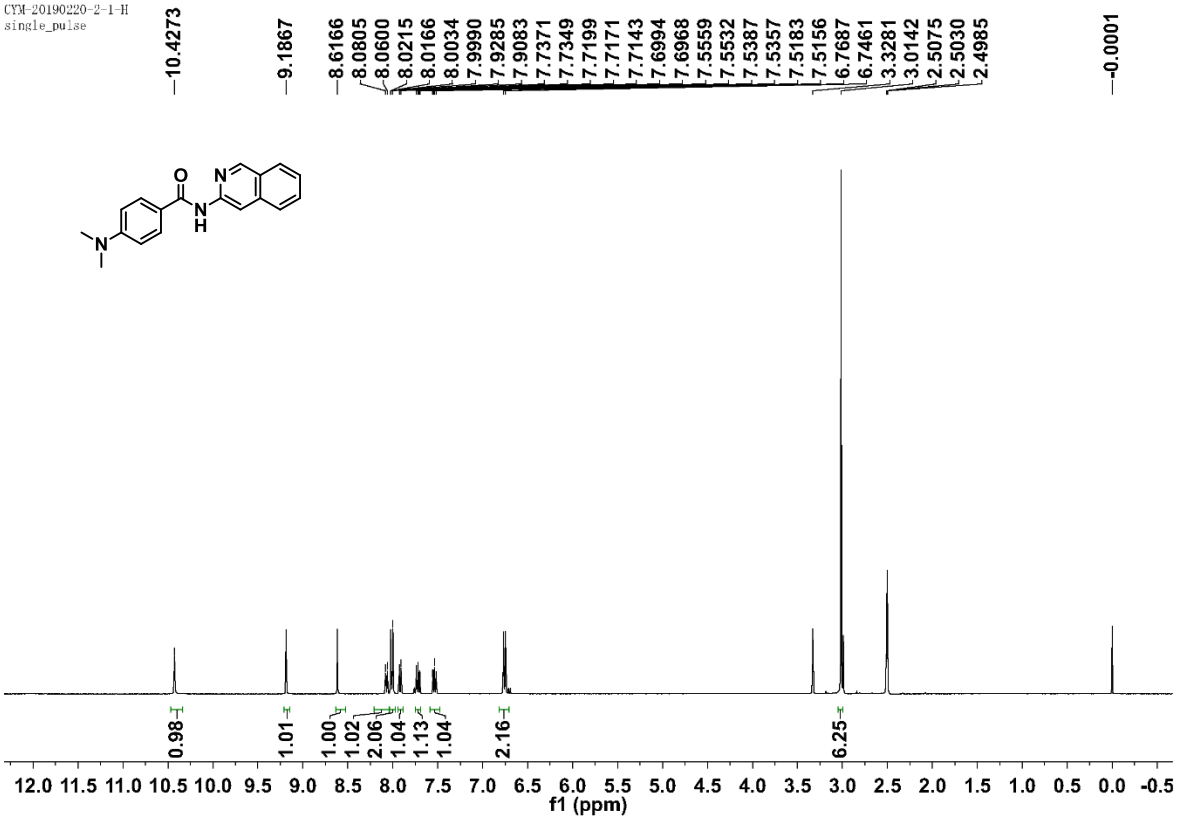

^{1}H NMR (DMSO-d_6) spectrum of compound **3a**

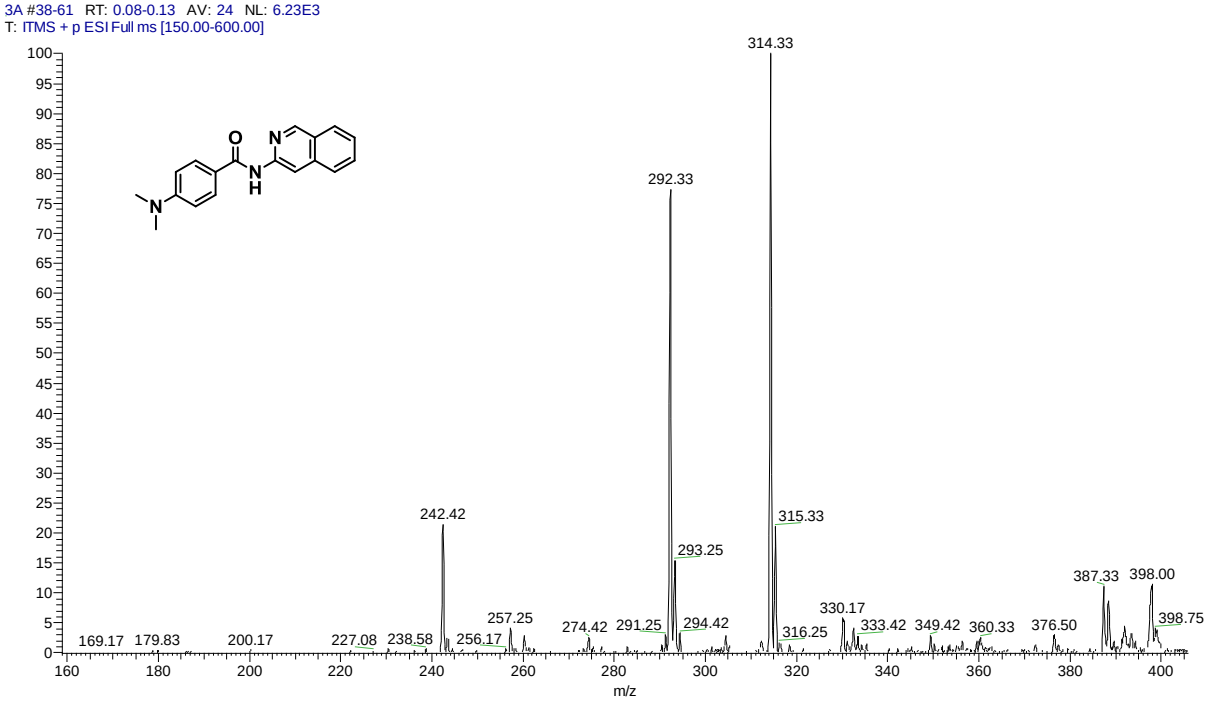

MS spectrum of compound **3a**

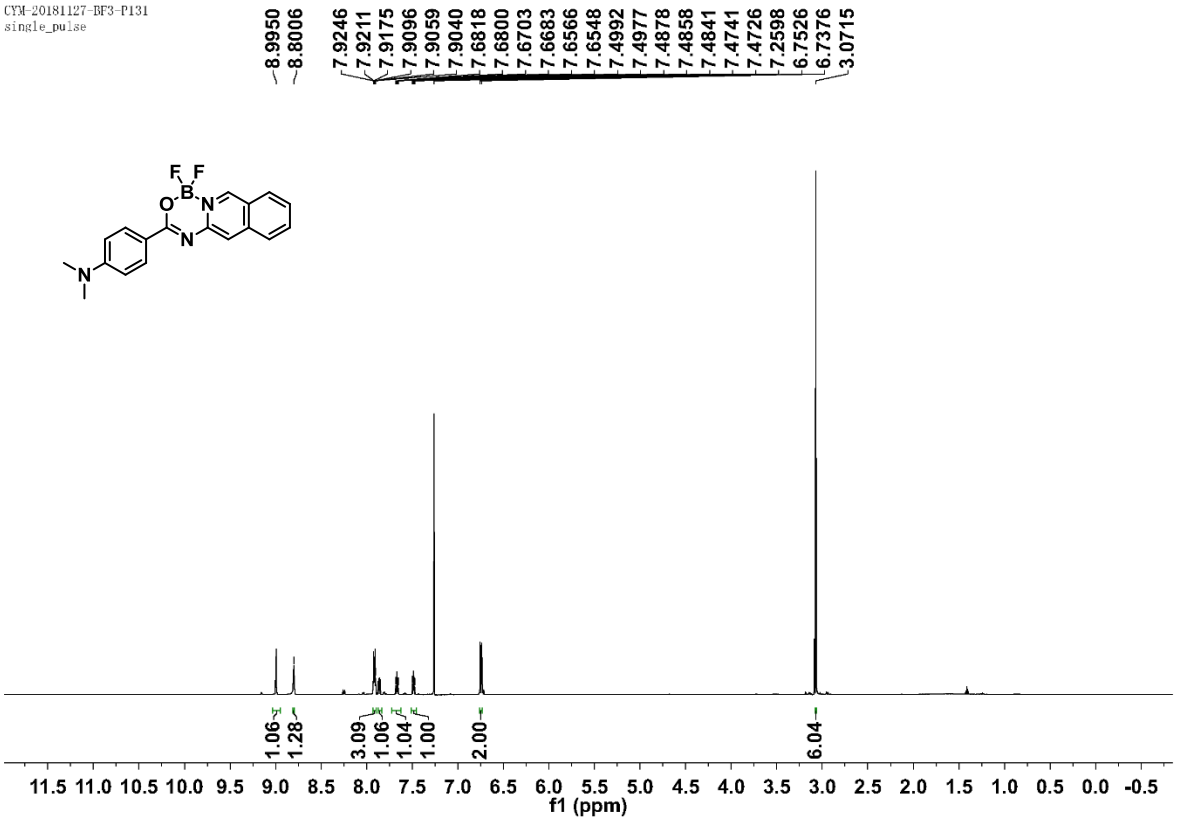

^{1}H NMR ($CDCl_3$) spectrum of compound **4a**

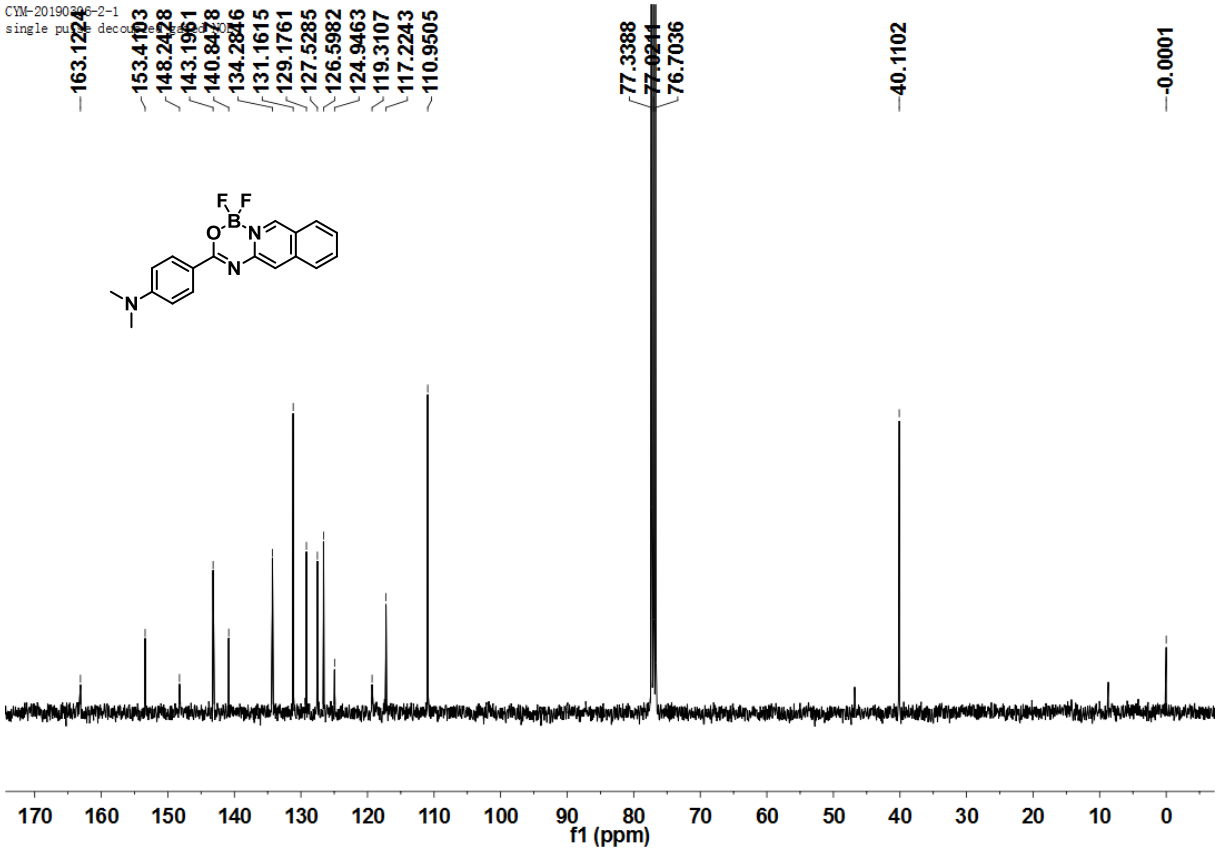

^{13}C NMR ($CDCl_3$) spectrum of compound **4a**

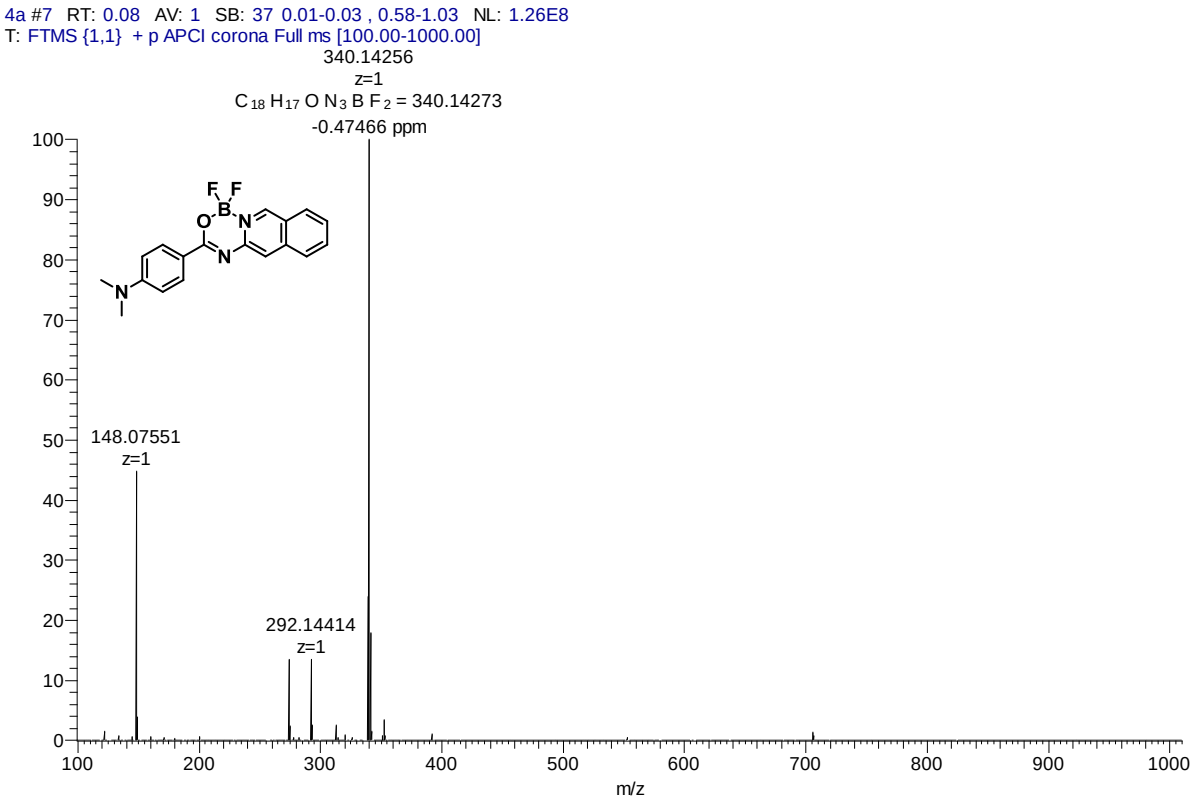

HRMS spectrum of compound **4a**

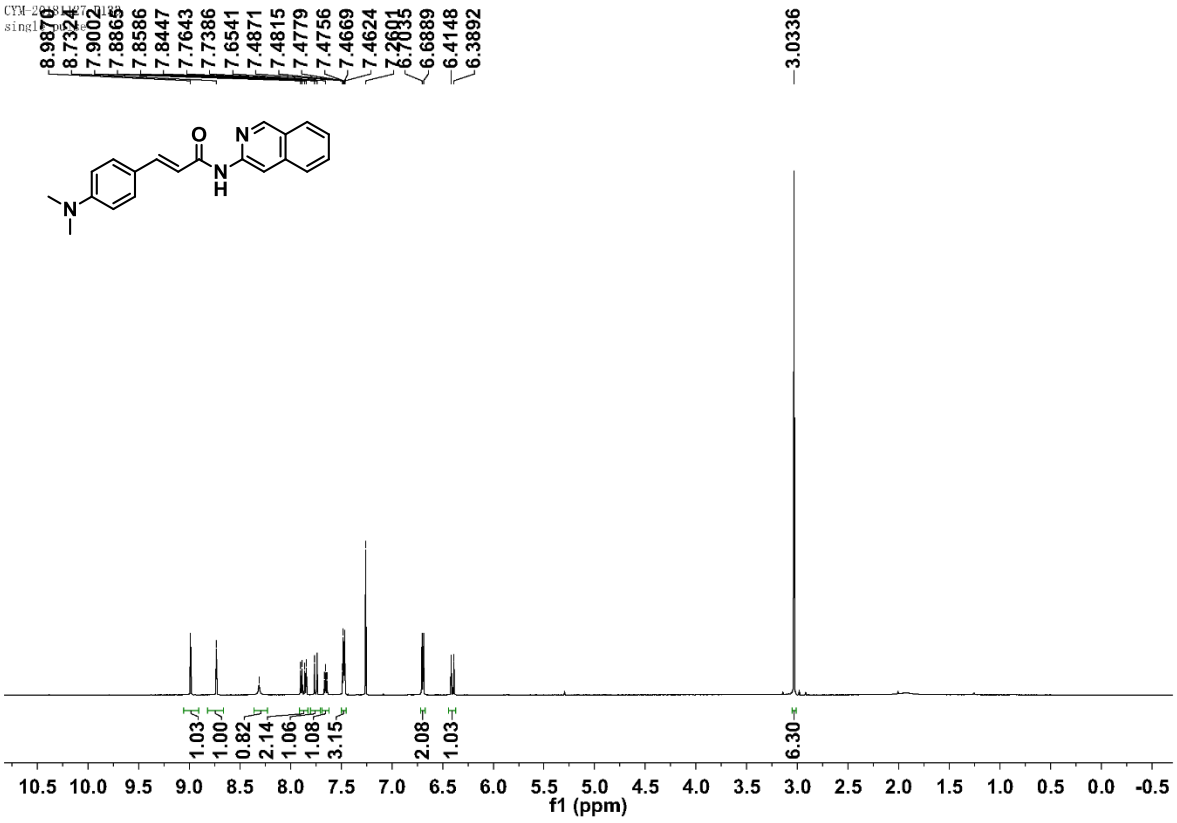

^{1}H NMR ($CDCl_3$) spectrum of compound **3b**

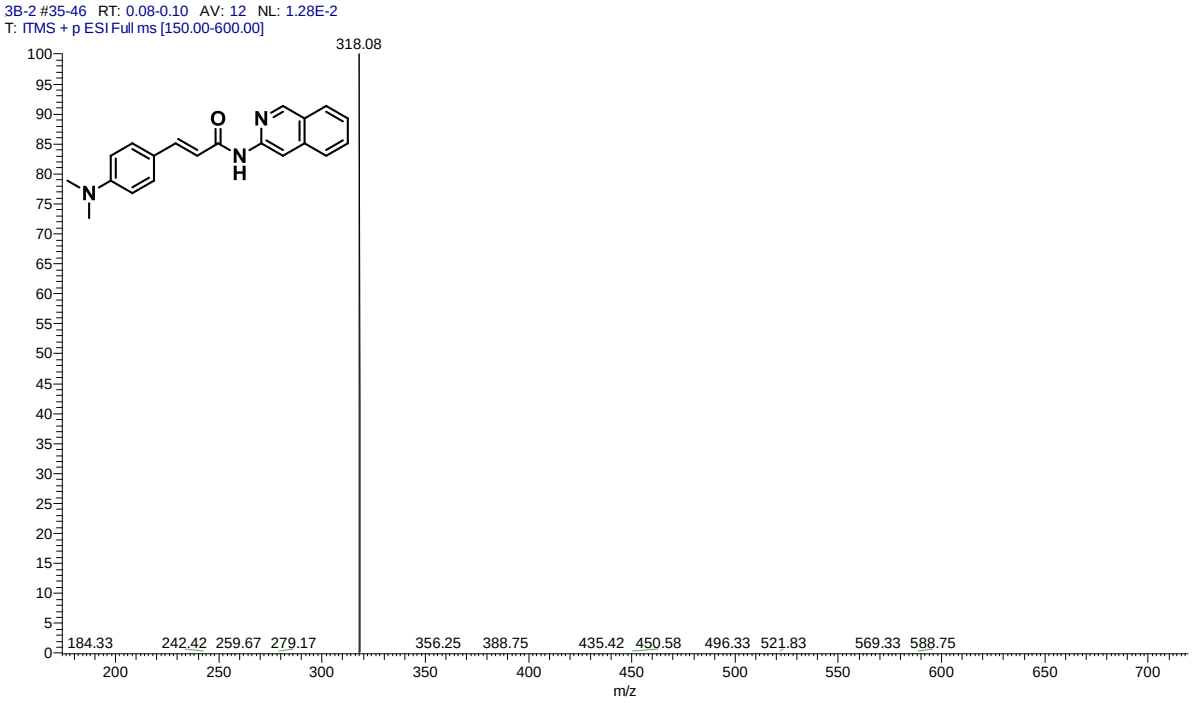

MS spectrum of compound **3b**

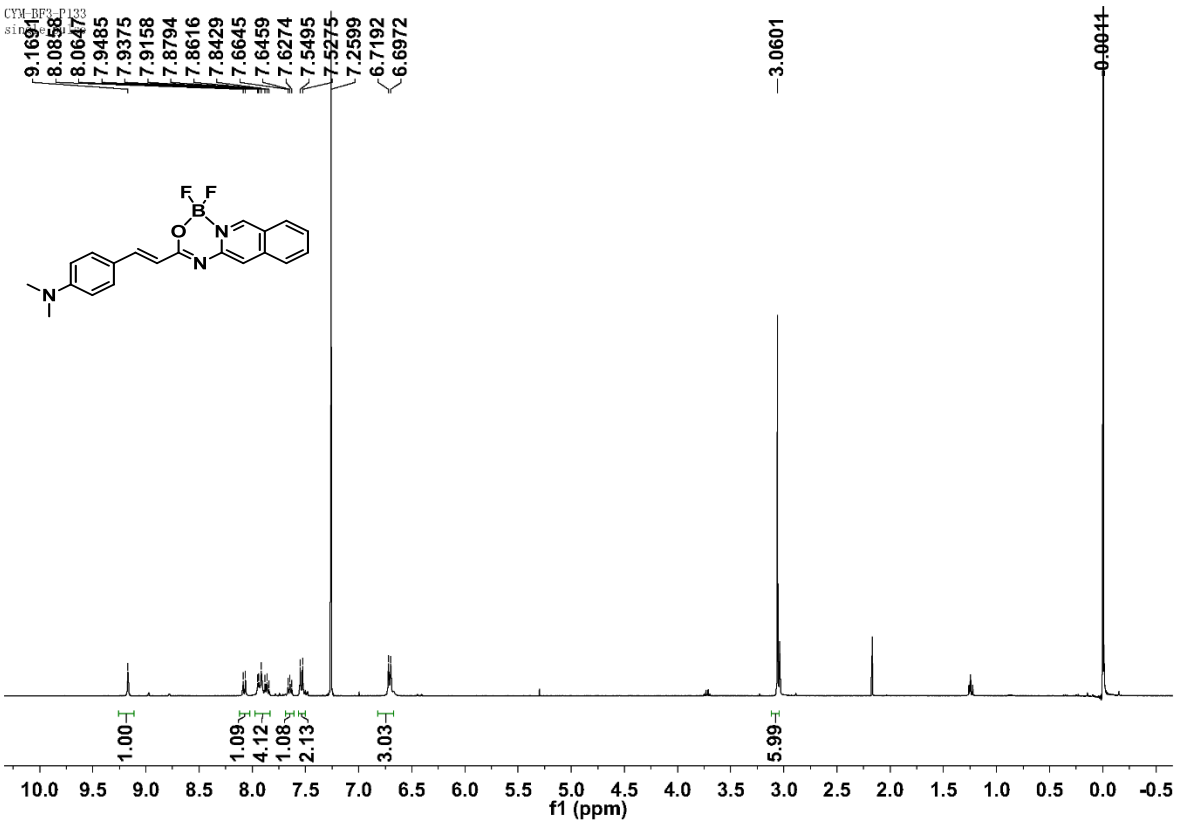

^{1}H NMR ($CDCl_3$) spectrum of compound **4b**

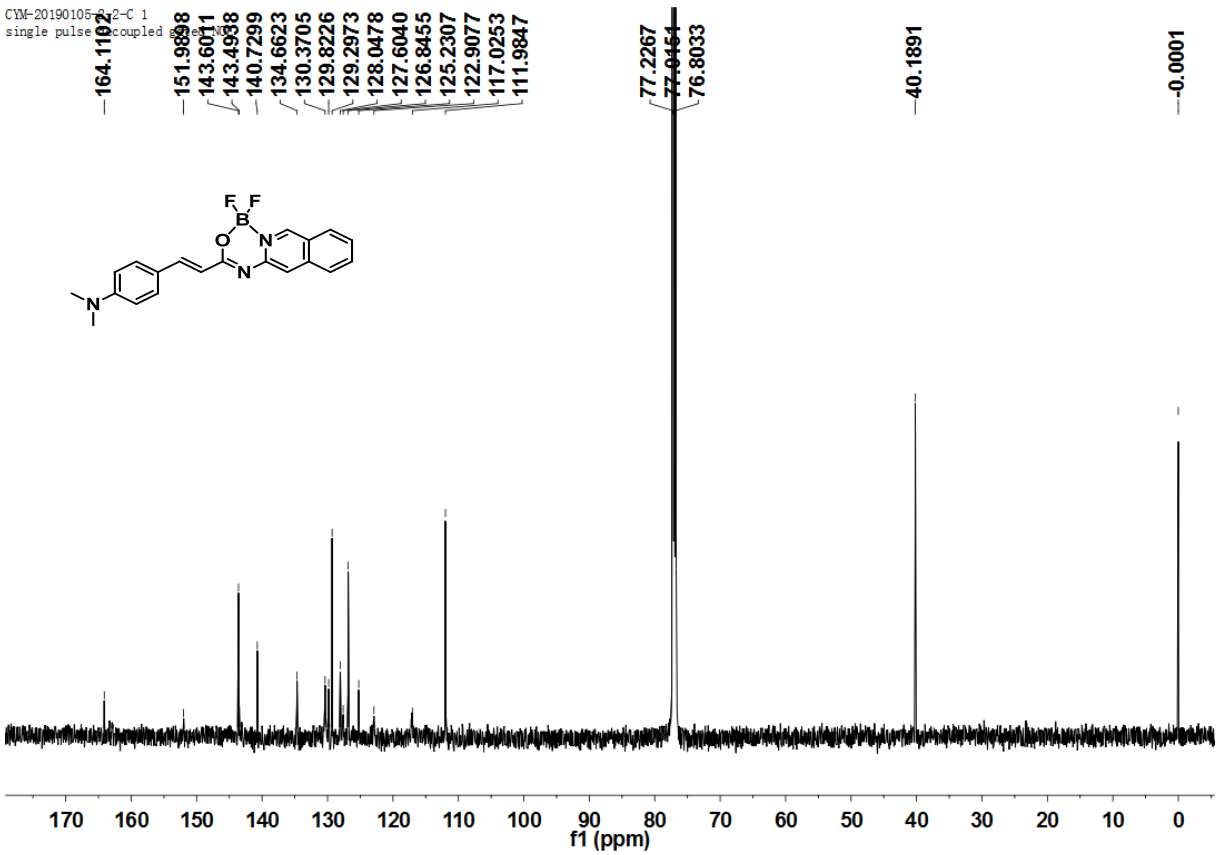

^{13}C NMR ($CDCl_3$) spectrum of compound **4b**

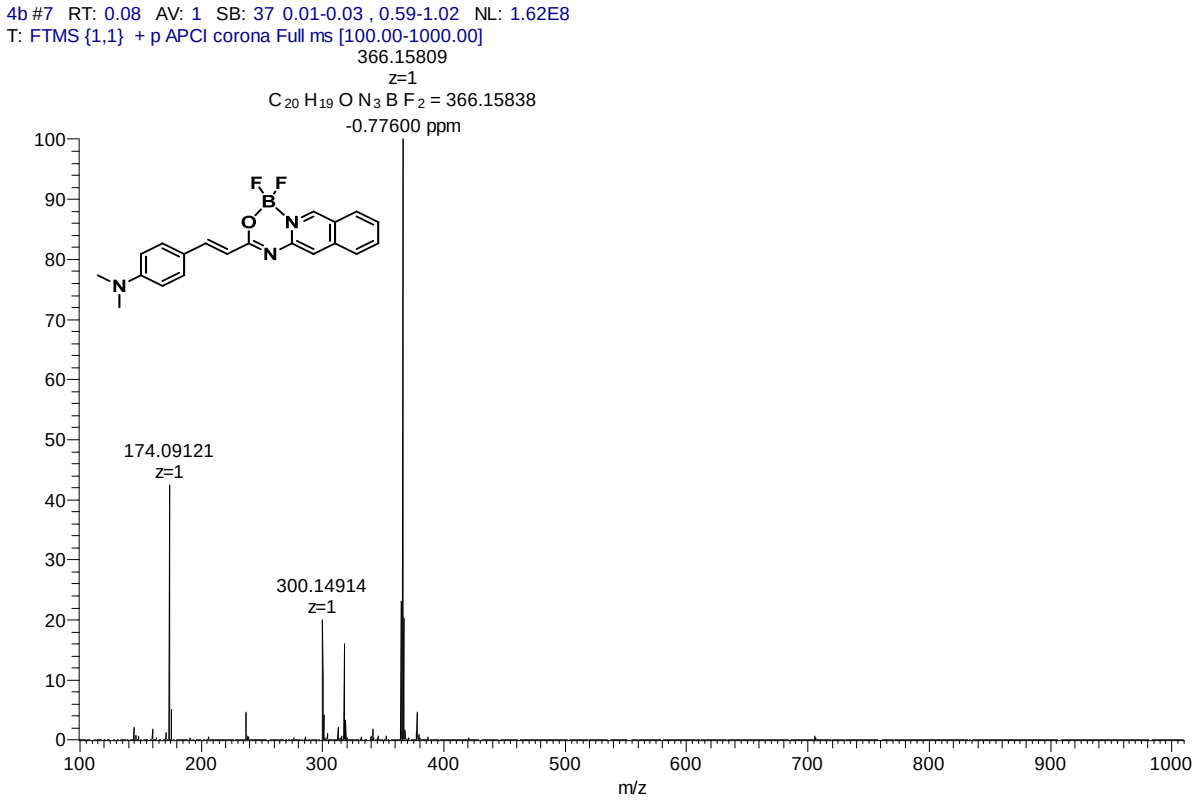

HRMS spectrum of compound **4b**

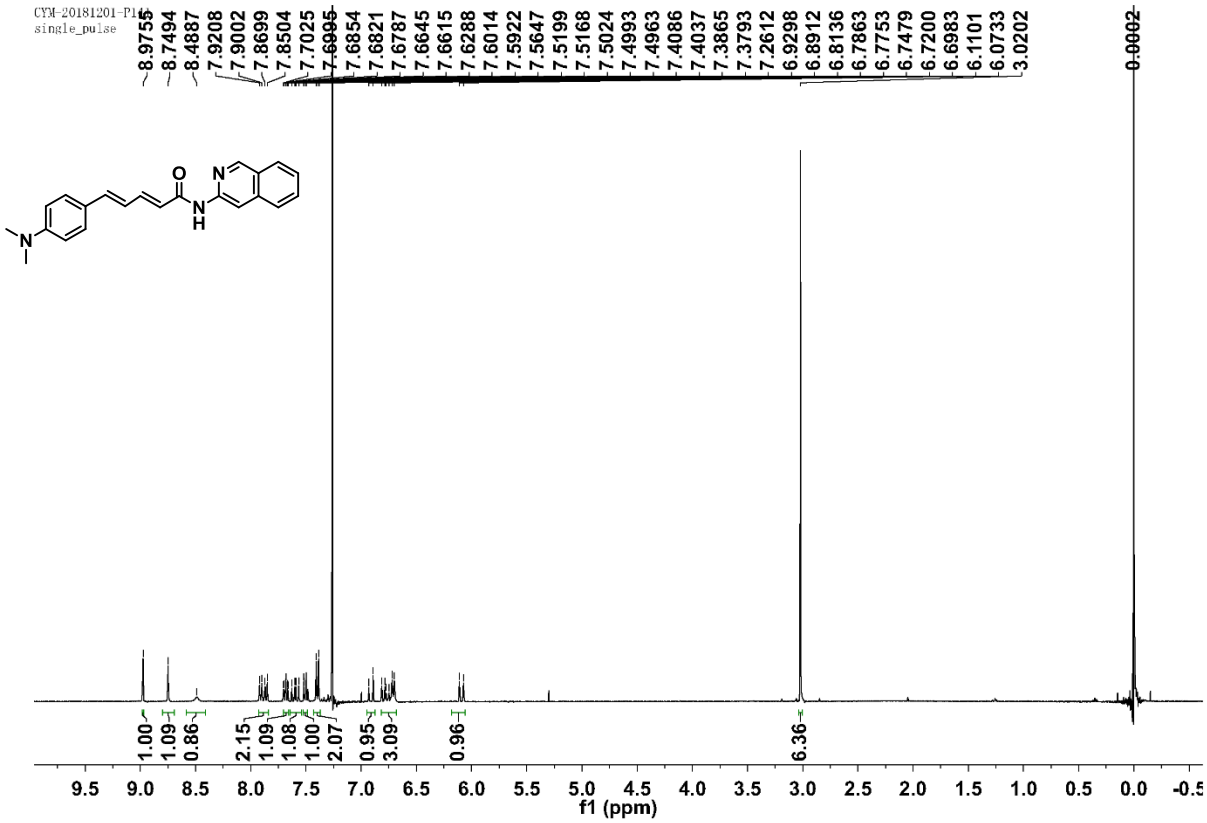

^{1}H NMR ($CDCl_3$) spectrum of compound **3c**

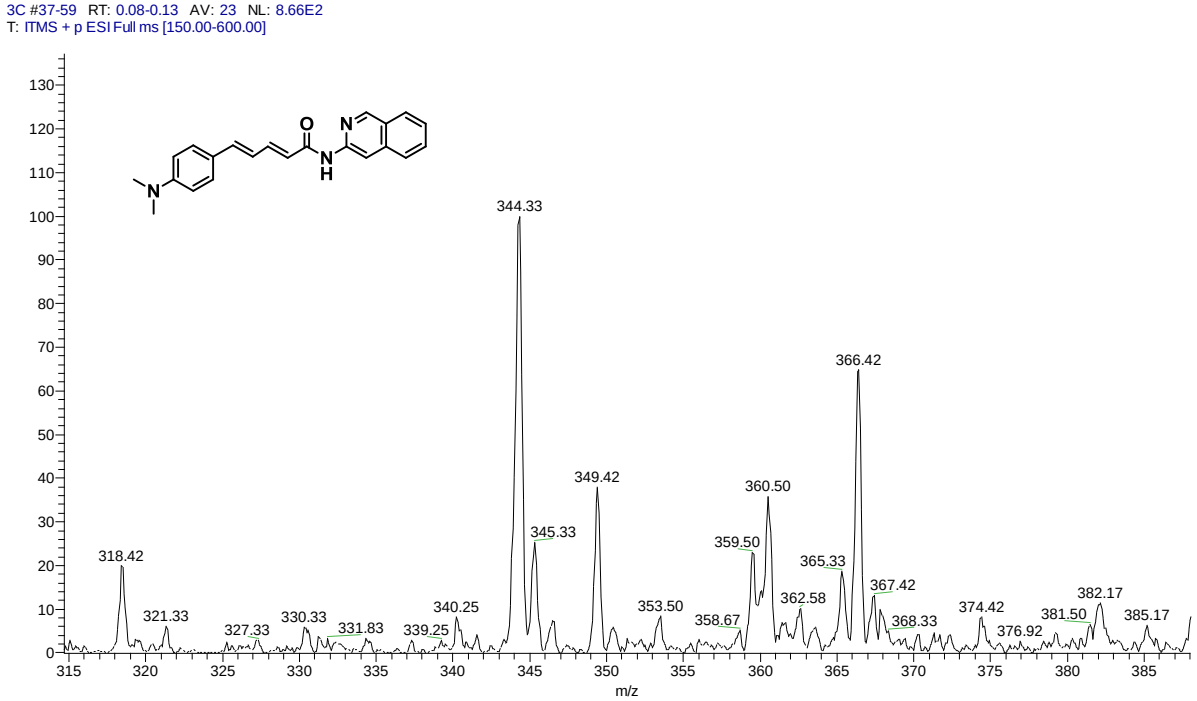

MS spectrum of compound **3c**

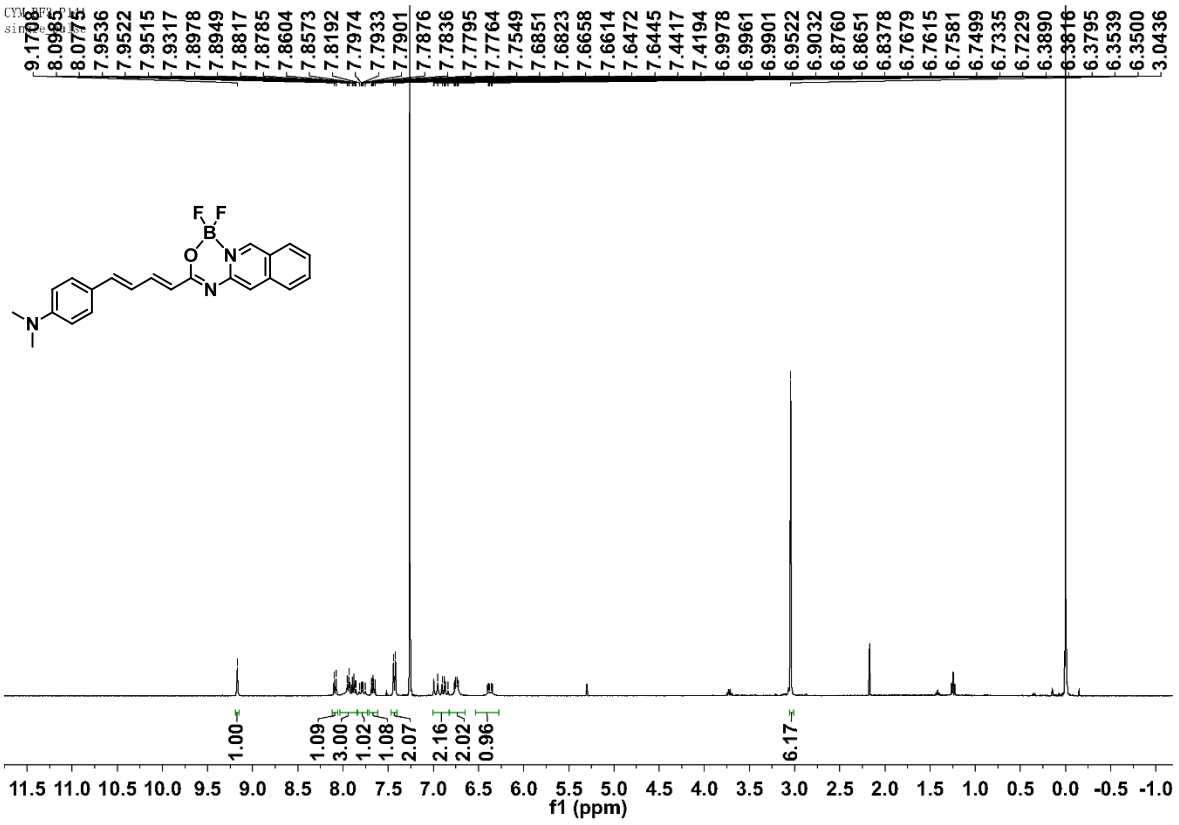

^{1}H NMR ($CDCl_3$) spectrum of compound **4c**

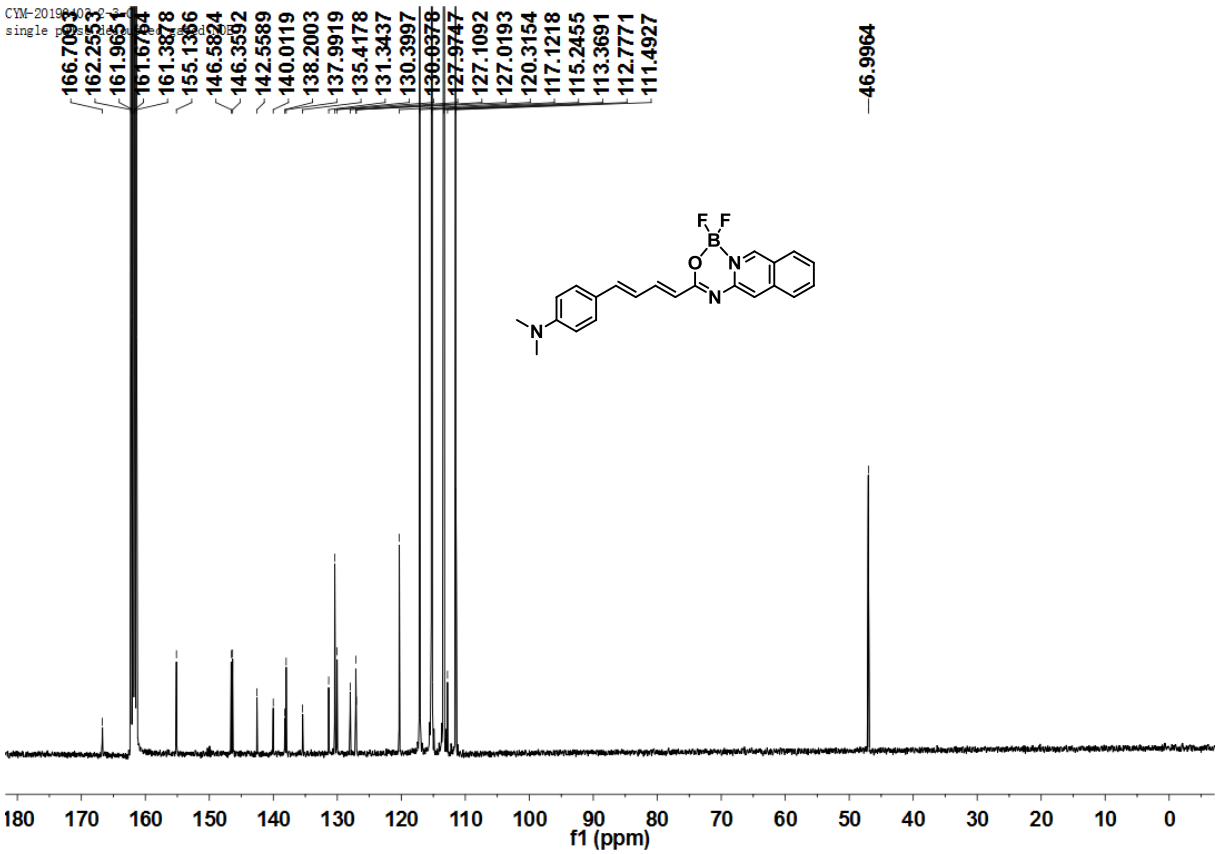

^{13}C NMR ($C_2DF_3O_2$) spectrum of compound **4c**

F F

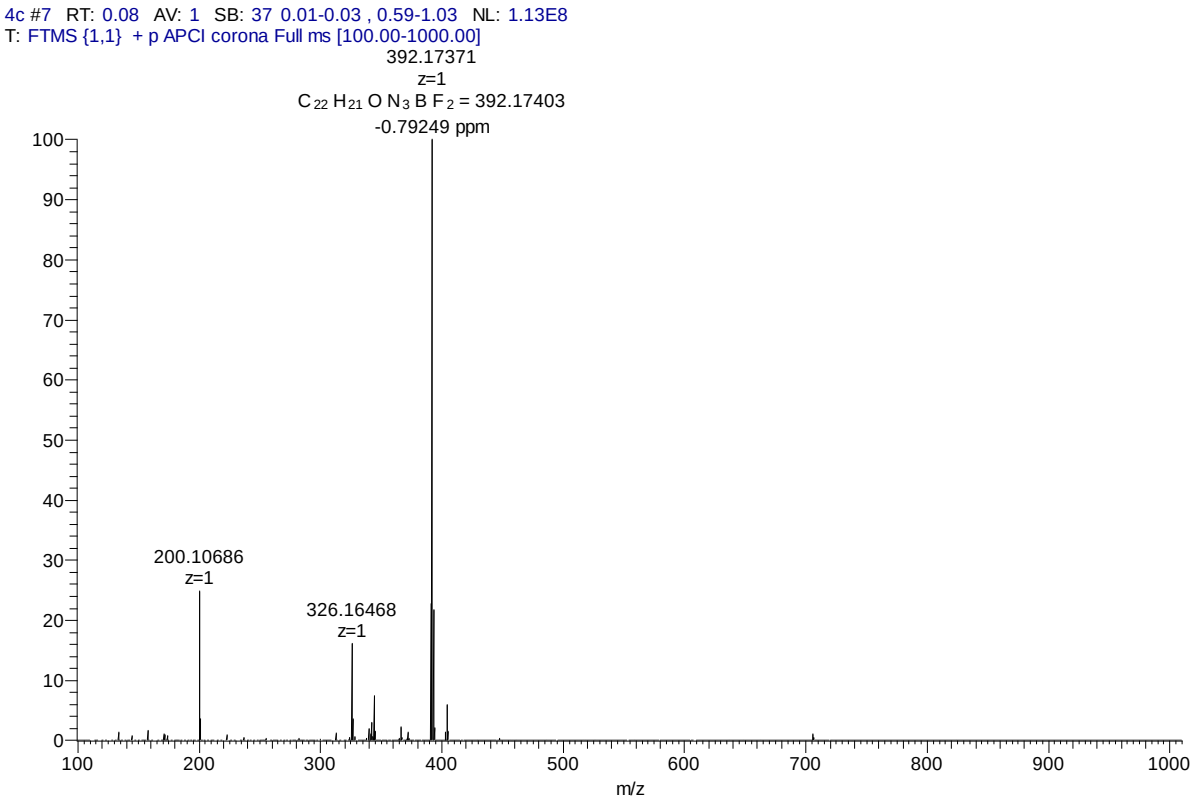

HRMS spectrum of compound **4c**

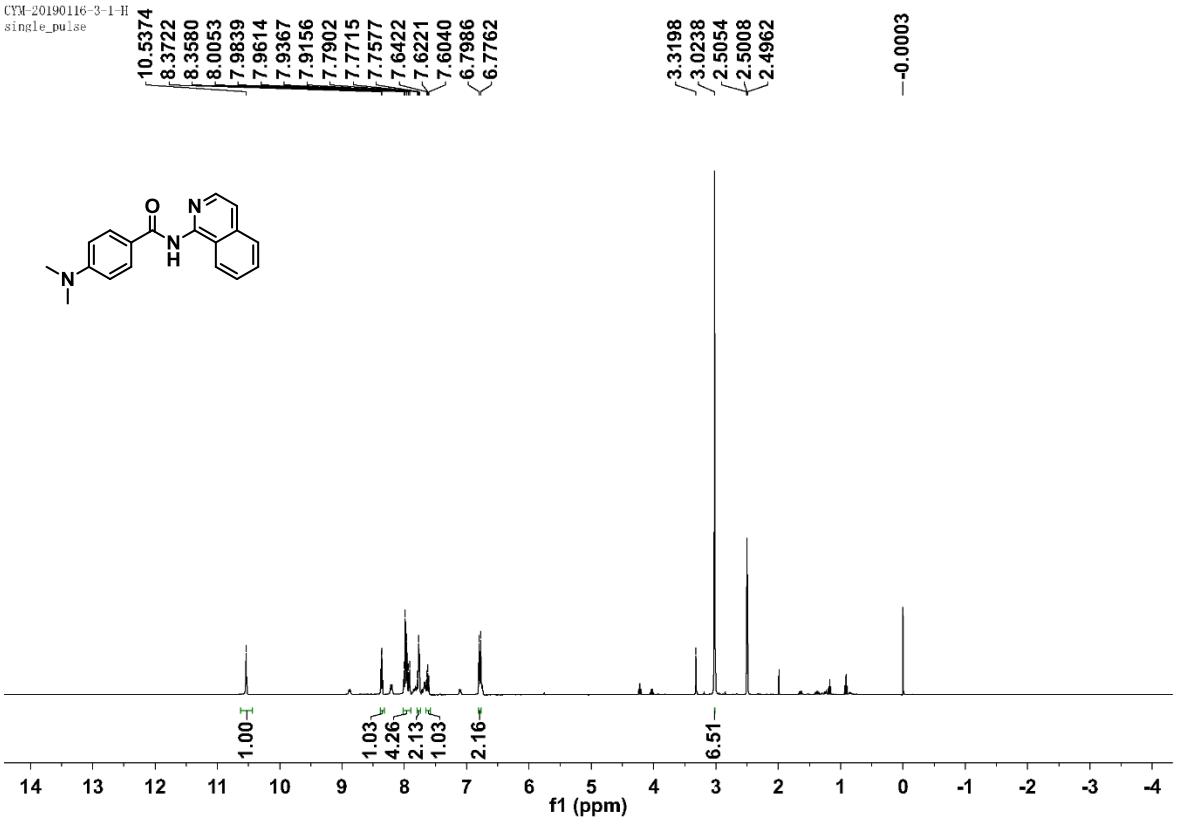

^{1}H NMR (DMSO-d_6) spectrum of compound **5a**

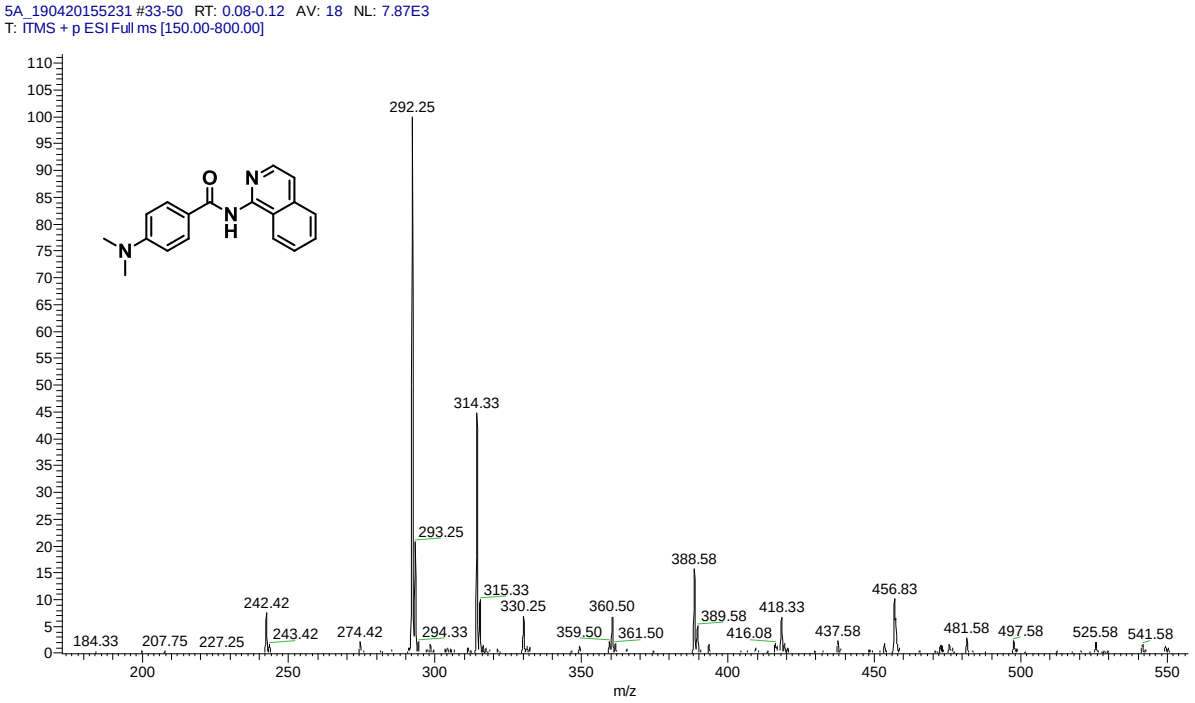

MS spectrum of compound **5a**

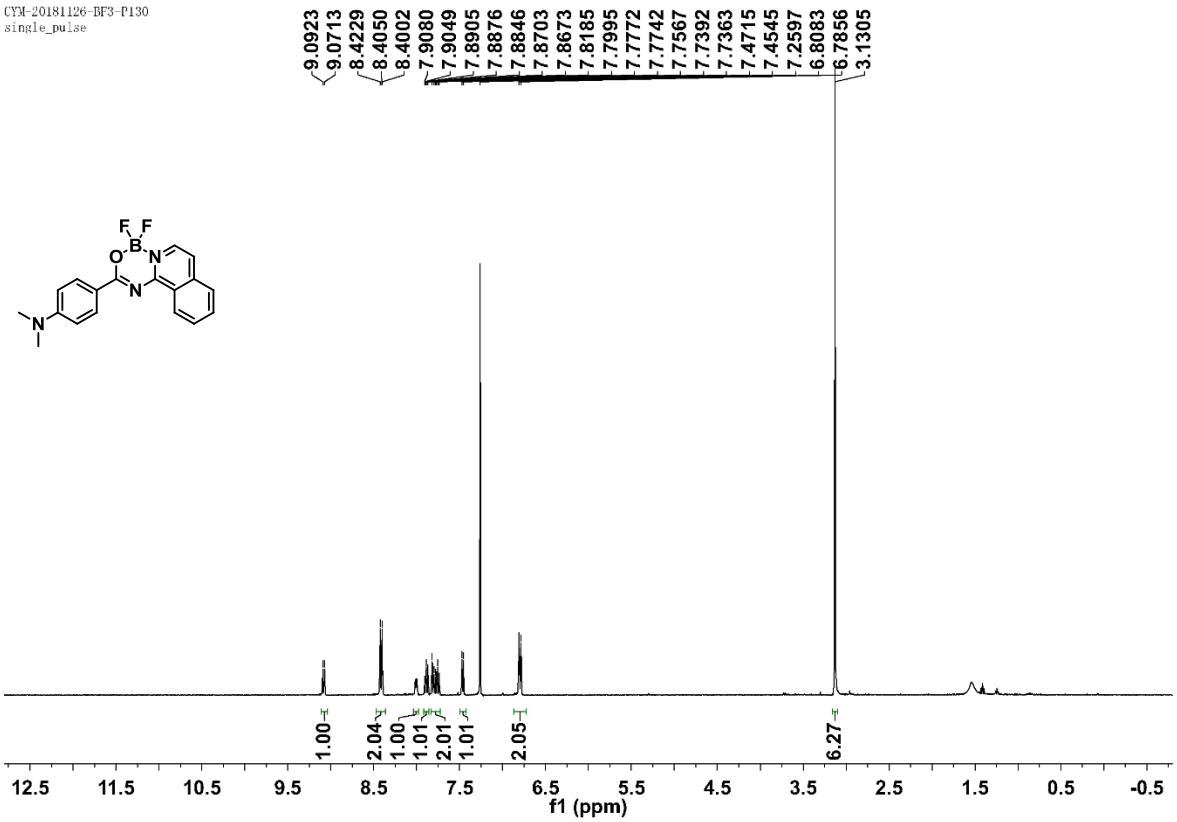

^{1}H NMR ($CDCl_3$) spectrum of compound **6a**

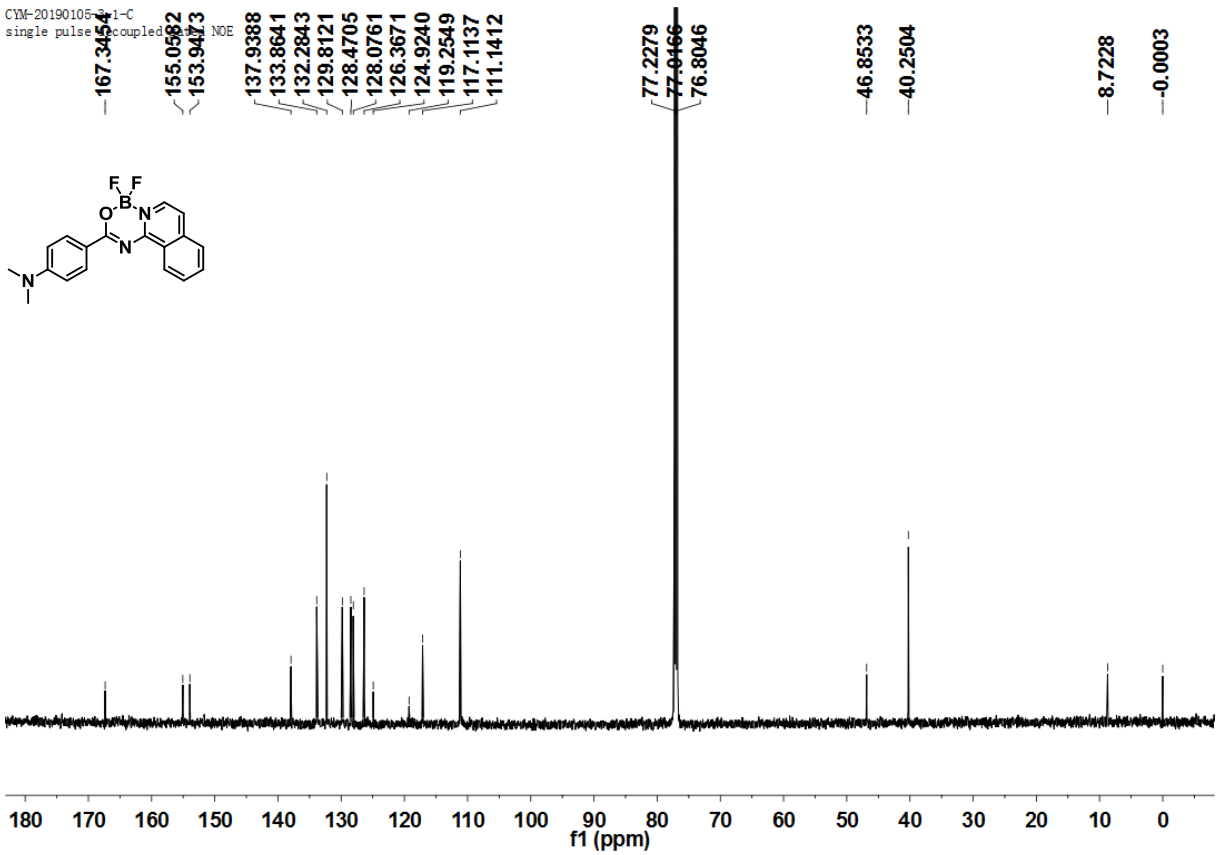

^{13}C NMR ($CDCl_3$) spectrum of compound **6a**

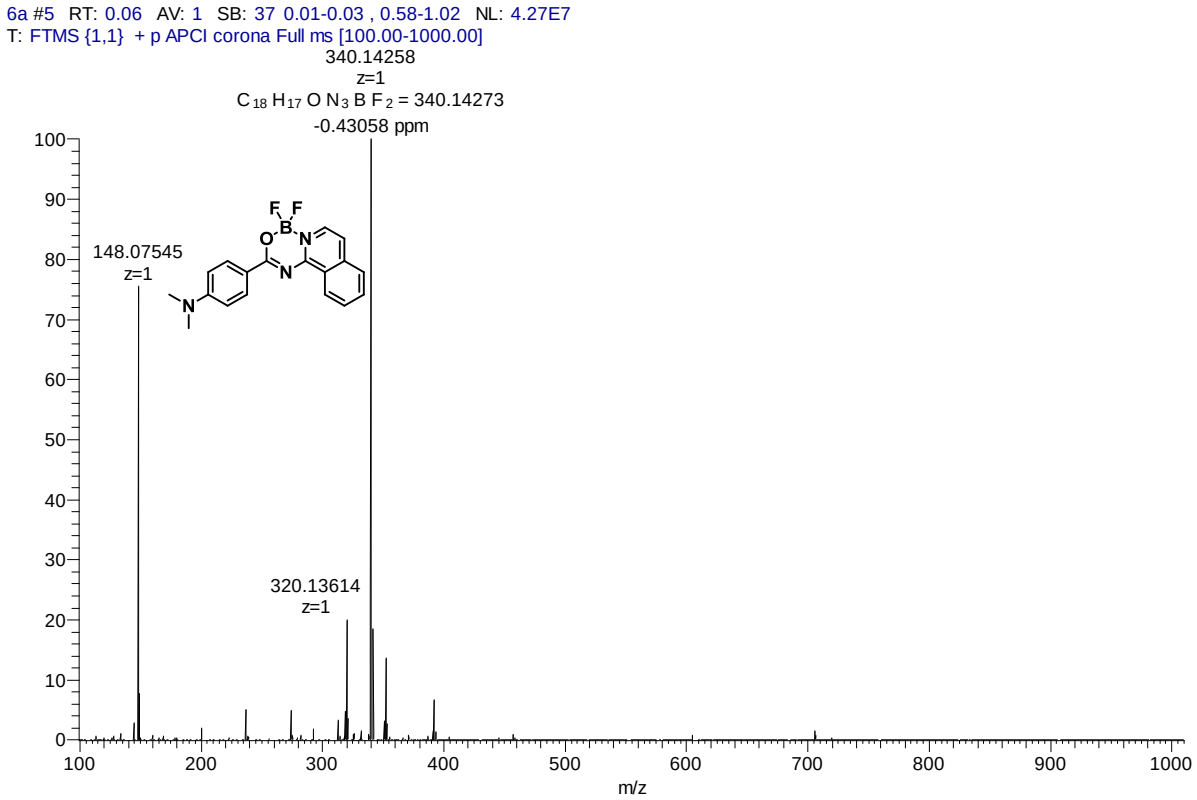

HRMS spectrum of compound **6a**

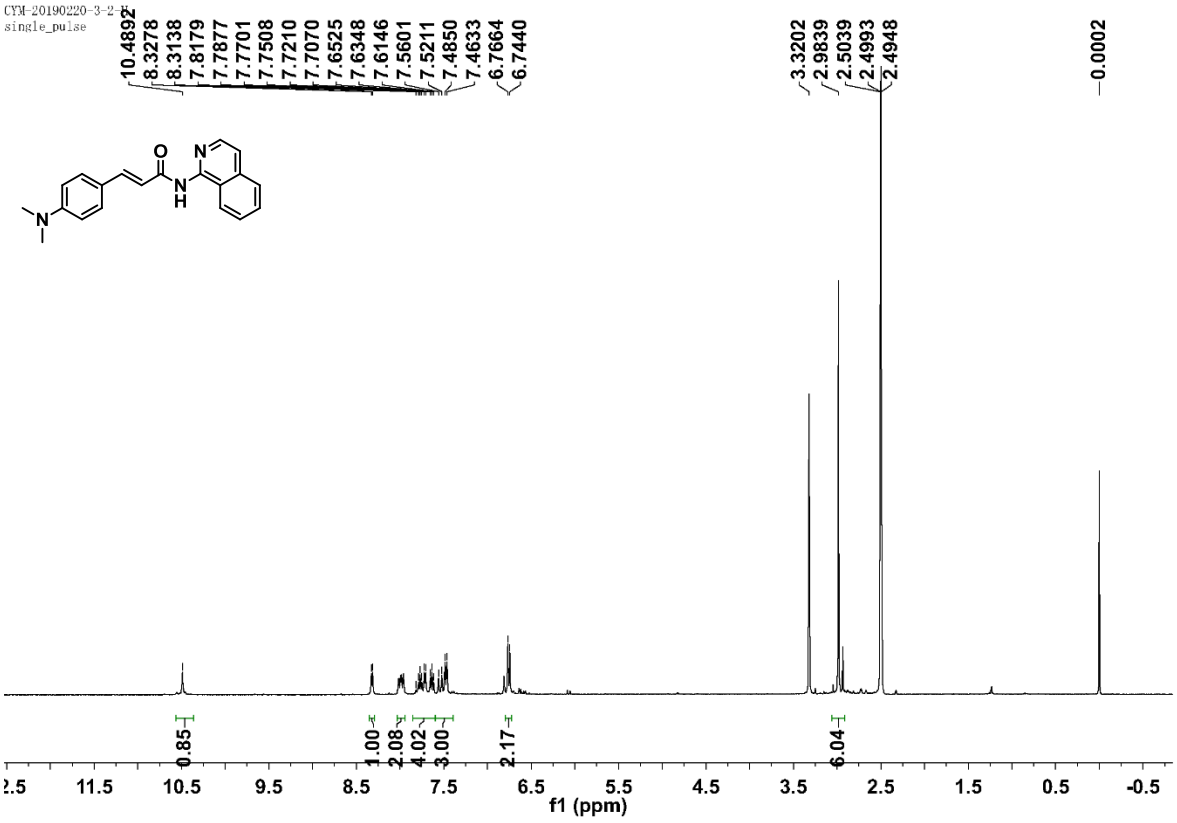

^{1}H NMR (DMSO-d_6) spectrum of compound **5b**

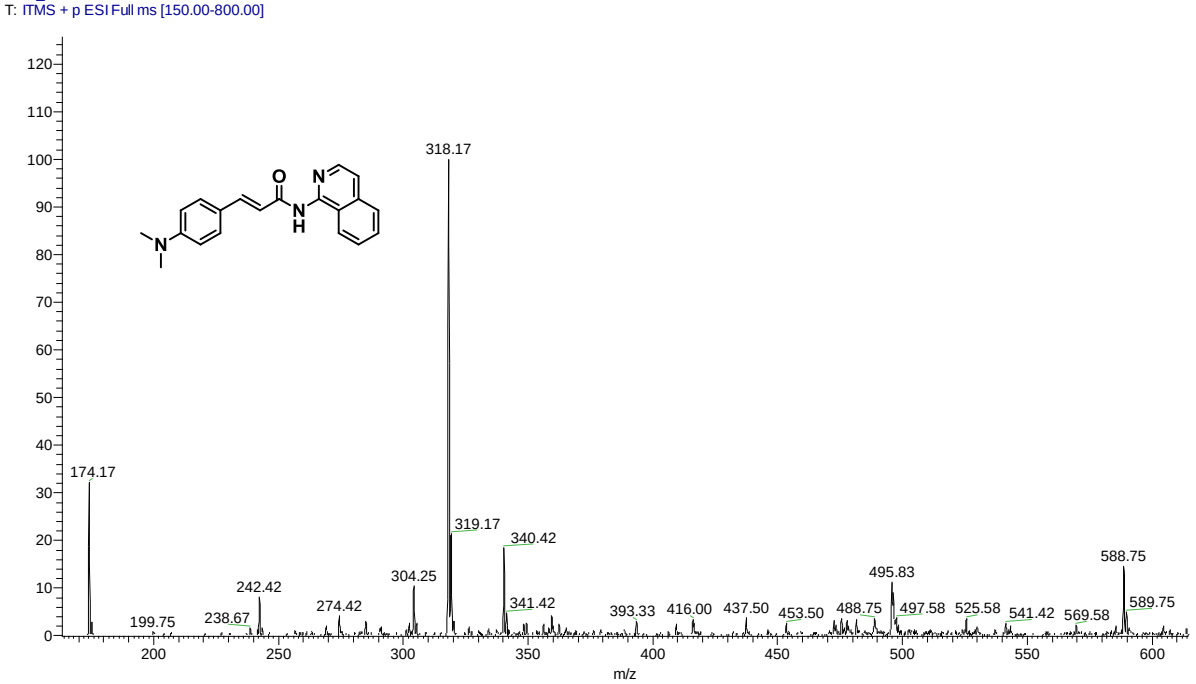

MS spectrum of compound **5b**

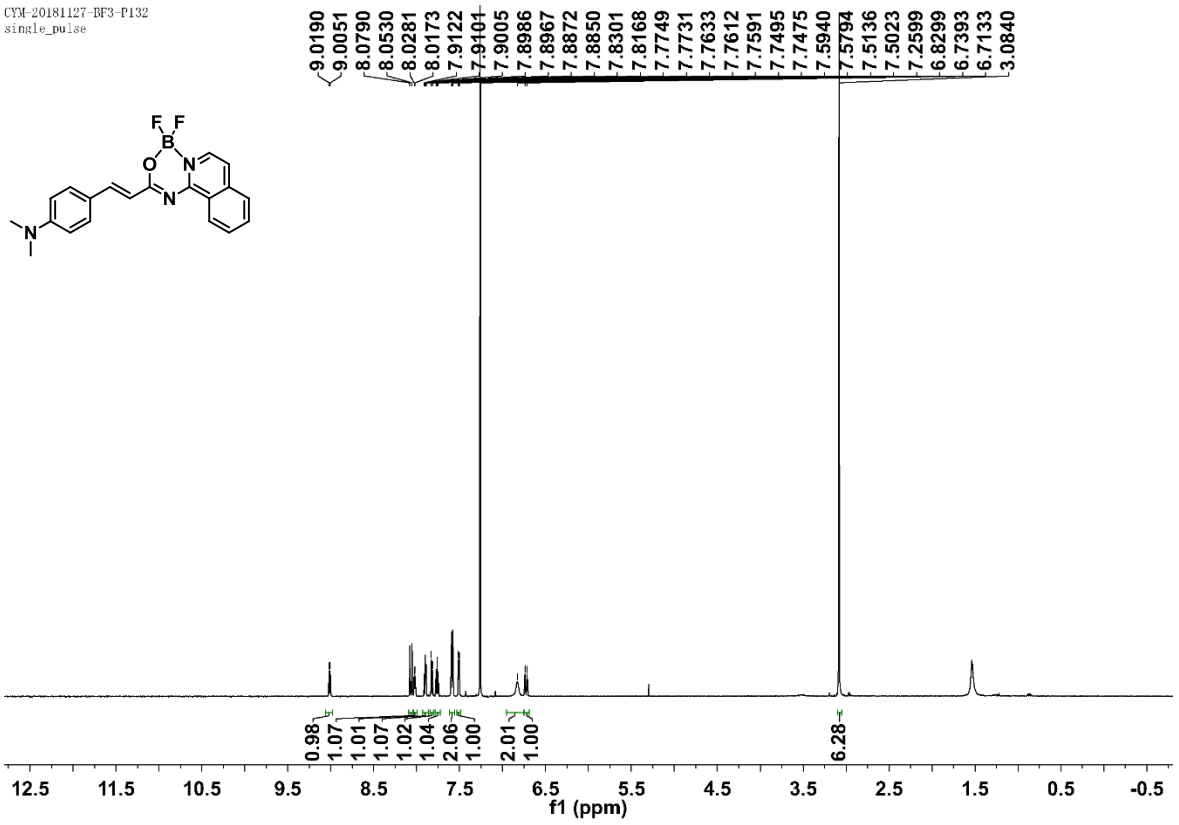

^{1}H NMR ($CDCl_3$) spectrum of compound **6b**

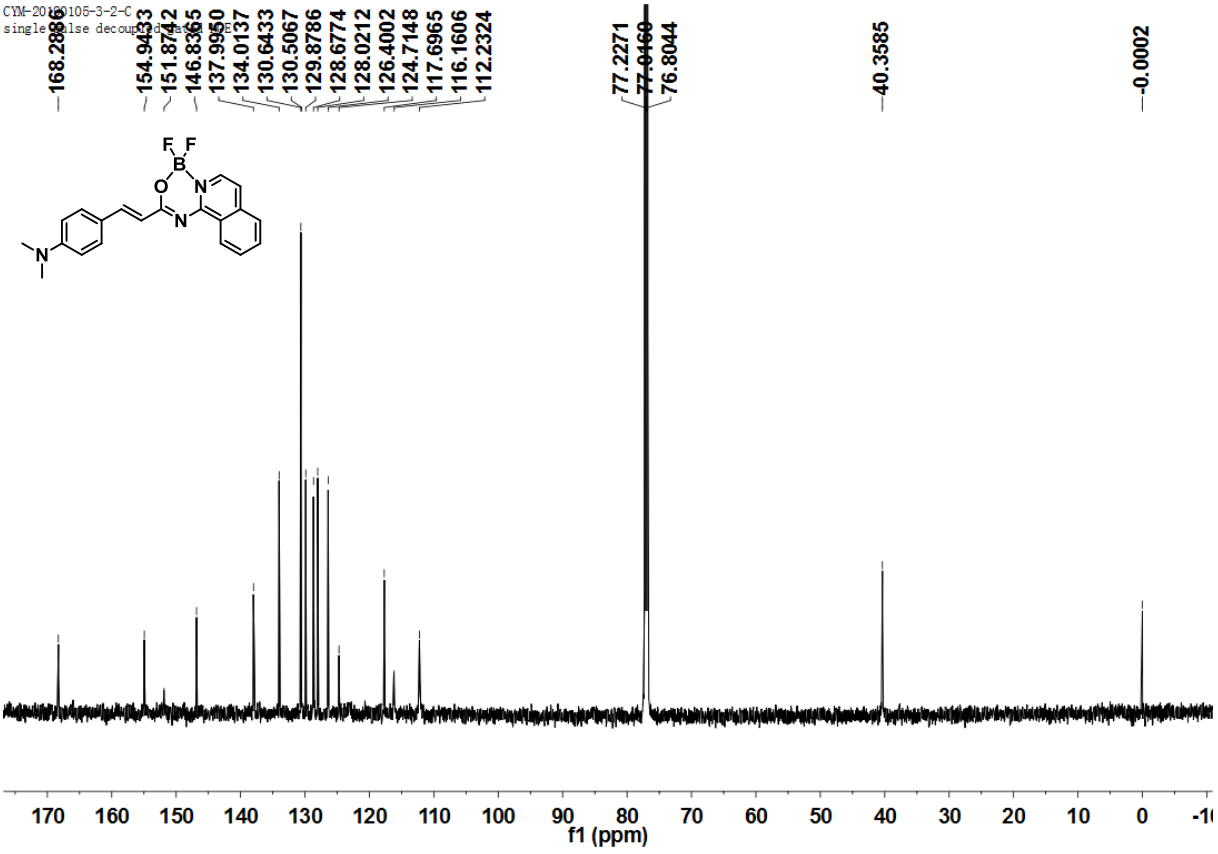

^{13}C NMR ($CDCl_3$) spectrum of compound **6b**

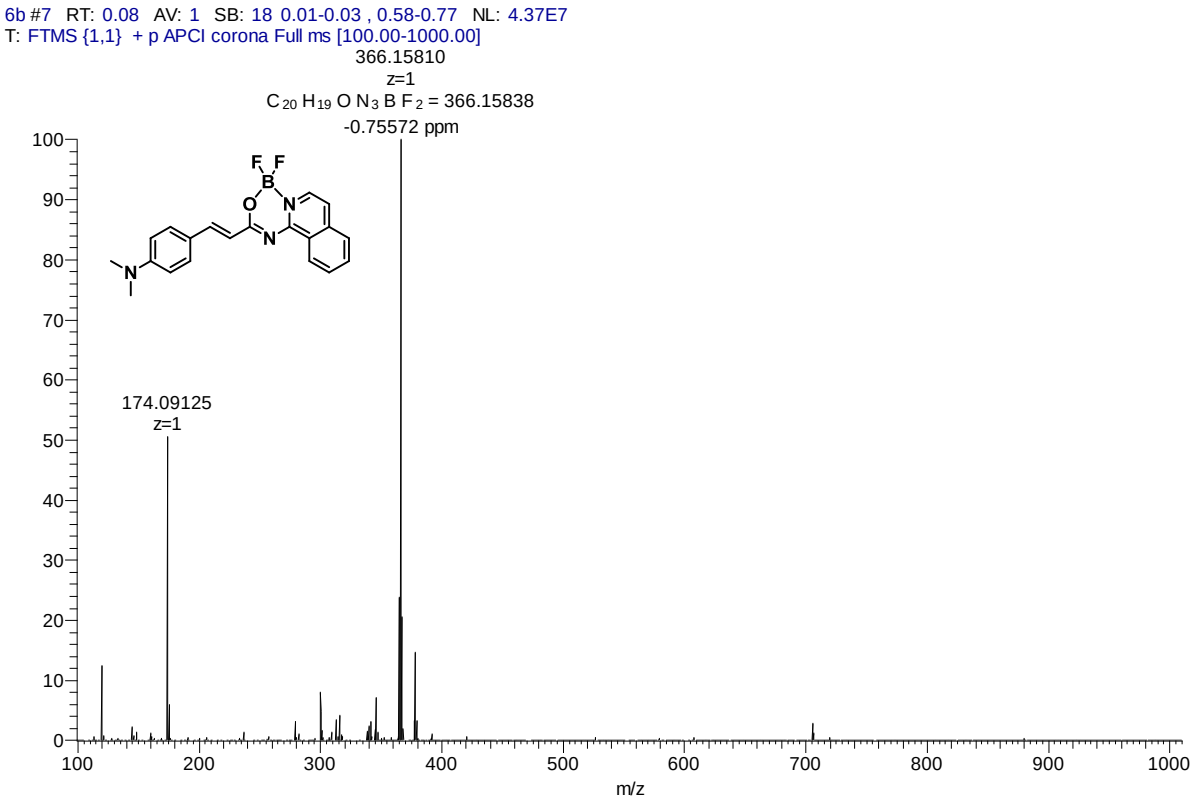

HRMS spectrum of compound **6b**

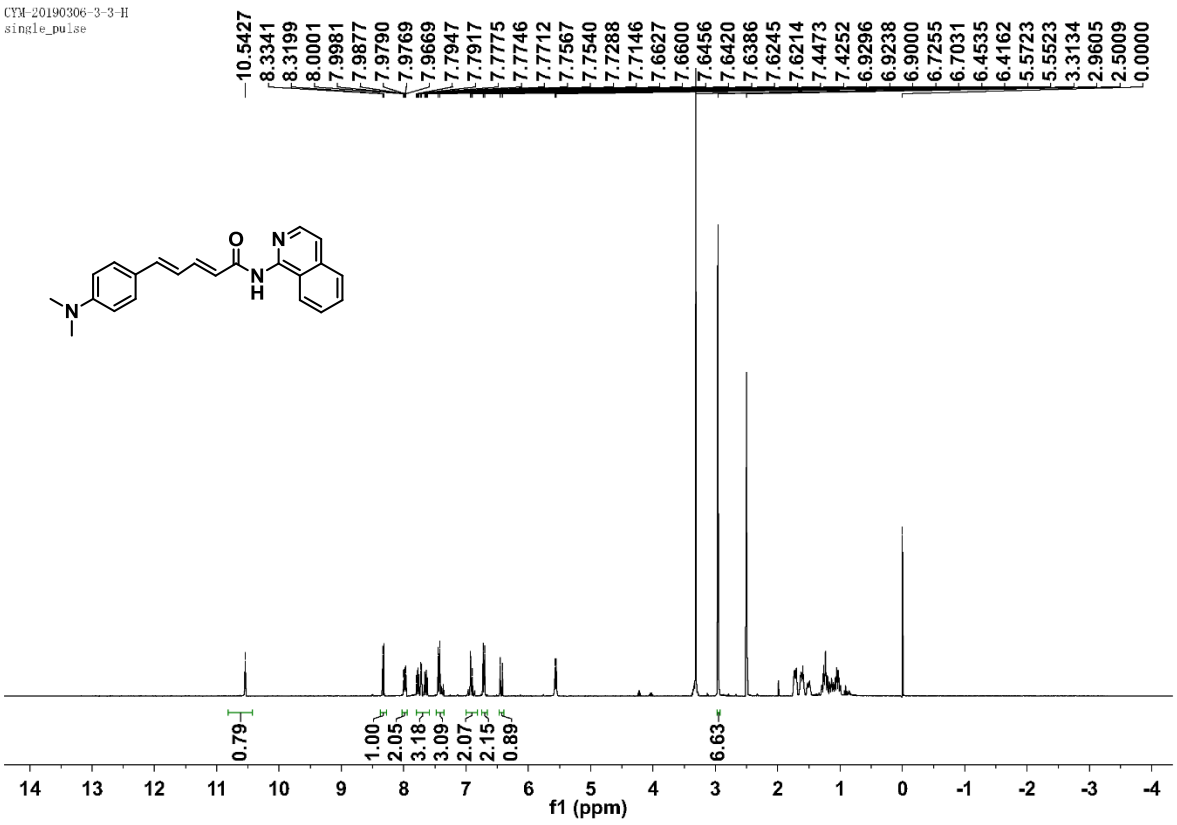

^{1}H NMR (DMSO-d_6) spectrum of compound **5c**

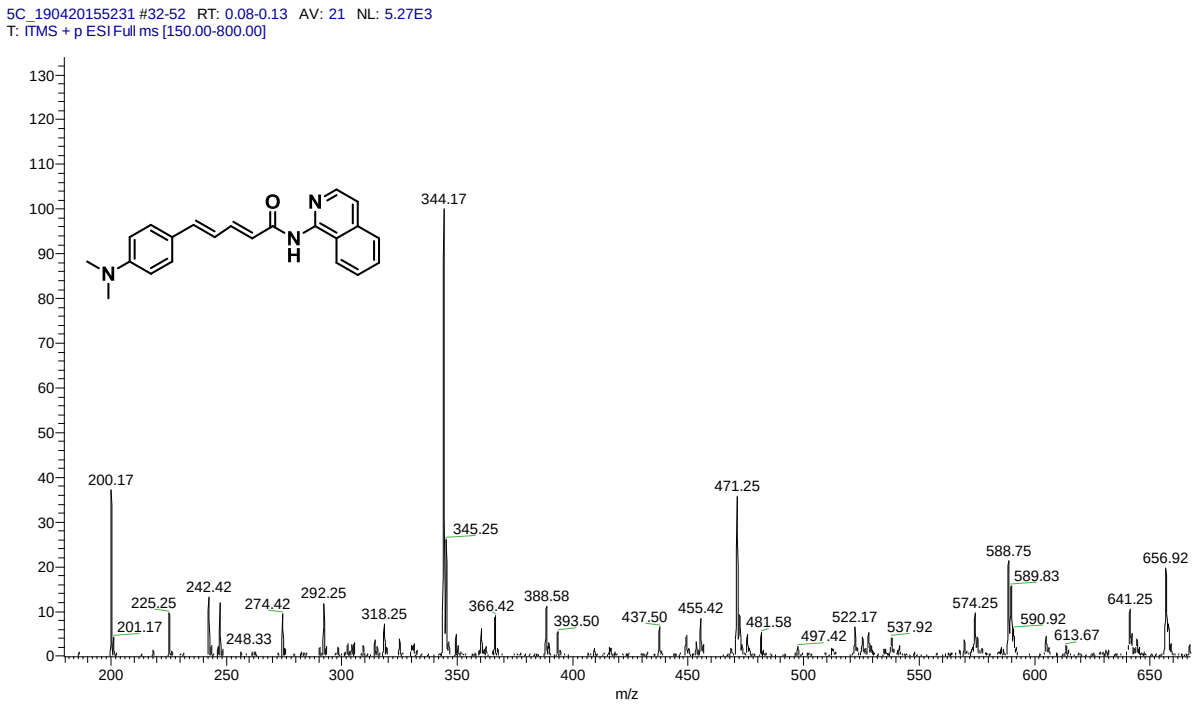

MS spectrum of compound **5c**

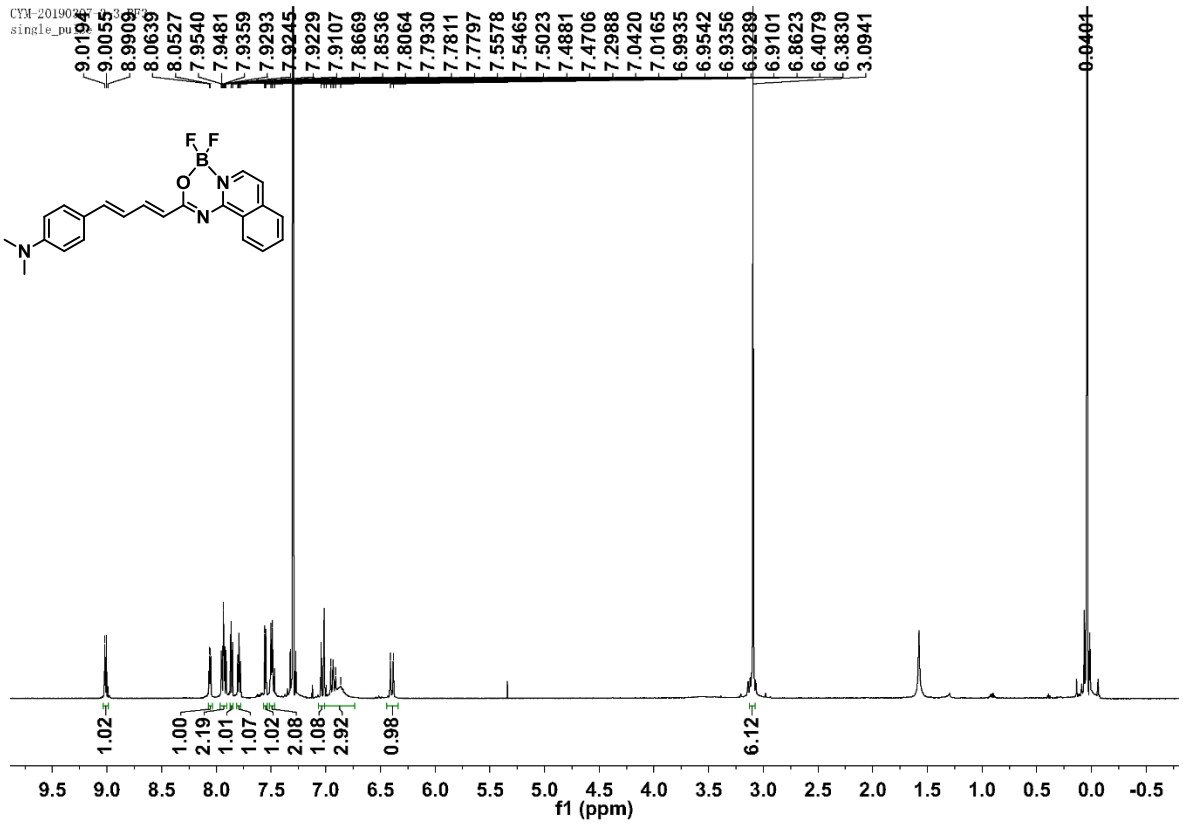

^{1}H NMR ($CDCl_3$) spectrum of compound **6c**

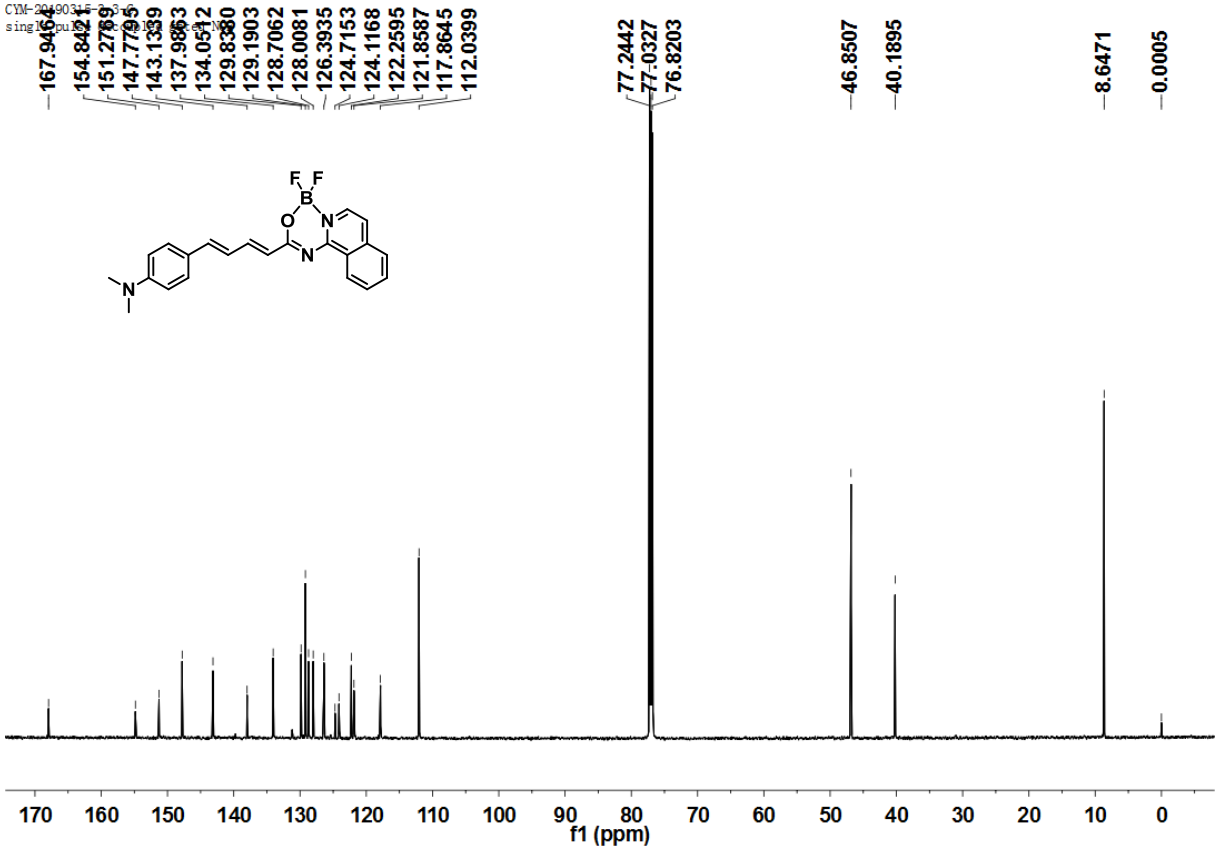

^{13}C NMR ($CDCl_3$) spectrum of compound **6c**

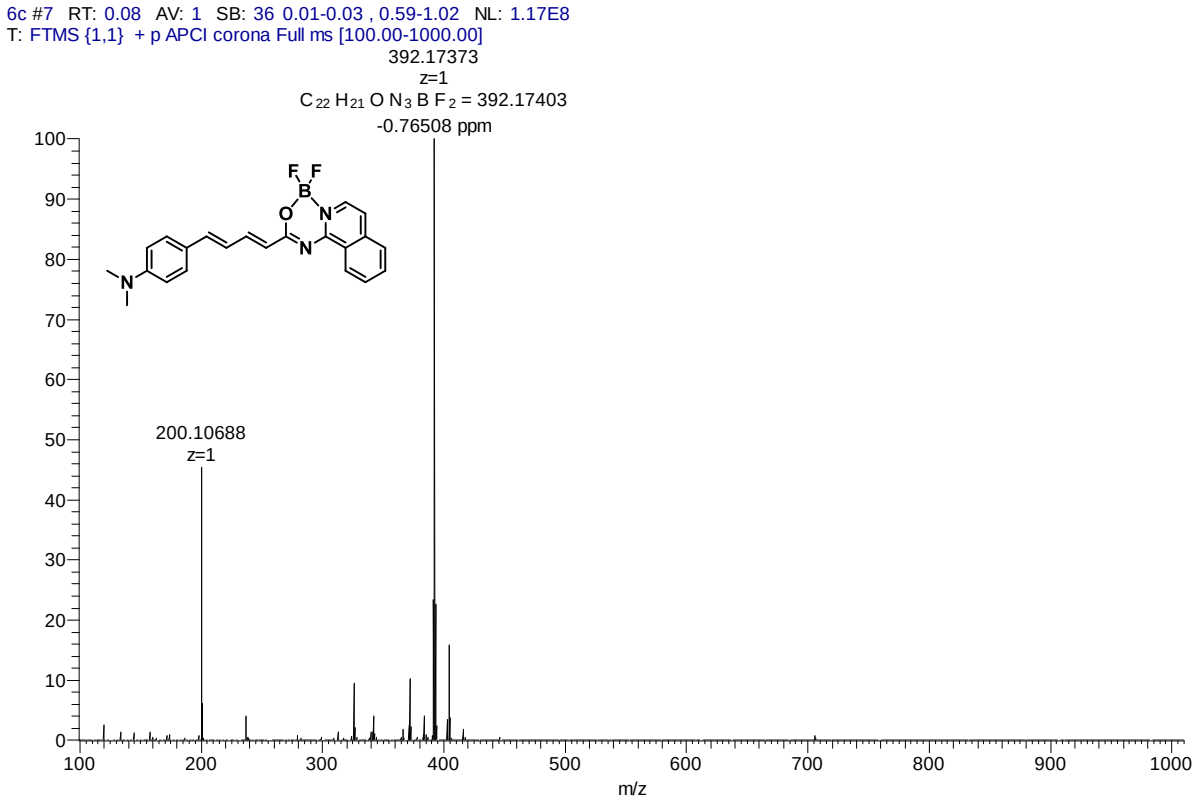

HRMS spectrum of compound **6c**

REFERENCE

1. M. Cui, M. Ono, H. Watanabe, H. Kimura, B. Liu and H. Saji, *J Am Chem Soc*, 2014, **136**, 3388-3394.
2. T. Yanai, D. P. Tew and N. C. Handy, *Chemical Physics Letters*, 2004, **393**, 51-57.
3. A. Schäfer, H. Horn and R. Ahlrichs, *J Chem Phy*, 1992, **97**, 2571-2577.
4. H. Matsusaka, K. Ikeda, H. Akiyama, T. Arai, M. Inoue and S. Yagishita, *Acta Neuropathol*, 1998, **96**, 248-252.
5. H. Fu, M. Cui, P. Tu, Z. Pan and B. Liu, *Chem Commun (Camb)*, 2014, **50**, 11875-11878.